Development of functional biopolymers with controlled architecture

Hang Shen

N° d'ordre: Année 2013

THESE

Présentée à

L'Université Jean Monnet, Saint Etienne

Ecole doctorale de Saint Etienne

Pour obtenir le diplôme de

DOCTEUR

Spécialité **Chimie et Science des Matériaux**

Par

Hang SHEN

Elaboration de polymères biosourcés fonctionnels à architecture controlée

Directeur de Thèse: Professeur Mohamed TAHA

Soutenue le : 17 Décembre 2013

Devant le jury composé par :

Monsieur Yves CHEVALIER Rapporteur

Madam Jianding CHEN Rapporteur

Monsieur Philippe CHAUMONT Examinateur

Monsieur Jean-claude JAMMET Examinateur

Madam Nathalie MIGNARD Examinatrice

Madam Cécile COUSTAL Examinatrice

Remerciements

The experiments in the present study were realized in the LABORATOIRE D'INGENIERIE DES MATERIAUX POLYMERES, CNRS UMR 5223, in site UNIVERSITE JEAN MONNET, SAINT ETIENNE, FRANCE.

Thanks to Professor Christian CARROT, for offering me such an opportunity to study in University Jean Monnet, welcoming me into this laboratory and treating me kindly in my three- year doctoral study.

I woluld like to send my deepest gratitude to Professor Mohamed TAHA, my supervisor and director of thesis, for his constant encouragement and guidance. He walked me through all the stages of the doctoral study. He is kind and warm heart, restrict to academic study but optimistic in cheering me up when I was frustrated, and he is a creative professor with ideas but also a practical chemist who always work and illustrate us in experiments. Without his consistent and illuminating instruction, this thesis could not have reached its present form.

I would like to express my gratitude to Dr Frédéric BECQUART, who offered a lot of help to let me accommodate myself to this new circumstance in France.

I am also greatly indebted to the professors Professor Jianding CHEN, from EAST CHINA UNIVERSITY OF SCIENCE AND TECHNOLOGY, CHINA. She cares her oversea students from academic research to their daily lives. From her visit to University Jean Monnet, I benefited the knowledge and experience from group discussion between Professor TAHA and her.

I also want to thank the financial support from China scholarship council (national scholarship fund) for their sponsorship during three years.

I am honored and appreciative to the participation of jury: Mr Monsieur Yves CHEVALIER and Madam Jianding CHEN as the reporters of thesis, and Philippe CHAUMONT, Jean-claude JAMMET and Nathalie MIGNARD as the examiner.

I would like to express my appreciations to the teachers who helped me in the laboratory during the writing of in this thesis: Nathalie MIGNARD, Corinne JEGAT, Caroline PILLON, Jean-Charles MAJESTE and Frédéric PROCHAZKA and my colleges Dalila, Kevin, Basak, Alix, Pierrick

and so on. They offer warm help in my daily life and useful suggest in study. I will always remember the happy and great time that we had spent together in the past 3 years.

Last but not the least, my thanks would go to my family, for their loving considerations and great confidence to me throughout these years; and my brothers for their consistent support and trust.

Publications and communications

Publications:

Hang SHEN, Jianding CHEN, Mohamed TAHA. Ring opening Copolymerization of caprolactone and glycidyl methacrylate and cross-linking of the issued methacrylated polycaprolactone (submitted)

Hang SHEN, Guilhem Quintard, Jianding CHEN, Mohamed TAHA. Multially Polycaprolactone based polyesterurethanes: synthesis, cross-linking with polyhydroxyethyl methacrylate and theromechanical properties (submitted)

Hang SHEN, Caroline PILLON, Jianding CHEN, Mohamed TAHA. Cross-linkable polylactic acid and polyhydroxybutyrate (submitted)

Hang SHEN, Jianding CHEN, Mohamed TAHA Hang SHEN, Jianding CHEN, Mohamed TAHA. Multi mercapto-functionalized PLA, PHB and PCL segmented polyurethanes (submitted)

Communications:

Oral presentation: Hang SHEN, Frédéric BECQUART, Jianding CHEN, Mohamed TAHA, Poly caprolactone Networks – PCL functionalization by copolymerization with GMA and thiol-ene network, 40èmes Journées d'Etudes des Polymères , Sept 30-Oct 5, 2012, Anduze (Gard), France.

Poster: Hang SHEN, Jianding CHEN, Mohamed TAHA. Ring opening copolymerization of caprolactone and glycidyl methacrylate and cross-linking of the issued copolymers. 4th International Conference on Biodegradable and Bio-based Polymers, 1-3 October 2013, Rome, Italy.

INDEX

Abbreviations

AIBN	2-azobis(2-methyl-propionitrile)
CL	caprolactone
GMA	Glycidyl methacrylate
H_{12}MDI	4, 4'-Methylenebis(cyclohexyl isocyanate)
HEMA	2-Hydroxyethyl methacrylate
LA	Lactide
M_c	Molecular weight between crosslinks
MMA	Methyl Methacrylate
PEU	Poly ester urethane
PHB	Polyhydroxybutyrate
$Sn(Oct)_2$	Tin(II)-bis-(2-ethylhexanoate)
T_g	Glass transition temperature
THF	Tetrahydrofuran
TGA	Thermogravimetrische Analyse
UV	Ultraviolet

Introduction générale

Depuis le siècle dernier, des matériaux polymères synthétiques ont été développés dans un des domaines les plus attrayants de la science des matériaux. Ces polymères formés principalement par des liaisons non carbone - carbone réversibles dans des conditions habituelles d'utilisations présentent des stabilités thermiques et biochimiques avantageuses dans les usages quotidiens. Leur faible coût, la reproductibilité de leurs synthèses et leur résistance relative au vieillissement physique leur permettront d'être les principaux matériaux utilisés dans l'industrie. Cependant, les propriétés de résistance des polymères synthétiques à la biodegrabilité sont devenues de plus en plus problématiques dans de nombreux domaines tels que la pharmacologie, l'agriculture, où ces matériaux sont utilisés pour une période de temps limitée avant de devenir déchets.

Pour résoudre ce problème, la nature des monomères des polymères en découlant doit être adaptée pour rendre ces matériaux bio-compatibles, non toxiques et biodégradables.. Les polyesters aliphatiques biodégradables tels que le polyhydroxybutyrate (PHB), le poly-(Ɛ-caprolactone) (PCL), ou un poly (α-hydroxy acide)s dérivés d' acides glycolique et lactique peuvent remplacer des polymères bio-stable dans le cas où leur utilisation est limitée dans le temps ou encore pour des applications spécifiques dans des domaines biomédicaux.

Ces polyesters sont habituellement linéaires et manquent de centres réactif ce qui limite leur réactivité. Pour élargir leurs domaines d'utilisation, on peut envisager des synthèses permettant d'y incorporer des fonctions réactives.

L'objectif de ce travail est d'une part de concevoir et préparer des pré polymères multifonctionnels bio-sourcés et / ou biodégradables utilisant de nouvelles voies de synthèse. Les fonctions que nous souhaitons introduire sont soit des liaisons doubles ou bien des mercaptans. Ces pré polymères seront ensuite utilisés pour préparer des réseaux ou des thermoplastiques contenant une partie biosourcée ou biodégradable et une autre synthétique.

Les pré polymères seront à base de polylacide lactique, polycaprolactone et polyhydroxybutyrate.

Deux voies de synthèse de prépolymères ont été envisagées.

La première consiste en une copolymérisation par ouverture de cycle du glycidyle méthacrylate avec le dimère cyclique « lactide » ou la caprolactone. La seconde approche, des polyesters uréthanes sont à préparer utilisant des oligomères hydroxy télécheliques. Ces synthèses seront envisagées en une ou deux étapes. Les fonctions visées ici sont soit des liaisons doubles ou des mercaptans.

Les prépolymères portant des liaisons doubles seront soit co polymérisés principalement avec le 2-hydroxylethylmethacrylate, ceux portant des fonctions mercaptan seront utilsés comme agents de transfert efficaces durant la polymérisation radicalaire de différents monomères.

General Introduction

Since the last century, synthetic polymeric materials have been developed in one of the most attractive materials science fields. These polymers formed mainly by carbon - carbon non-reversible under normal conditions, and present uses thermal and biochemical stabilities advantageous in everyday use. Their low cost, reproducibility of their synthesis and their relative resistance to physical aging allow them to be the main materials used in the industry. However, the strength properties of synthetic polymers biodegradability have become increasingly problematic in many areas such as pharmacology, agriculture, where these materials are used for a limited period of time before becoming waste.

To solve this problem, the nature of the monomers in polymers arising must be adapted to make them biocompatible, non-toxic and biodegradable materials. The biodegradable aliphatic polyesters such as polyhydroxybutyrate (PHB), poly (Ɛ-caprolactone) (PCL) , or poly (α-hydroxy acid) s derived from glycolic and lactic acids can replace permanent bio-polymers in the cases where their use is limited in time or for specific applications in biomedical fields. These polyesters are usually linear and lack of reactive centers which limits their reactivity. To expand their areas of application, we can consider allowing synthesis to incorporate reactive functional groups.

The objective of this work is a part of designing and preparing bio-sourced and / or biodegradable multifunctional polymers using new synthetic routes. The functions that we want to introduce are either double bonds or mercaptos. These pre-polymers are then used to prepare networks or thermoplastic containing a bio-based or biodegradable fraction and another synthetic. Prepolymers are based on polylacide lactic polyhydroxybutyrate and polycaprolactone.

Two synthetic routes prepolymers were considered:

The first step consist a ring-opening copolymerization of glycidyl methacrylate with cyclic dimer “lactide” or caprolactone. The second approach, urethane polyesters are prepared

using hydroxy telechelic oligomers. These summaries will be considered in one or two stages. The functions described here are either double bonds or mercaptans.

Prepolymers carrying double bonds are polymerized or co mainly with 2-hydroxylethylmethacrylate, those bearing mercaptan functions as will use effective transfer agents during the radical polymerization of different monomers.

Chapter 1

Bibliography

Résumé

Ce chapitre présente une étude bibliographique concernant la conception de la structure ainsi que la synthèse par polymérisation par ouverture de polymères fonctionnalisés biodégradables. Des mécanismes de ces réactions sont présentés. Les propriétés des matériaux à base de ces polymères en fonction de leurs structures sont reportées.

Les techniques décrites sont des moyens précieux pour orienter la suivante de cette étude.

Abstract

This chapter presents a literature review on the design of the structure and synthesis opening polymerization of functionalized biodegradable polymers. Mechanisms of these reactions are presented. The properties of materials based on these polymers in terms of their structures are reported.

The techniques described are valuable means to guide the following of this study.

This Chapter introduced the general conceptions and former studies of bio-resourced cyclic esters and their ring opening (co)polymerization to obtain degradable polymers. Syntheses strategies were adapted to obtain homo (co) polyesters with different functions. Based on which, more complicated structured polymers were designed by these linear, star-shaped or polyester networks. Properties and applications of these polymers are also discussed in this chapter.

1.1 Degradable polymers based on cyclic esters and the ring opening polymerization

1.1.1 Ring opening polymerization of cyclic esters

Dependence on petroleum-derived plastics has increased considerably since the last century. However, the rapid depletion of crude oil and the increasing apprehension to the environmental effects of synthetically produced materials has prompted much interest in biologically derived polymers, particularly of renewable, biodegradable and biocompatible class [1-5]. Among this materials, aliphatic polyesters are promising sustainable alternatives to commodity plastics such as polyethylene and polypropylene. Ester linkages are frequently encountered in nature and hence it is expected that synthetic polymers containing such linkages and an appropriate structure would be environmentally degradable. The traditional way of synthesizing polyesters has been by polycondensation using diols and a diacid (or derivative), or from a hydroxyl acid. This method suffers from some major shortcomings need for (a) high temperature, (b) long reaction times, (c) removal of reaction by-products, and (d) a precise stoichiometric balance between reactive acid and hydroxyl groups. On the other hand, the ring opening polymerizations (ROPs) of lactones, cyclic diesters including lactide and glycolide, and cyclic ketene acetals is an alternative method, which has been successfully employed to yield high molecular mass polymers under relatively mild conditions. This poly addition reaction can be carried out with no or limited side-reactions, and this makes it possible to control properties like molecular weight and molecular weight distribution (MWD).

The generally accepted mechanism for ring opening polymerization involves initiation by

either an anionic [6-9], cationic [10-13], coordination–insertion [14-17] or an activated monomer mechanism. The coordination–insertion mechanism is commonly used as it is a living polymerization, enables access to high molecular weight polymers and does not epimerize stereo centers such as those found in lactide. The mechanism operates via the coordination of the lactone to a Lewis acidic metal alkoxide complex, which activates and attacks the lactone at the carbonyl carbon. Acyl bond cleavage results in ring opening and the generation of a novel metal alkoxide species from which the cycle can re-initiate. Many metals have precedent for initiating the coordination–insertion polymerization, the common features being that they are Lewis acidic with a labile metal alkoxide or amide bond from which to initiate the polymerization; several excellent reviews already cover the selection and range of initiators tested [10].

The ROPs are typically carried out in the melt, using a catalyst along with a low molecular weight nucleophile, usually an alcohol, to co-initiate the polymerization and control the molecular weight of the resulting polymer. Despite its potential toxicity, stannous 2-ethylhexanoate is frequently used as the catalyst by Coordination-insertion mechanism, and in fact, this organometallic is used in commercially prepared biodegradable sutures. Temperatures ranging from 90 to 180^{o}C have been used with a variety of monomers such as ε-caprolactone, lactide, glycolide, trimethylene carbonate, p-dioxanone, and δ-valerolactone [18-21]. In recent communications, polymerization of these lactone can also be carried out by the activation of alcohol by a strong guanidine base, such as 1,5,7-triazabicyclo [4.4.0] dec-5-ene (TBD), 1,8-diazabicyclo[5.4.0]-undec-7-ene (DBU) and N-methyl-1,5,7-triazabicyclo[4.4.0]dec-5-ene (MTBD) , which were shown [22, 23] uniquely capable of inserting into the ester of the cyclic ester monomer, and subsequent hydrogen bonding of the adjacent nitrogen to an incoming alcohol to complete a transesterification cycle to form the polyester (Scheme 1).

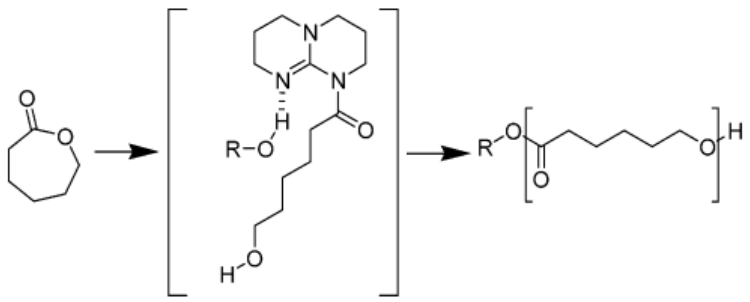

Scheme 1.1 Ring-Opening Polymerization of caprolactone through dual activation by TBD, cited from [22]

1.1.2 Bio-sourced cyclic esters and commercial available polyesters

For ROPs, variety of monomers provides for facile manipulation of polymer properties such as degradation rate and modulus when altering these monomers by sorts and amounts, listed on Table 1.

Among these monomers, the most commercially viable to date is lactide, derives from biomass such as corn or wheat, which can ring opening polymerize into polylactide (PLA). Polylactide has good mechanical and physical properties and therefore is suitable for use in disposable consumer articles as well as fiber applications, a key advantage being its hydrolysis to lactic acid, a metabolite in the carboxylic acid cycle. The applications for polylactide are enhanced by its biocompatibility and its ability to be absorbed and degraded in natural environment, It has been used for some time in biomedical applications such as sutures, dental implants, vascular grafts, bone screws and pins [24-27]. It has also been investigated as a vector for drug delivery, for example in the long-term antimicrobial drugs delivery, contraceptives and prostate cancer treatments [28]. LA has been widely used in the field of tissue engineering as a scaffold material to support cell and tissue growth. However, for many applications, PLA is not an ideal material due to its high crystal ability, brittleness, lack of total absorption and thermal instability. Further drawbacks are that it is unfunctionalized and hydrophobic; these properties impede its biodegradation and prevent targeting of the treatment.

Monomer	Structure	T_g/°C	Ref.
ε-Caprolactone	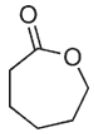	−60 to −65	18
D,L-Lactide / L-Lactide	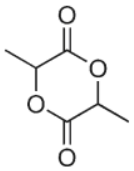	57 / 65	19
Glycolide	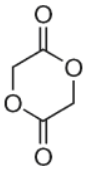	35	19
δ-Valerolactone	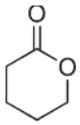	−63	20
Trimethylene carbonate	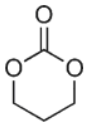	−26	21

Table 1.1 Structure of monomers commonly used in ring-opening polymerization and glass transition temperature of their homopolymers. [18-21]

Poly caprolactone (PCL) was firstly synthesized by researchers in the early 1930s [29], which can be prepared by either ring opening polymerization with a variety of mechanisms discussed above and became commercially available due to its properties that could be degraded by microorganisms [30]. PCL is also a hydrophobic, semi-crystalline polymer, its crystal ability decreases with increasing molecular weight. The good solubility, low melting point (59–64°C) and exceptional blend-compatibility has stimulated extensive research into its potential application in the biomedical fields [31] being a number of drug-delivery devices. Attention was drawn to these biopolymers owing to their numerous advantages such as tailorable degradation kinetics and mechanical properties, ease of shaping and manufacture enabling appropriate pore sizes conducive to tissue in-growth, and the controlled delivery of drugs contained within their matrix. Due to the fact that PCL degrades at a slower rate than polyglycolide (PGA), poly D, L-lactide (PDLA) and its copolymers (in drug-delivery devices that PCL or caprolactone copolymers remain active for over 1 year and in slowly degrading suture

materials.), PCL was soon overwhelmed by the popularity of other degradable polymers such as PLA and PGA, which were studied in applications which demanded the polymer matrix to release encapsulated drugs within days or weeks with a complete intracorporal degradation 2-4 months after implantation. Furthermore, PCL do not have the mechanical properties to be applied in high load bearing applications. By these disadvantages, PCL was almost forgotten for two decades. However, It should be kept in mind that PCL possesses superior rheological and viscoelastic properties over many of its degradable polymer counterparts which renders it easy to manufacture and manipulate into a large range of scaffolds [32-35]. In reality, PCL can be used in a wide range of scaffold fabrication technologies and its relatively inexpensive production routes, compared with other aliphatic polyesters, is hugely advantageous. Furthermore, the fact that a number of drug-delivery device fabricated with PCL already have FDA approval and CE Mark registration enables a faster avenue to market.

The use of poly hydroxyalkanoates (PHA) as biomaterials has been investigated for many years [36]. PHA is a group of biodegradable polyesters accumulated by many bacteria under unbalanced growth conditions [37, 38], which means its ultra biocompatible and biodegradable properties. The first constituent of PHA that identified in 1920s is [R]-3-hydroxybutyric acid (3HB) [39], Since then, for a long time it was thought that 3-HB was the only constituent of PHA, hence the term PHB (poly hydroxybutyrate) was widely used to refer to this bacterial polyester. Now, over 100 different types of PHA have been reported [40], and poly (3-hydroxybutyrate) (PHB) is still the most common short chain length PHA synthesized by various bacteria grown on different types of substrates [41, 42]. PHA has been evaluated for a variety of applications, which include environmentally friendly materials and biomedical materials such as controlled release, surgical sutures, wound dressings, lubricating powders, tissue engineering, and so on [43, 44]. Meanwhile, it is a kind of thermoplastic biomass, which makes them suitable for melt processing [45]. Even though the biomedical applications of PHA have been investigated for many years and much attention was paid [32-35], the overall results seemed not satisfied for the practical applications. The main reason is that PHB has several inherent deficiencies that limit its medical applications, including its brittleness due to its high crystal ability and narrow thermo-processing window because of its thermal instability [46, 47]. High costs compared to petroleum-based commodity plastics, its relatively low impact resistance [48] and low interfacial adhesion between PHA and other polymer phases

[49] (which cause poor mechanical performances due to miscibility) are believed to be another factors that hinder its applications. To improve these properties, different strategies were used. its blending with reactive compatibilizer EVOH by reactive extrusion was conducted and the mechanism was studied [50], meanwhile, strategies of the block copolymers based on PHA syntheses and its introduction in polyurethane as hydrophobic segment are intensively investigated [51-54], which makes PHA again the promising materials in all fields.

1.2 Structure design and properties of polymers based on degradable polyesters

1.2.1 Syntheses strategies for functionalized polyesters

As discussed above, the common disadvantages of these commercial degradable polyesters are the lack of reactive center on their backbones, highly crystal ability and weak mechanic properties of their homo or copolymers. So it is important to develop syntheses strategies of functionalized aliphatic polyesters or in particular develop routes to functionalize them with biologically relevant and compatible molecules, based on which the application of these polyester can be broaden and furthermore replace the petroleum based polymers. To achieve this goal, two syntheses ways can be adapted: 1) functionalization of cyclic esters and their homo / co polymerization with other monomers; or 2) modification of the polyester to endow functions on them. By doing so further syntheses of complicated polymers will be available based on functions on these polyesters, and structures of polymer can be designed due to multi functions on the polyesters.

1.2.1.1 Fuctionalization and copolymerization of cyclic esters

Fuctionalization of different cyclic esters with different functions was investigated by researchers. Among them, the functionaliztion of CL with different functions were intensively reported, Mecerreyes [55] reported the synthesis and copolymerization of 4-(acryloyloxy)-ε-caprolactone (in Scheme 1.2). This new monomer can be polymerized in a living / controlled way by two different polymerization mechanisms, atom transfer radical polymerization (ATRP)

and ROP. As a potential application of ROP product, introduction of acrylate pendant groups into the polyesters facilitated the preparation of cross-linked biodegradable materials either thermally or by irradiation with ultraviolet light radical curing. With same mechanisms, caprolactone with other functions such as epoxy were synthesized and its copolymerization with CL are confirmed [56]. Including pendant double bonds of polymer, back bone unsaturated polyester based on PCL were also synthesized. Lou et al polymerized 6,7-dihydro-2(5H)-oxepinone using Schrock's molybdenum catalyst [57]. The unsaturated group is potentially useful for crosslinking or epoxidation reactions. Halide, hydroxyl and carbonyl functionalized PCL were also reported separately [58-60]. Similar study was carried by Chen [61]. In his research, acryloyl cyclic carbonate monomers are prepared with good overall yields (40%). ROP of these multi functional monomers with lactones can yield degradable networks by cooperating with ε-caprolactone and lactide, shown in scheme 1.2.

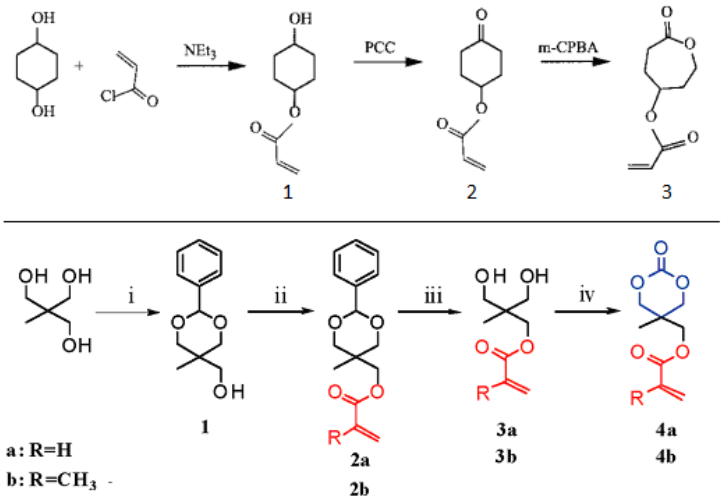

Scheme 1.2 Syntheses of pendant double bond functionalized cyclic esters polymerizable with lactones, cited from [55]

1.2.1.2 Copolymerization of cyclic esters and other monomers

Copolymerization of cyclic esters with designed monomers, for example, amino acid derivates, is another way to obtain functionalized polyesters. Tatsuro claimed the synthesis of copolymer with pendant thiol groups also using cysteine as reagent [62]. Cysteine was firstly protected for its mercapto group using methoxybenzyl groups and then made into cyclodepsipeptide, which can homopolymerize or copolymerize with lactide and give polyesters with pendant mercapto after deprotection (Scheme 1.3). The complicated multi-step synthesis and the low yield limit its applications.

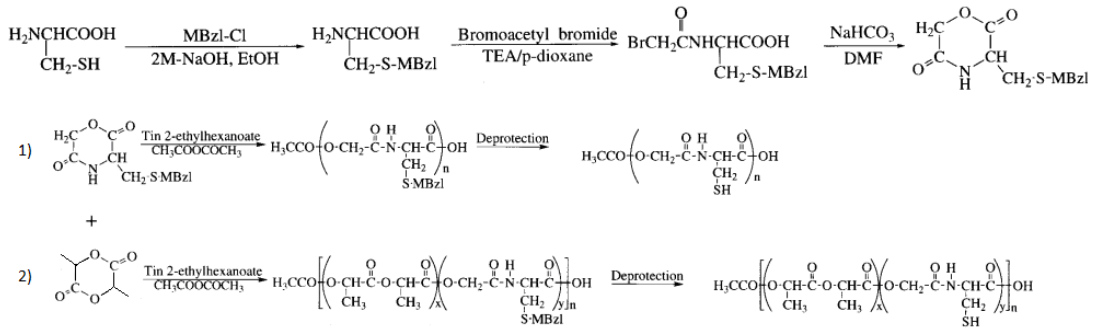

Scheme 1.3 Syntheses of pendant mercapto functionalized cyclic esters polymerizable with lactide, cited from [62]

Sun developed another way to synthesis the PLA-b-PCys copolymers [63]. The PLA block with amino end group was firstly synthesized by ROP using 2-benzyloxycarbonyl amino ethanol as the initiator, and then this block was used as a macroinitiator to introduce cysteine blocks using the N-carboxyanhydride of β-benzyloxycarbonyl-L-cysteine as monomer, Block polymer with pendant -SH groups can also be obtained by deprotection of benzyl groups, shown in Scheme 1.4

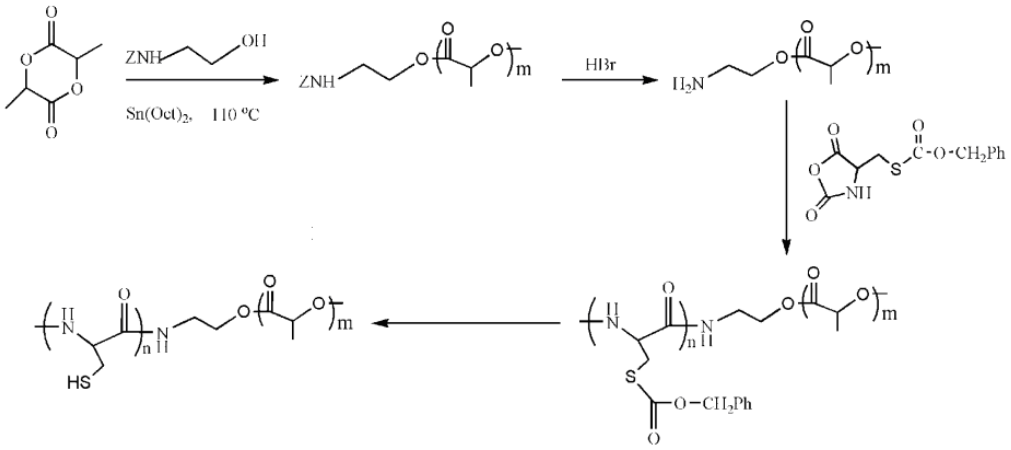

Scheme 1.4 Syntheses of pendant mercapto functionalized cyclic esters than can copolymerize with lactide, cited from [62]

Copolymerization between cyclic esters and epoxies was rarely reported, but it is confirmed to be an available way to prepare polymer with epoxy repeat units. Copolymerization of ε-caprolactone with ethylene oxide (EO) in cationic mechanism was claimed by Bednarek [64] with diol / BF3 etherate as initiator / catalyst pair, and the products were verified by Nuclear magnetic resonance (NMR) and matrix-assisted laser desorption/ionization time-of-flight (MALDI-TOF) mass spectrometry MALDI-TOF to prove the copolymerization. The ROP of bis

(γ-lactone), 2,8-dioxa-1-methylbicyclo[3.3.0]octane-3,7-dione, and glycidyl phenyl ether (GPE) / glycidy1 methacrylate (GMA) were performed with anionic mechanism [65, 66] and the structures were proved also by MALDI-TOF analysis (in Scheme 1.5)

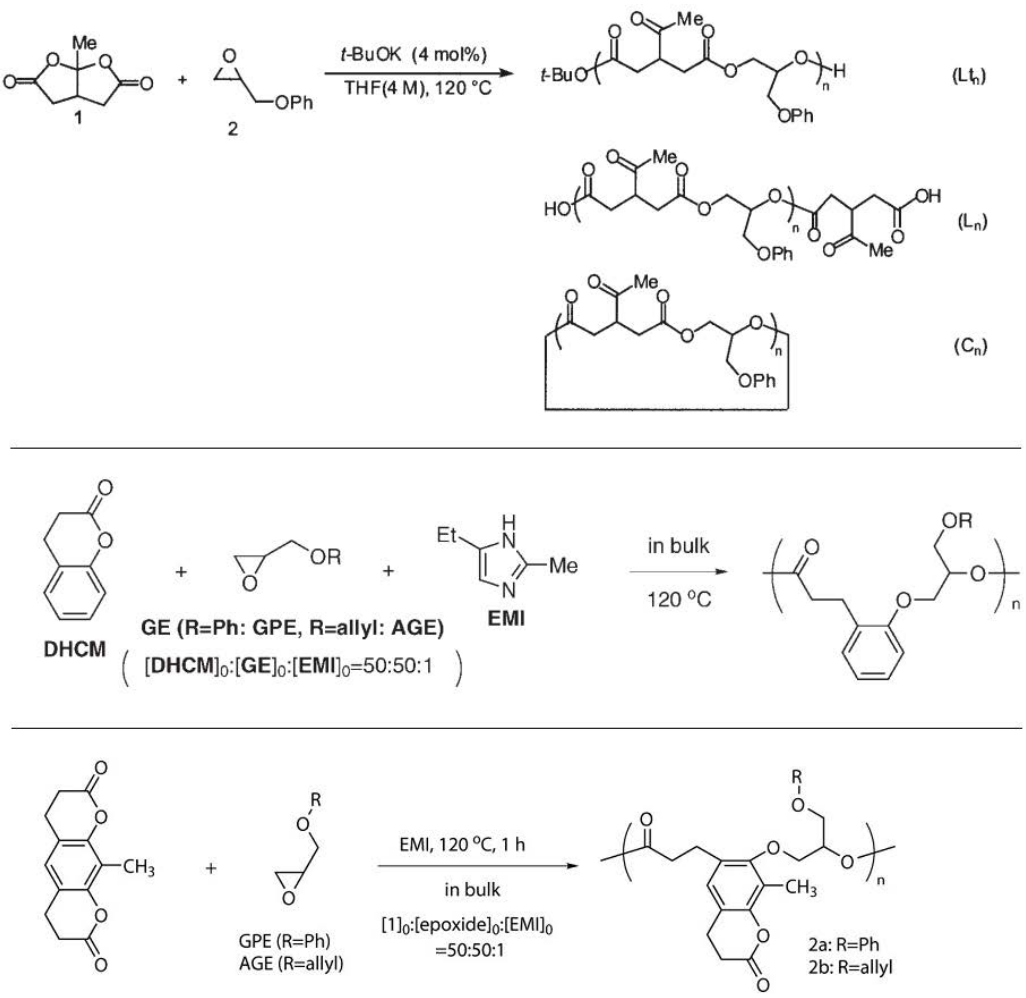

Scheme 1.4 Copolymerzations between bis-lactone and epoxides, cited from [62]

Recently, this group proved again the copolymerization between cyclic ester and epoxide by copolymerize 10-Methyl-2H,8H-benzo-[1,2-b:5,4-b']bipyran-2,8-dione or 3,4-dihydrocoumarin with GPE [67, 68], shown in Scheme 1.4, these reports are good proof of the copolymerization between the epoxides and cyclic esters. Adaptation of this mechanism to natural sourced cyclic esters will board the way of functionalization of degradable polyesters.

The copolymerization of bio-sourced cyclic esters and functionlized lactone or lactame, and the post modification of the product is another way to obtain polyester with targeted functions. John [69] prepared linear poly (ε-caprolactone-co-glycolic acid-co-serine) by ring-

opening polymerization of a protected glycolic acid and acrylated the serine hydroxyl groups following their deprotection (Scheme 1.5) . This is also a good way to obtain specially functionalized polyesters.

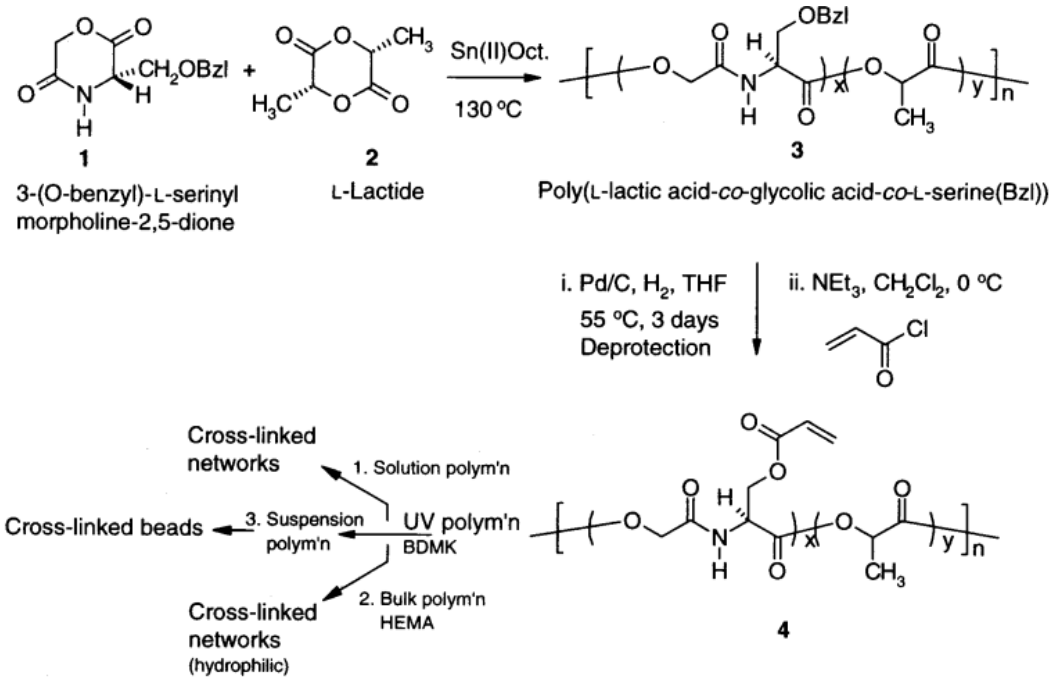

Scheme 1.5 Copolymerzations and post-modification to obtain targeted functionalized polyesters, cited from [62]

1.2.1.3 End group fuctionalization of polyesters

ROP controls the polymer's starting moiety according to the type of initiator used; therefore, by plenty choices of initiator containing alcohol or amine groups it is possible to install functionality to the chain ends as ester or amide groups. Furthermore, star-shaped polyester can be obtained when using polyol (for example glycerol) as initiator, which bear multi polyester arms and reactive end groups (usually hydroxyl groups) that makes the further syntheses of more complicated polymers available [70]. This strategy will be later discussed in chapter 1.2. The majority of ROP studies focus on the use of mono alcohols such as benzyl alcohol or ethanol, however, researchers addressed the application of functionalized initiators. Kricheldorf and Kreiser-Saunders reported interesting synthesis, which was applied by Stupp, using vitamins, hormones and drugs to initiate lactide polymerization [71, 72]. Another paper [64] describes an alternative method to functionalize the chain ends, which involves coupling the secondary alcohol terminus of the PLA with carboxylic acids using diimide. The coupling methods were useful due to the mild conditions and good yield, which enabled attachment

of bioactive substituents such as drugs or fluorescent tags that might not have been compatible with metal initiators. Using functional end groups to initiate ROP is a well established and large research area, so this section is restricted to the incorporation of carbohydrates at the end of aliphatic polyester chains. This is relevant as they are biocompatible, renewable resources with large numbers of functional groups and also provides an interesting contrast to the methods applied for incorporating carbohydrates into condensation polymerizations.

1.2.1.4 Surface modification of polyester to endow functions

As discussed above, the polyester chains composed by unfunctionalized cyclic esters are lack of reactive centers, which hinder the further modification of their backbone to improve their chemical and physical properties. Take PCL for example, their rather low wettability and surface energy adversely give rise to inefficient cell attachment and cell growth. Hence modification and surface treatment are necessary for the broadening of these polyesters' application. However, wet-chemical treatments do not only induce irregular polymeric surface etching, but also leave harmful chemical residues on the polyester scaffolds, so physical treatment including plasma treatment [73-75], UV-initiation [76], and high energy irradiation [77] are preferred by researches. Among these technology, Plasma treatment is a versatile and effective method for modifying the surface properties or introducing desired chemical groups at the surface of a material without affecting its bulk properties [78]. Ohrlander et al. [78] reported the graft of acrylic amine onto PCL chains. In their study, electron beam irradiation at a dose of 5 Mrad was used to generate initiating species in the polyester. Kosorn et al. [79] discovered that the low pressure oxygen plasma treatment of polycaprolactone (PCL) and alkaline hydrolyzed polycaprolactone (HPCL) scaffolds resulted in the surface roughness, increased surface hydrophilicity, and generation of oxygen-containing functional groups at the surfaces of the scaffolds. Jacobs [73] examined the chemical changes on the plasma-treated surfaces using contact angle measurements and XPS analysis. Results show that discharge gas can have a significant influence on the chemical composition of the PCL surfaces: air and argon plasmas introduce oxygen containing groups, while helium plasmas incorporate both oxygen and nitrogen-containing functionalities. To sum up, the plasma treatment is a convenient and fast procedure to functionalize the polyester with activated reactive centre on the chain, but the requirement of equipment limits its wide use for applications.

1.2.2 Structure design for star-shaped polymers and networks, and structure dependent properties

1.2.2.1 Syntheses of polymer network and star-shaped polymers

To establish more complicated structured polymers based on degradable polyesters, many strategies have been examined. These strategies can be generally classified into one of 3 categories: 1) monomer copolymerization with multifunctional monomers including click reactions; 2) polymerization of a prepolymer with a multi functional monomer; or 3) polymerization of a prepolymer followed by an additional cross-linking reaction. And mechanisms of these methods include ring-opening polymerization, polycondensation, polyaddition, and various radical polymerization mechanisms.

For category 1), Polyester networks prepared via polycondensation of multifunctional carboxylic acids and polyols are typically carried out at high temperatures under vacuum to remove the water by-product formed. Polycondensation curing can be done with a wide variety of monomers, thus allowing ready manipulation of the properties of the polyester. Another advantage is that catalysts are not required. However, long reaction times, high temperatures, and the need for precise stoichiometry and low vacuum conditions in some situations are disadvantages. Moreover, it is difficult to achieve high degrees of polymerization and controlled chain lengths because of potential sidereactions and monomer volatilization, which results in a change in monomer stoichiometry during reactions [4, 10].

For categories 2) and 3), prepolymers are needed to construct the more complicated polymers. Polymer architecture is an important design criterion. In general, star or linear polyesters synthesized by methods in chapter 1.2.1 have been used as prepolymers, and both lead to effective networks. But there are distinct advantages for using a star-shaped architecture: the mechanical properties of the final network can be easily altered based on the number and molecular weight of arms in the star prepolymer, which directly controls the cross-link density. Furthermore, mechanical properties of the network prepared by star shaped polymer have better performance to those linear prepolymer crosslinked networks, proved by the elastomers prepared from (3-isocyanatopropyl) triethoxy-silane-terminated star-poly(lactide) versus its linear counterpart, from Helminen's research [80]. This result was attributed to the

higher cross-link density from star prepolymer architecture. Additionally, star-shaped polymers with low molecular weights have a lower melt viscosity than the same molecular weight linear polymer [81], which may benefit the fabrication of different devices.

To obtain only ester bond contained networks (completely composed by cyclic esters), monomers with 2 or more cyclic functions are always adapted. Pitt and co-workers [82] copolymerized ε-caprolactone and δ-valerolactone with 2,2-bis(e-caprolactone-4-yl)propane (BCP). The resulting elastomers had alterable Young's moduli ranging from 0.38 to 4.69MPa and sol contents of only approximately 4%. In a similar approach Palmgren [83] prepared elastomer networks by copolymerizing 1,5-dioxepan-2-one with either BCP or bis(e-caprolactone-4-yl) with higher sol contents ranged from 5 to 20%, shown in Scheme 1.6

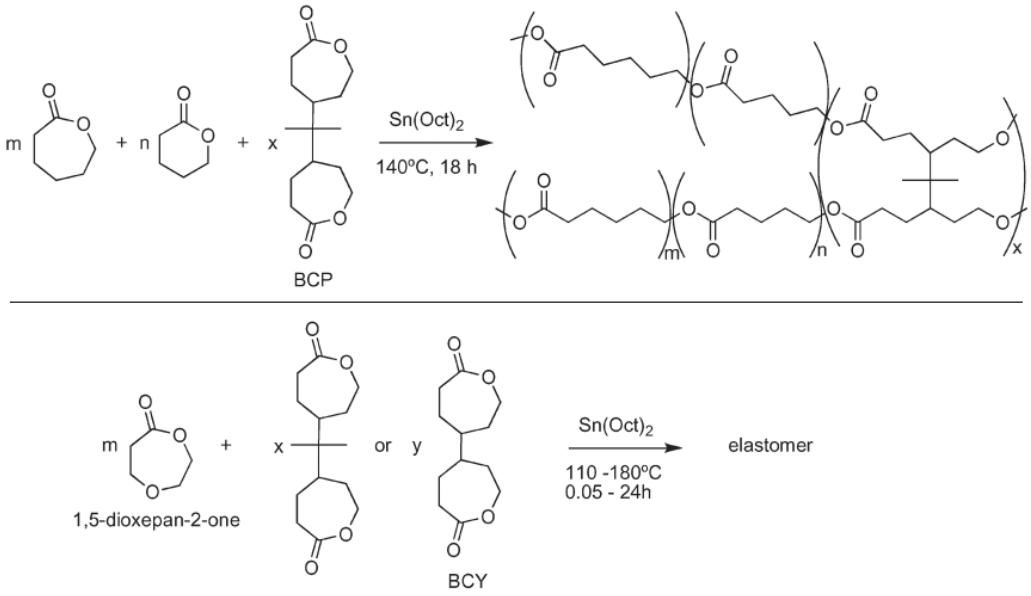

Scheme 1.6 Copolymerization of multi functional lactones and CL to obtain elastomers, cited from [62]

The only ester bond contained star shaped polyesters can be obtained using polydiol as initiator with variety of examples discussed in chapter 1.2.1, as mentioned above, Ring-opening polymerization results in a hydroxyl group at the chain ends and thus a living polymer is formed, by this mechanism further modification or polymerization is available by reacting these hydroxyl groups, among which, the most frequency studied subject is the crosslinking of polyol prepolymers with polyisocyanates. Pitt reacted 3-arm-star-poly(ε-caprolactone-co-δ-valerolactone) with hexane 1,6-diisocyanate at 100°C for 90 minutes [84]. These elastomers had Young's moduli ranging from 0.07–3.83MPa, ultimate stresses of 0.59–2.45MPa, and

ultimate strains that can reach to 1940%. Bruin reacted 6-arm-star-poly(e-caprolactone-co-glycolide) with ethyl-2,6-diisocyanatohexanoate at room temperature for 24 hours, followed by post-curing at 100–110°C for 3 hours [85], ultimate stresses of the products ranged from 8 to 40MPa, and their ultimate strains were 300–500%. The good strength performance of these elastomers was likely due to the higher cross-link density afforded by using star-shaped polyester with a greater number of arms.

The most popular method of preparing polyester based polymers in the literature has been through radical curing of prepolymers, belonged to category 2). In this strategy, unsaturated groups are incorporated in the prepolymer, either along the backbone, at the chain end, or as pendant groups. Cross-linking can then be accomplished via either thermal or photo initiation. Prepolymer poly(hydromuconic acid-co-diethylene glycol-co-adipic acid) containing unsaturated moiety along main chain have been reported by Olson et al [86]. This prepolymer was thermally initiated with either benzoyl peroxide or 2, 2'-azobis(2-methylpropionitrile) (AIBN) with reaction times reaching 24 hours, reactive diluents N-vinylpyrrolidone were required to increase the cross-linking efficiency. The mechanical properties of the product were markedly influenced by the presence of the N-vinylpyrrolidone (NVP), while at the same time only relatively small changes in the ultimate stress and strain were noted. For prepolymer containing pendant double bonds, John [69] employed UV-initiated polymerization along with the cross-linker ethylene glycol dimethacrylate. The acrylated PLA(Glc-Ser) cross-linked polymer networks obtained were glassy and transparent and showed relatively low swelling in water due to their cross-linked nature, but were easily swelling in chloroform and in dimethyl sulfoxide. The acrylate polymers on copolymerization with 2-hydroxyethyl methacrylate (HEMA) resulted in cross-linked networks [PLA (Glc-Ser)/HEMA], which were swelling in water and in DMSO showing the potential of the polymer in hydrogel applications.

There are more examples of prepolymers containing unsaturated functions at the end chain. This strategy is popular because end chain double bonds are more reactive than those on the backbone, and more efficient network formation can be achieved without adding reactive diluents. A common strategy is to prepare linear or star-shaped polymers via ring-opening polymerization, followed by functionalization of the end hydroxyl groups with an acrylate (e.g. acryloyl chloride) or anhydrides (e.g. methacrylic anhydride)

The anhydride approach has been reported to produce molecular weight broadening due to chain scission [87] while the chloride approach requires anhydrous conditions and careful temperature control to avoid side reactions between the basic proton scavenger (typically triethylamine) and the acid chloride [88]. However, both approaches can produce high degrees of end functionalization. Storey et al. prepared 3-arm-star-poly (ε-caprolactone) methacrylate and 3-arm-star-poly(D,L-lactide) methacrylate and cured them thermally using 2-butanone peroxide at 60 uC for 60 hours. 60 The cured networks had sol contents of less than 10% in every case, without the need for reactive diluents. They had high Young's moduli but not elastic, possessing strains only 7–10% at break. Helminen [80] prepared 4 arm-star (ε-caprolactone-co-D,L-lactide) methacrylated prepolymers with different molecular weight and monomer compositions, and thermally cured these prepolymers to form elastic networks. These examples demonstrated that the mechanical properties of the networks could be readily manipulated by adjusting both the molecular weight and the composition of the prepolymer. At given monomer composition, the moduli and stress at break decreased as the molecular weight increased, while the strain at break increased.

Specially in polymer network established by radical polymerization, there is another way to crosslink the prepolymer and polymer chains from reactive dilute, that is, by thiol-ene clicks. Known for over 100 years[89], the thiol-ene reaction is simply the hydrothiolation of a C=C bond. In the polymer / materials fields the reaction has been most widely employed as a means of preparing near-perfect networks and films [90, 91]. There are several features associated with the thiol-ene reaction that make it a particularly attractive, facile and versatile process [92]: Firstly, such hydrothiolation reactions can process under a variety of conditions including by a radical pathway, via catalytic process mediated by nucleophiles, acids, bases, in the apparent absence of an added catalyst in highly polar solvents such as water or DMF or via supramolecular catalysts. Secondly, a wide range of enes serve as suitable substrates, including activated and non-activated species as well as multiply-substituted olefinic bonds. However, reactivity can vary considerably depending on reaction mechanism and substitution pattern at the C=C bond. Thirdly, virtually any thiol can be employed, including highly functional species, although reactivity can cover several orders of magnitude depending on the S–H bond strength and the cleavage mechanism. Finally, such reactions are generally

extremely rapid and can be complete in a matter of seconds (even at ambient temperature and pressure), are tolerant to the presence of air/oxygen and moisture (provided the concentration of oxygen does not approach that of the thiol), and proceed with (near) quantitative formation of the corresponding thioether in a regioselective fashion. The mechanism of thiol-ene click is illustrated in Scheme 1.6, generally, the thiol-ene reaction has been conducted under radical conditions, often photo-chemically induced [93]. Under such conditions it proceeds via a typical chain process with initiation, propagation and termination steps.

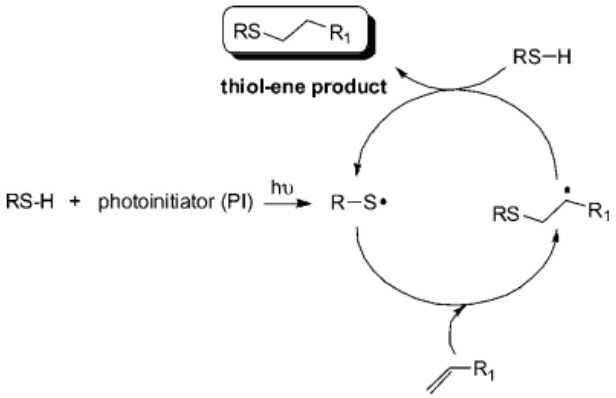

Scheme 1.6 Photo initiated thiol-ene reaction, cited from [62]

It should be notice that this facile technology with huge advantages can be adapted in establishing degradable networks by cooperating double bond functionalized prepolymer and multi thiols, or mercapto functionalized prepolymer and multi double bond containing monomers. UV crosslinkable, water-based polyurethane polymers bearing pendant unsaturation was synthesized by Otts [94], he used this prepolymer with polyfunctional thiol crosslinkers to prepare uniform aqueous colloidal dispersions capable of forming crosslinked films upon UV exposure at 254 nm. Lin [95] began the research for utilization of the thiol–acrylate Michael addition reaction to form hydrogel biomaterials for controlled drug-delivery application. These hydrogels were formed in aqueous environment from PEG-containing multi-acrylates or vinyl sulfones and a variety of thiols, and particularly those from cysteine units in peptide sequences. Niu [96] utilized a similar approach to react PEG-poly(propyleneoxide)-PEG triblock copolymers that were end-functionalized with acrylates and thiols to form a thermo sensitive hydrogel material. The experimental results indicated the potential applications of reactive thermal-sensitive hydrogel in drug delivery, tissue engineering, and cell encapsulation. From these studies it can be concluded that with thiol-ene click technology is a feasible way to construct polyester based network or structured

polymers.

From the strategies discussed above, it can be seen that photo induced radical polymerization were widely used in building structured polymers with double bond functionalized prepolymers. Photo initiated cross-linking has many advantages over thermal initiation for biomedical applications, including more rapid reaction, effective cross-linking at low temperatures thus reducing possible denaturation of biological compounds, application in minimally invasive surgery by injection followed by cross-linking, and facile microfabrication and coating onto other devices and materials. Free-radical polymerization requires the use of photo initiators that dissociate into radicals upon the absorption of light energy. While cross-linking is rapid and effective, these photo initiators may be a source of toxicity. Photo dimerization does not require a photo initiator, however, longer cross-linking times are required.

1.2.2.2 The structure dependent polymer properties

Rheology properties by dynamic mechanical analysis (DMA)

Rheological properties of polymers are often analyzed as a means of examining differences in polymer structure. Molecular weight, molecular weight distribution, and long-chain branching are the primary factors affecting polymer viscoelasticity, and all of them can be studied through rheological measurements. Rheological properties can also be used to predict the behavior of a polymer during processing in conventional equipment [97]. Indeed, rheological characterization is gaining in importance in the development phase of biodegradable polymers, because of the close relationship between rheology and processing. PCL, PLA and PHA have all been investigated [98-100]. Furthermore, for materials with more complicated structures and compositions, for example, the polymer blends, the hybrid polymers, the inter penetrating network (IPN), the DMA or dynamic mechanical thermal analysis (DMTA) is useful to verify the immiscibility and the interactions of the polymer phases. The storage / loss modulus and their ratio, loss factor, indicate the relaxation of different polymer segments, glass transition behaviors in temperature zones and the rubber plateau of the storage shear modulus described crosslink density of the obtained polymers. Remis [101] and Valette [102] synthesized polyurethane-unsaturated polyester interpenetrating polymer network or hybrid polymers, and analyzed their properties by DMTA. According to the DMTA results, they

explained the relationship between the elastic modulus and crosslink density in function of the proportion used, the relaxation associated glass transition due to semi-immiscible behavior and intermediate formulations and furthermore phase inversion in the range of intermediate compositions. Ljungberg [103] blended PLA with 5 plasticizers in a batch wise mixer and pressed into films. The films were analyzed by means of dynamic mechanical analysis and differential scanning calorimetry to investigate the properties of the blends, the immiscibility of the two compounds and phase separations were investigated. Tang [104] investigate the influence of filler $BaTiO_3$ on polyurethane / unsaturated polyester resin interpenetrating polymer networks, he claimed that types of filler and filling amount both have great influence on maximum tanδ and E" values of IPNs. Fiber-like filler can improve areas of E" and shift effective damping temperatures to higher temperatures dramatically, mainly because of strong frictional action between two apparent different modulus materials. In Trakulsujaritchok [105] and Babkina's work [106], the strengthened damping properties of the interpenetrating polymer networks were illustrated by their DMA curves. The striking features of the tanδ curves of in IPN DMA graphs were an increase in intermediate plateau between the two composition transitions and a reduction in tanδ peaks, which broaden the working area of damping for the materials. By the examples listed above, it can be clearly seen that the DMA is a very useful tool in evaluating the thermal properties of polyester based polymers.

Degradation properties depend on syntheses strategies

Regardless of the syntheses strategies adapted, the final goal of achieving biodegradability is the preparation of polymer backbone containing hydrolyzable bonds. With consideration to manipulating hydrolysis, there are a number of ways accomplished. The degradation rate can be controlled by the nature of the bond and the rate of water penetration into the materials. It is well known that incorporating more hydrophobic monomers, such as CL, as opposed to more hydrophilic monomers, such as glycolide or ethylene glycol, inhibits water penetration into polyesters, resulting in a decreased degradation rate [107]. The diffusion of water into the bulk is also ruled by the glass transition temperature of the polymer, the lower the glass transition temperature, the greater the diffusion rate of water into the bulk. However, most monomers used to lower T_g also decrease the water concentration in the polymer. For example, PCL has a glass transition temperature of -60^oC is often incorporated ring opening

copolymerizations approaches to control the glass transition temperature, but, as it is hydrophobic, the result is that the degradation rate of the polymer decreases. Furthermore, increasing the crosslink density of the polymer for increasing modulus and strength also results in an increase in the degradation time, demonstrated by Pitt and co-workers [82]. Highly cross-linked elastomers of star-poly (ε-caprolactone-co-D,L-lactide) triacrylate were found to degrade in a manner consistent with a surface erosion mechanism, that is an almost constant mass loss with time, whereas less cross-linked polymers degraded in a bulk degradation fashion [81]. This difference in degradation mechanism was attributed to the slower rate of water. So when designing the structure of the polyester based polymer, these points are important factors for their degradation abilities.

1.3 Achievements for the Ph.D study

The work of my Ph.D study can be divided into 3 parts, the first one includes (co)polymerization and functionalization of the polyesters by different syntheses strategies. Telechelic hydroxyl groups, mercapto and double bond are the main functions I should endow onto polyesters including PCL, PLA and PHA. Syntheses optimization and characterizations for these polyesters were investigated throughout the process. After obtaining the targeted polyesters, the polyesters were synthesized into poly ester urethanes by structure design with different parameters in the second step, Characterizations were also carried out to confirm the structures. Then, these double bond or mercapto containing polyesters / poly ester urethanes are cooperated with biocompatible (meth)acrylic monomers to form networks or star-shaped polymer, applications of these structured polymers such as damping materials or hydrogel will be studied for the final step.

References:

1. Amass W, Amass A, and Tighe B. Polymer International 1998;47(2):89-144.
2. Gross RA and Kalra B. Science 2002;297(5582):803-807.
3. Ikada Y and Tsuji H. Macromolecular Rapid Communications 2000;21(3):117-132.
4. Okada M. Progress in Polymer Science 2002;27(1):87-133.
5. Rezwan K, Chen QZ, Blaker JJ, and Boccaccini AR. Biomaterials 2006;27(18):3413-3431.
6. Azechi M, Matsumoto K, and Endo T. Journal of Polymer Science Part A: Polymer Chemistry 2013.
7. Gädda TM, Nelson AK, and Weber WP. Journal of Polymer Science Part A: Polymer Chemistry 2004;42(20):5235-5243.
8. Kim J-B and Cho I. Tetrahedron 1997;53(45):15157-15166.
9. Kurcok P, Kowalczuk M, Hennek K, and Jedlinski Z. Macromolecules 1992;25(7):2017-2020.

10. Albertsson A-C and Varma IK. Aliphatic polyesters: synthesis, properties and applications. Degradable Aliphatic Polyesters: Springer, 2002. pp. 1-40.
11. Crivello J, Falk B, and Zonca M. Journal of Polymer Science Part A: Polymer Chemistry 2004;42(7):1630-1646.
12. Liu Y and Pittman CU. Journal of Polymer Science Part A: Polymer Chemistry 1997;35(17):3655-3671.
13. Ariga T, Takata T, and Endo T. Macromolecules 1997;30(4):737-744.
14. Ling J, Shen J, and Hogen-Esch TE. Polymer 2009;50(15):3575-3581.
15. Mecerreyes D, Jérôme R, and Dubois P. Novel macromolecular architectures based on aliphatic polyesters: relevance of the "coordination-insertion" ring-opening polymerization. Macromolecular Architectures: Springer, 1999. pp. 1-59.
16. Wheaton CA and Hayes PG. Comments on Inorganic Chemistry 2011;32(3):127-162.
17. Stevels WM, Ankoné MJ, Dijkstra PJ, and Feijen J. Macromolecules 1996;29(26):8296-8303.
18. Hofman A, Slomkowski S, and Penczek S. Die Makromolekulare Chemie, Rapid Communications 1987;8(8):387-391.
19. Löfgren A, Albertsson A-C, Dubois P, Jérôme R, and Teyssié P. Macromolecules 1994;27(20):5556-5562.
20. Dubois P, Jérŏme R, and Teyssie P. Aluminium alkoxides: A family of versatile initiators for the ring-opening polymerization of lactones and lactides. Makromolekulare Chemie. Macromolecular Symposia, vol. 42: Wiley Online Library, 1991. pp. 103-116.
21. Dubois P, Ropson N, Jérôme R, and Teyssié P. Macromolecules 1996;29(6):1965-1975.
22. Lohmeijer BG, Pratt RC, Leibfarth F, Logan JW, Long DA, Dove AP, Nederberg F, Choi J, Wade C, and Waymouth RM. Macromolecules 2006;39(25):8574-8583.
23. Simón L and Goodman JM. The Journal of Organic Chemistry 2007;72(25):9656-9662.
24. Mäkelä P, Pohjonen T, Törmälä P, Waris T, and Ashammakhi N. Biomaterials 2002;23(12):2587-2592.
25. Morris HF, Ochi S, and Winkler S. Annals of Periodontology 2000;5(1):157-165.
26. Jukkala-Partio K, Pohjonen T, Laitinen O, Partio E, Vasenius J, Toivonen T, Kinnunen J, Törmälä P, and Rokkanen P. Biodegradation and strength retention of poly-L-lactide screws in vivo. An experimental long-term study in sheep. Annales chirurgiae et gynaecologiae, vol. 90, 2001. pp. 219.
27. Inoguchi H, Kwon IK, Inoue E, Takamizawa K, Maehara Y, and Matsuda T. Biomaterials 2006;27(8):1470-1478.
28. Albertsson A-C and Varma IK. Biomacromolecules 2003;4(6):1466-1486.
29. Natta FJv, Hill JW, and Carothers WH. Journal of the American Chemical Society 1934;56(2):455-457.
30. Baldan A. Journal of materials science 2004;39(1):1-49.
31. Chandra R and Rustgi R. Progress in Polymer Science 1998;23(7):1273-1336.
32. Luciani A, Coccoli V, Orsi S, Ambrosio L, and Netti PA. Biomaterials 2008;29(36):4800-4807.
33. Marrazzo C, Di Maio E, and Iannace S. Polymer Engineering & Science 2008;48(2):336-344.
34. Huang H, Oizumi S, Kojima N, Niino T, and Sakai Y. Biomaterials 2007;28(26):3815-3823.
35. Lee K, Kim H, Khil M, Ra Y, and Lee D. Polymer 2003;44(4):1287-1294.
36. Chen G-Q and Wu Q. Biomaterials 2005;26(33):6565-6578.
37. Greco P and Martuscelli E. Polymer 1989;30(8):1475-1483.
38. Chen G-Q and Page WJ. Biotechnology Techniques 1997;11(5):347-350.
39. Diard S, Carlier J-P, Ageron E, Grimont PA, Langlois V, Guérin P, and Bouvet OM. Systematic and applied microbiology 2002;25(2):183-188.
40. Chen G, Wu Q, Xi J, Yu HP, and Chan A. Progress In Natural Science 2000;10(11):843-850.
41. Kato M, Bao H, Kang C-K, Fukui T, and Doi Y. Applied microbiology and biotechnology 1996;45(3):363-370.

42. Sudesh K. Polymers for Advanced Technologies 2000;11(8-12):865-872.
43. Zinn M, Witholt B, and Egli T. Advanced Drug Delivery Reviews 2001;53(1):5-21.
44. Williams SF, Martin DP, Horowitz DM, and Peoples OP. International journal of biological macromolecules 1999;25(1):111-121.
45. Liu W, Yang H, Wang Z, Dong L, and Liu J. Journal of Applied Polymer Science 2002;86(9):2145-2152.
46. Khanna S and Srivastava AK. Process Biochemistry 2005;40(2):607-619.
47. Häberlein H, Seliger H, Kohler R, and Sulzberger P. Polímeros 2005;15(2):122-126.
48. Avella M, Errico ME, Rimedio R, and Sadocco P. Journal of Applied Polymer Science 2002;83(7):1432-1442.
49. Ha C-S and Cho W-J. Progress in Polymer Science 2002;27(4):759-809.
50. Sadik T, Massardier V, Becquart F, and Taha M. Polymer 2012.
51. Lynn DM and Langer R. Journal of the American Chemical Society 2000;122(44):10761-10768.
52. Chen Z, Cheng S, and Xu K. Biomaterials 2009;30(12):2219-2230.
53. Loh XJ, Tan YX, Li Z, Teo LS, Goh SH, and Li J. Biomaterials 2008;29(14):2164-2172.
54. Li X, Loh XJ, Wang K, He C, and Li J. Biomacromolecules 2005;6(5):2740-2747.
55. Mecerreyes D, Humes J, Miller R, Hedrick JL, Detrembleur C, Lecomte P, Jérôme R, and San Roman J. Macromolecular Rapid Communications 2000;21(11):779-784.
56. Mecerreyes D, Miller RD, Hedrick JL, Detrembleur C, and Jérôme R. Journal of Polymer Science Part A: Polymer Chemistry 2000;38(5):870-875.
57. Lou X, Detrembleur C, Lecomte P, and Jérôme R. Macromolecules 2001;34(17):5806-5811.
58. Riva R, Schmeits S, Stoffelbach F, Jérôme C, Jérôme R, and Lecomte P. Chemical communications 2005(42):5334-5336.
59. Liu MJ, Vladimirov N, and Frechet JMJ. Macromolecules 1999;32(20):6881-6884.
60. Latere Dwan'Isa J-P, Lecomte P, Dubois P, and Jérôme R. 2003.
61. Chen W, Yang H, Wang R, Cheng R, Meng F, Wei W, and Zhong Z. Macromolecules 2009;43(1):201-207.
62. Ouchi T, Seike H, Nozaki T, and Ohya Y. Journal of Polymer Science Part A: Polymer Chemistry 1998;36(8):1283-1290.
63. Sun J, Chen X, Lu T, Liu S, Tian H, Guo Z, and Jing X. Langmuir 2008;24(18):10099-10106.
64. Bednarek M and Kubisa P. Journal of Polymer Science Part A: Polymer Chemistry 2005;43(17):3788-3796.
65. Zhang C, Ochiai B, and Endo T. Journal of Polymer Science Part A: Polymer Chemistry 2005;43(12):2643-2649.
66. Chung K, Takata T, and Endo T. Macromolecules 1995;28(11):4044-4046.
67. Uenishi K, Sudo A, and Endo T. Journal of Polymer Science Part A: Polymer Chemistry 2009;47(14):3662-3668.
68. Uenishi K, Sudo A, and Endo T. Macromolecules 2007;40(18):6535-6539.
69. John G and Morita M. Macromolecules 1999;32(6):1853-1858.
70. Xue L, Dai S, and Li Z. Macromolecules 2009;42(4):964-972.
71. Klok H-A, Hwang JJ, Iyer SN, and Stupp SI. Macromolecules 2002;35(3):746-759.
72. Kricheldorf HR and Kreiser-Saunders I. Polymer 1994;35(19):4175-4180.
73. Jacobs T, De Geyter N, Morent R, Desmet T, Dubruel P, and Leys C. Surface and Coatings Technology 2011;205:S543-S547.
74. Martins A, Pinho ED, Faria S, Pashkuleva I, Marques AP, Reis RL, and Neves NM. Small 2009;5(10):1195-1206.
75. Ohrlander M, Palmgren R, Wirsen A, and Albertsson AC. Journal of Polymer Science Part A: Polymer

Chemistry 1999;37(11):1659-1663.
76. Allméar K, Hult A, and Rårnby B. Journal of Polymer Science Part A: Polymer Chemistry 1988;26(8):2099-2111.
77. Kaji K, Abe Y, Murai M, Nishioka N, and Kosai K. Journal of Applied Polymer Science 1993;47(8):1427-1438.
78. Loh Ih, Chu C, Blumenthal N, Alexander H, and Turner D. Journal of biomedical materials research 1994;28(3):289-301.
79. Janvikul W, Uppanan P, Thavornyutikarn B, Kosorn W, and Kaewkong P. Procedia Engineering 2013;59:158-165.
80. Helminen A. Branched and crosslinked resorbable polymers based on lactic acid, lactide and ε-caprolactone: Helsinki University of Technology, 2003.
81. Amsden B, Wang S, and Wyss U. Biomacromolecules 2004;5(4):1399-1404.
82. Pitt CG, Hendren RW, Schindler A, and Woodward SC. Journal of Controlled Release 1984;1(1):3-14.
83. Palmgren R, Karlsson S, and Albertsson AC. Journal of Polymer Science Part A: Polymer Chemistry 1997;35(9):1635-1649.
84. Pitt CG, Gu ZW, Ingram P, and Hendren RW. Journal of Polymer Science Part A: Polymer Chemistry 1987;25(4):955-966.
85. Bruin P, Veenstra G, Nijenhuis A, and Pennings A. Die Makromolekulare Chemie, Rapid Communications 1988;9(8):589-594.
86. Olson DA, Gratton SE, DeSimone JM, and Sheares VV. Journal of the American Chemical Society 2006;128(41):13625-13633.
87. Lang M and Chu CC. Journal of Applied Polymer Science 2002;86(9):2296-2306.
88. Zhang Y, Won CY, and Chu CC. Journal of Polymer Science Part A: Polymer Chemistry 1999;37(24):4554-4569.
89. Posner T. Berichte der deutschen chemischen Gesellschaft 1905;38(1):646-657.
90. Zhou H, Li Q, Shin J, and Hoyle CE. Macromolecules 2009;42(8):2994-2999.
91. Clark T, Kwisnek L, Hoyle CE, and Nazarenko S. Journal of Polymer Science Part A: Polymer Chemistry 2009;47(1):14-24.
92. Lowe AB. Polymer Chemistry 2010;1(1):17-36.
93. Hoyle CE, Lee TY, and Roper T. Journal of Polymer Science Part A: Polymer Chemistry 2004;42(21):5301-5338.
94. Otts DB, Heidenreich E, and Urban MW. Polymer 2005;46(19):8162-8168.
95. Lin C-C and Anseth KS. Pharmaceutical research 2009;26(3):631-643.
96. Niu G, Zhang H, Song L, Cui X, Cao H, Zheng Y, Zhu S, Yang Z, and Yang H. Biomacromolecules 2008;9(10):2621-2628.
97. Dealy JM and Wissbrun KF. Melt rheology and its role in plastics processing: theory and applications: Springer, 1999.
98. Ramkumar D and Bhattacharya M. Polymer Engineering & Science 1998;38(9):1426-1435.
99. Choi H, Park S, Yoon J, Lee HS, and Choi S. Polymer Engineering & Science 1995;35(20):1636-1642.
100. Melik D and Schechtman L. Polymer Engineering & Science 1995;35(22):1795-1806.
101. Ramis X, Cadenato A, Morancho J, and Salla J. Polymer 2001;42(23):9469-9479.
102. Valette L and Hsu C-P. Polymer 1999;40(8):2059-2070.
103. Ljungberg N and Wesslen B. Journal of Applied Polymer Science 2002;86(5):1227-1234.
104. Tang D, Zhang J, Zhou D, and Zhao L. Journal of materials science 2005;40(13):3339-3345.
105. Trakulsujaritchok T and Hourston D. European Polymer Journal 2006;42(11):2968-2976.

106. Babkina N, Lipatov YS, and Alekseeva T. Mechanics of Composite Materials 2006;42(4):385-392.
107. Li S. Journal of biomedical materials research 1999;48(3):342-353.

Chapter 2

Multi ally polycaprolactone based polyesterurethanes: synthesis, cross-linking with polyhydroxyethyl methacrylate and theromechanical properties

Hang SHEN [1, 2, 3], Guilhem Quintard [4], Jianding CHEN [5], Mohamed TAHA [1, 2, 3]*

1 Université de Lyon, F-42023, Saint-Etienne, France

2 CNRS, UMR 5223, Ingénierie des Matériaux Polymères, F-42023, Saint-Etienne, France

3 Université de Saint-Etienne, Jean Monnet, F-42023, Saint-Etienne

4 INSA-Lyon, IMP, UMR5223, Université de Lyon, F-69621 Villeurbanne, France

5 Laboratory of Advanced Materials Processing, East China University of Science and Technology, 200237 Shanghai, China

*correspondence：Mohamed.Taha@univ-st-etienne.fr

Résumé

De nouveaux poly (polycaprolactone uréthane) (PEUs) segmentés ayant des structures différentes fonctionnalisés allyle (PEU-g-allyle) ont été conçus et préparés en deux étapes. Les synthèses ont été suivies par FTIR et les structures des produits obtenus ont été vérifiées par ^{1}H RMN, SEC et DSC. Par copolymérisation UV de PEU-g-allyle avec le 2–hydroxyethyle méthacrylate, des réseaux ont été obtenus. Les propriétés thermo-mécaniques de ces réseaux dépendent de la structure des unités d'exécution utilisées. Des propriétés d'amortissement particulières ont été obtenues. Les PEU et les réseaux obtenus ont été caractérisés et leur dégradation a été étudiée par TGA.

Mots-clés: photo durcissement, CL, biodégradable, poly (ester-uréthane) s, réseau

Abstract

A new two-step allyl-functionalized polycaprolactone segmented poly(ester urethane)s (PEUs) synthesis is reported. Oligomers having different branched architectures were designed and prepared. The syntheses were monitored by FTIR and the structures of the obtained products were verified by ^{1}H NMR, SEC and DSC. Through UV initiated copolymerization of the PEUs with 2-hydroxyl methacrylate, networks were obtained. These networks' thermo mechanical properties depend on the structure of the used PEUs. Particular damping properties were obtained. The degradation behavior of the PEUs and the obtained networks were investigated by TGA.

Keywords: Photo curing, CL, biodegradable, poly (ester- urethane)s, network

2.1 Introduction

Poly ester urethanes (PEUs) are particularly versatile polymers that can form materials ranging from stiff thermoplastics to rigid thermosets by changing the combinations of monomers and additives. They can be used as coating material, optical fiber coating or to prepare high-strength composites,[1-3] and nowadays used as scaffolds in tissue engineering.[4, 5] Compared with PEUs, poly(meth)acrylates show good performance in heat / solvent resistance and weather ability. Therefore, there is a complement in the performance of PEUs and poly(meth)acrylates, and this effect was often investigated by co-crosslinking of poly(meth)acrylates and PEUs.[6, 7] Oprea et al. [8] synthesized double bond telechelic PEUs then copolymerized them with acrylated soybean oil and acrylic acid. Films of this network were obtained and their mechanical properties analyzed. Polyester urethane acrylates containing PLGA, HEMA and ethyl ester lysine diisocyanate were investigated for their hydrolytic degradation by A. Ghaffar et al.[9] All these studies show the potential applications in both industry and medical fields.

Generally the syntheses of polyurethane-acrylate prepolymers can be carried out in 2 steps: first an excess diisocyanate is reacted with dialcohol leading to generally linear prepolymers. Then, the end chain remaining isocyanate reacts with the hydroxyl group of a (meth)acrylic monomer. During the second step, the reaction temperature and time should be carefully controlled to avoid the double bound radical polymerization that could lead prematurely to a non-controlled cross-linking.[10, 11] Recently, biodegradable segmented polyurethanes were synthesized for biomedical applications.[12-15] They have been mainly synthesized by reacting polyester diols with slightly toxic diisocyanates such as isophorone diisocyanate (IPDI) or hexamethylene diisocyanate (HDI). The objective of this study is to prepare hydrophilic materials combining polyester urethane properties with those of a biodegradable polymer and having controllable viscoelastic and thermal properties as well as good dimensional stability.

Bio-resourced polyesters such as polylactide (PLA) and polyhydroxybutyrate (PHB) are often used[16-19] but they also exhibit obvious defects, for example, brittleness and weak heat resistance for PLA, and narrow processing windows for PHB,[20] which is also unstable upon its melting temperature. At the same time, unsuitably high Young's modulus and rather low elongation at break values of PHB is clearly inappropriate for numerous clinical uses. Therefore,

a particular interest was given again to Poly (ε-caprolactone) (PCL). PCL has been produced and commercialized as biodegradable materials since the 1930s.[21] The good solubility of PCL, its low melting point and exceptional blend-compatibility has stimulated extensive research for its potential application in biomedical fields.[22-25] Furthermore, tailorable degradation kinetics and mechanical properties, ease of shaping and ability to be used in controlled delivery of drugs have drawn the attention of researches to PCL more than other biopolymers.[26] For these reasons, the PCL was chosen as the biodegradable polymer in this study. A new approach has been used to prepare tailored segmented PEU acrylates based on PCL. By copolymerization of the PEU acrylates with 2-Hydroxyethyl methacrylate, networks were synthesized and characterized principally for biomedical domains.

2.2 Experimental Section

Materials

Dihydroxyl-terminated polycaprolactone oligomers CAPA@ 2100A, 2200A and 2402 were purchased from Solvay. Their M_n are respectively 1000, 2000 and 4000 Da as indicated by the supplier and confirmed by ^{1}H NMR. 2-Hydroxyethyl methacrylate was purchased from Röhm GmbH. 4, 4'-Methylenebis(cyclohexyl isocyanate) (H_{12}MDI), Glycerol, 1,4-butanediol, Dibutyltin dilaurate, Allylamine, Tin(II)-bis-(2-ethylhexanoate) were purchased from SIGMA-ALDRICH (France). Anhydrous DMF and diethyl ether were purchased from Carlo Erba Reagents™. The photo initiator was composed as follows: 60wt% of CN381 from Sartomer (containing copolymerisable amine acrylate as synergist), 20wt% of Benzophenone (99%) from Aldrich, and 20wt% of 2, 2-Diethoxyacetophenone from Aldrich. 2-Hydroxyethyl methacrylate was distilled before use; glycerol was dehydrated by molecular sieves 3 Å (rod shape, size 1/16 inch, Fluka) for 1 week before use. All other reagents were used as received without further purification.

Synthesis

Synthesis of PCL-segmented prepolymer

A typical synthesis procedure of multi functionalized PEU is illustrated by Scheme 1: glycerol and the hydroxyl-terminated PCL oligomer were first introduced into a 2-neck flask equipped

with previously dried nitrogen flow and condenser. Then anhydrous DMF was injected in as the solvent and the reactive system was magnetically stirred until it became homogeneous at room temperature. Then the H_{12}MDI was injected in and mixed for 5 minutes. Finally the dibutyltin dilaurate was introduced as the catalyst and the system was placed in an oil bath at 80°C for 55 minutes. During the reaction, the FTIR was used to monitor the consumption of isocyanate group.

End-capping of the prepolymers using bifunctional monomers

The obtained PEU solution above was diluted with anhydrous DMF and placed in the ice-water bath with magnetic stirring. Then allylamine was dropwise added to react with the remaining isocyanate groups. The reaction monitored by FTIR was kept for 30minutes until the complete reaction of isocyanate groups. Then the product was precipitated in a large amount of ethyl ether, the precipitator was three times re-dissolved in chloroform and re-precipitated in ethyl ether. Then, the solid was collected and dried under vacuum at room temperature for 24 hours and stored at -20°C.

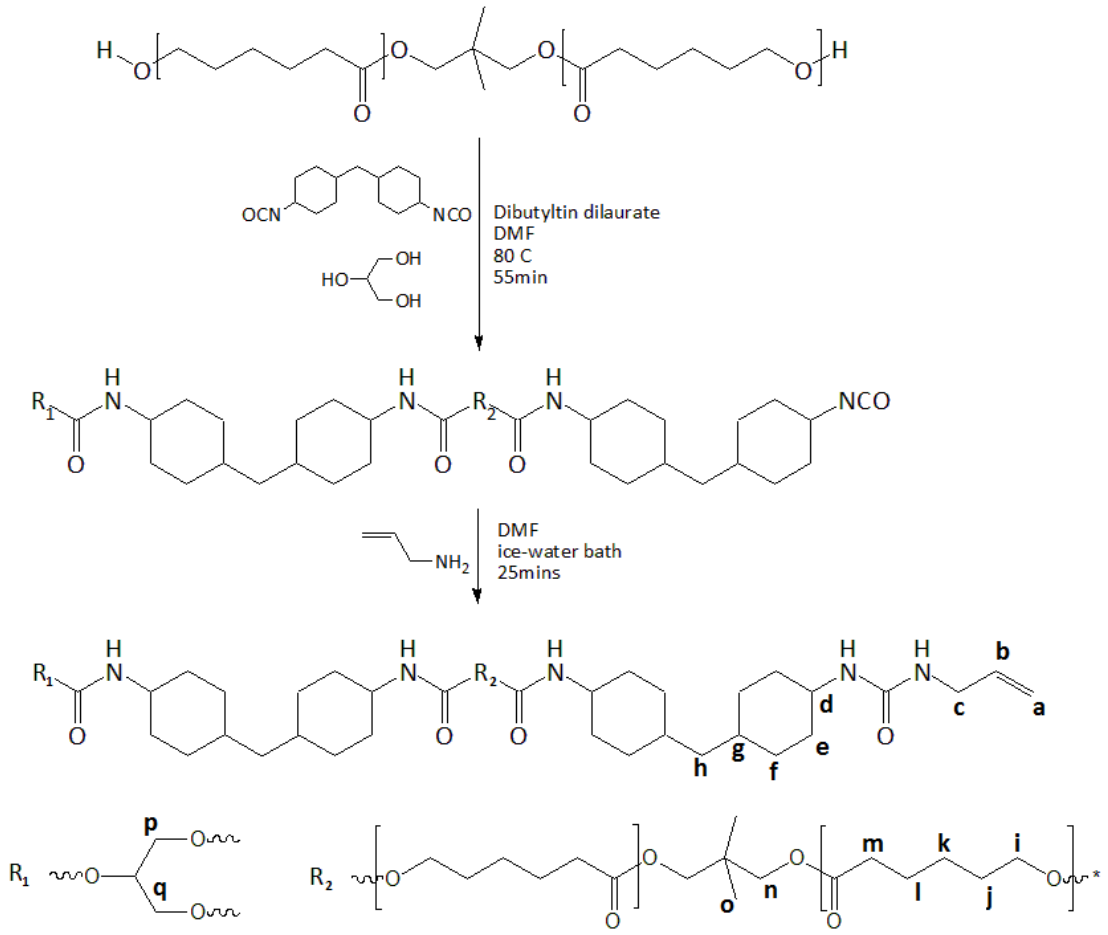

Scheme 1. The 2-step synthesis of allyl functionalized and PCL segmented PEUs labeled for ^{1}H NMR

Structure design and nominate of the poly (ester urethane)s

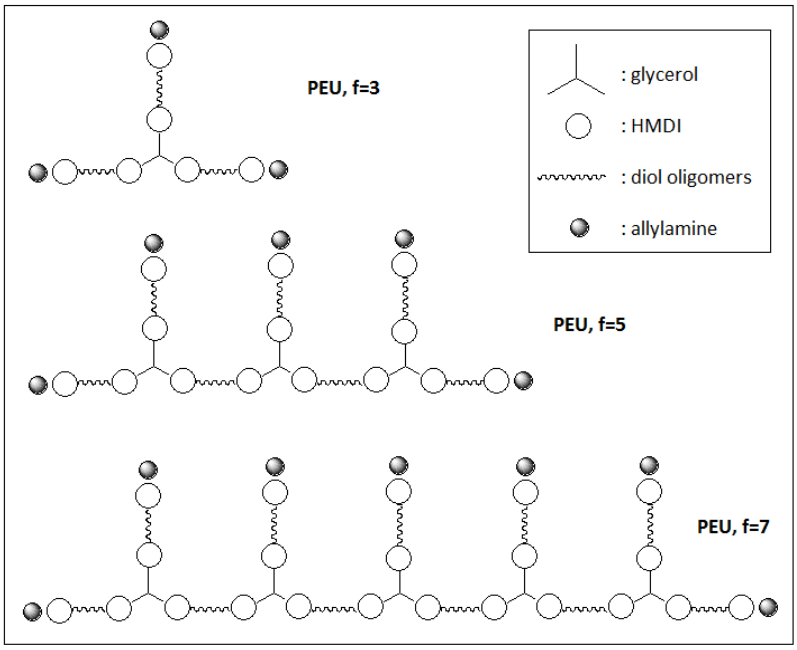

Figure 1. Expected structures of the PCL segmented allyl functionalized PEUs

To endow the poly(ester urethane) with different functionalities, different structures were designed and illustrated in Figure 1. The mole ratio of the components was determined by the expected structure and the gel point calculated by equations based on Miller-Macosko's theory [27] from eq1 to eq3:

$$P^2_{gel} = \frac{1}{(\overline{f}_A - 1)(\overline{f}_B - 1)} \times \frac{1}{r} \quad \text{Eq.1}$$

$$\overline{f}_i = \frac{\sum n_i f_i^2}{\sum n_i f_i} \quad \text{Eq.2}$$

$$r = \frac{n_A f_A}{n_B f_B} \quad \text{Eq.3}$$

Herein f_i means the the functionality of each compound (glycerol, PCL, etc...), $\overline{f}_i$ means the average functionality of polyol (A) or diisocyanate (B), n is the amount of monomer in mole, and r means the function mole ratio of polyol to isocyante (r<1), by which the gel point P_{gel} can becalculated.

In order to clearly identify the different PEUs with different structures, samples in this study are named as **U (or N)-FX-AY-MZ**. In which, 'U' means polyurethane, 'N' means PU network cooperated with HEMA, 'F' means expected functionality, 'A' means number of oligomer chain(s) introduced into the expected structures and 'M' means the M_n of the oligomers. For instance: U-F3-A3-M1000 means polyurethane with expected functionality 3 and having 3 oligomer arms with molar mass 1000.

Network films preparation through UV irritation

Different allyl-functionalized PCL-segmented PEUs were dissolved in HEMA with mass ratio M_{HEMA} : M_{PEU} = 1.5 : 1 at room temperature in the shaker until the solution became homogeneous. Then, the photo initiator was fully dispersed into the system by oscillation at room temperature for 3mins. The mixture was placed in an ultrasonic oscillator to remove the air bubbles before curing.

To initiate the UV irritation, the mixtures were placed in LDPE molds (100mm x 10mm x 100µmm) and cured in air with a fluorescent lamp, JAD STS-350, equipped with 8W x 3

fluorescent tubes offering λ=250nm UV light. The mixtures were exposed at 3cm from the lamps for 24hrs. After the curing, the sample bars were collected for mechanical analyses.

Instrumentation

IR

FT-IR was used to monitor the reaction of isocyanate group with absorption at 2260cm^{-1}, and quantitatively characterize the PEUs. The absorption spectra of the polymer were recorded on a Nicolet Nexus spectrometer (700-3500 cm^{-1}) using attenuated total reflectance (ATR) technique.

NMR analysis

NMR analyses were performed with a Bruker Advance II spectrometer operating at 250MHz for ^{1}H NMR. The analyses were performed with 5mm diameter tubes containing about 25mg of polymer in 0.5mL chloroform-D, with tetramethylsilane as the internal reference at 0ppm. And each sample was scanned for 64 times at 300K.

DSC

Differential scanning calorimetry (DSC) measurements for the allyl functionalized PCL segmented PEUs and PEU / PHEMA networks were carried out with a Q10 calorimeter from TA Instruments. Samples were transferred to hermetic pans and sealed, and analyzed from -80°C to 210°C with a cooling / heating rate of 10°C·min^{-1}. The glass transition temperatures were evaluated from the data recorded during heating by identifying the inflection points. Each sample underwent two cycles of heating-cooling cycles.

SEC

For the analyses of allyl functionalized PCL segmented PEUs, Size exclusion chromatography (SEC) was conducted using a system equipped with refractive index (Waters 2414) and light scattering (Wyatt MiniDawn Treos) detectors. Two columns HR1 and HR3 from Waters were used. The eluent was tetrahydrofuran (THF) with a flow rate of 1 mL·min^{-1} and the elution temperature is 35°C. The copolymer molecular weights were determined using a calibration

curve established on a set of narrow polystyrene standards of different molecular weights ranging from 500 to 700 000.

Dynamic Mechanic Analysis

The dynamic mechanical thermal analyses of the PEU / PHEMA network films were performed with Rheometrics Solids Analyzer (RSA II, TA-Instruments) to obtain tensile dynamic mechanical spectra. Test samples were cut from the previously cured strips with a predetermined shape (40mm x 10mm x 100µm). For dynamic tensile measurements, a nominal strain of 0.1% was adapted, with an applied frequency of 1Hz. Storage modulus E', loss modulus E", and loss factor tan δ were determined as a function of temperature. Data were taken from -90 °C to 150 °C using a heating rate of $3^{o}C \cdot min^{-1}$. Each sample was equilibrated in the same chamber under dry nitrogen at the starting temperature prior to running the test.

2.3 Results and discussions

2.3.1 Syntheses and characterizations of PCL segmented multi allyl functionalized poly(ester urethane) prepolymers

Structure design of the PEUs mainly focused on two aspects: the content of PCL segments that affects the flexibility and biodegradability of the issued material, and the allyl functionality of PEUs, which concerns the network structure prepared using the PEU as cross-linker.

The syntheses were performed in 2 steps: first, prepolymers were obtained by reactions between glycerol, polycaprolactone diols and excess H_{12}MDI (according to eq1-eq3). Secondly, the double bond functionalization was achieved by reaction of the remaining isocyanate groups with allylamine. The synthesis procedure and characterizations of these products are discussed in this part.

Synthesis monitor by FTIR

Syntheses of PEU-functionalized allyl were monitored with FTIR (Figure 2). After the isocyanate absorption at 2259 cm^{-1} decreased during 55mins, it became constant, indicating the total consumption of the alcohol groups and the end of the first step. This was confirmed by the disappearance of the alcohols' absorption at 3476 cm^{-1} , the appearance of the

absorption peak at around 3330-3350 cm^{-1} (assigned to the -NH group) as well as the C=O stretching at 1725 cm^{-1} and C-N-H bending at 1540 cm^{-1} of the urethane group. At the end of the second step, the N=C=O absorption disappeared, confirming the total reaction of isocyanate with the amine groups of allylamine.

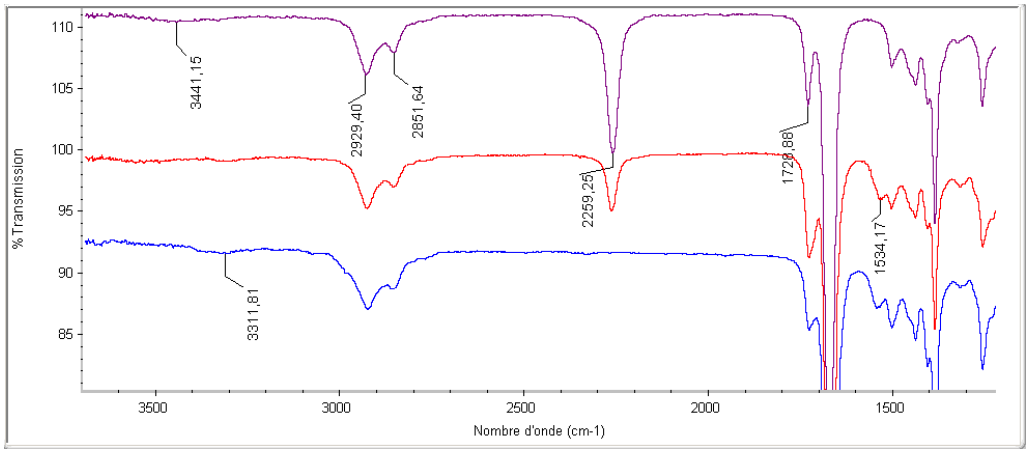

Figure 2. FTIR spectra monitoring PCL segmented allyl functionalized PEU U-F3-A3-M1000 syntheses, from 1200cm^{-1} to 3600cm^{-1}: (a) reactants at initial time, (b) PCL segmented PEU U-F3A3M1000 prepolymer after the first step of synthesis, (c) PCL segmented allyl functionalized PEU after the second step.

Allyl functionalized PEU Structure evolution by ^{1}H NMR

The structure of allyl functionalized PCL segmented PEU illustrated above in Scheme 1 was analyzed by ^{1}H NMR, and a spectrum is shown as example in Figure 3. The attributions of the protons are shown in Table 1.

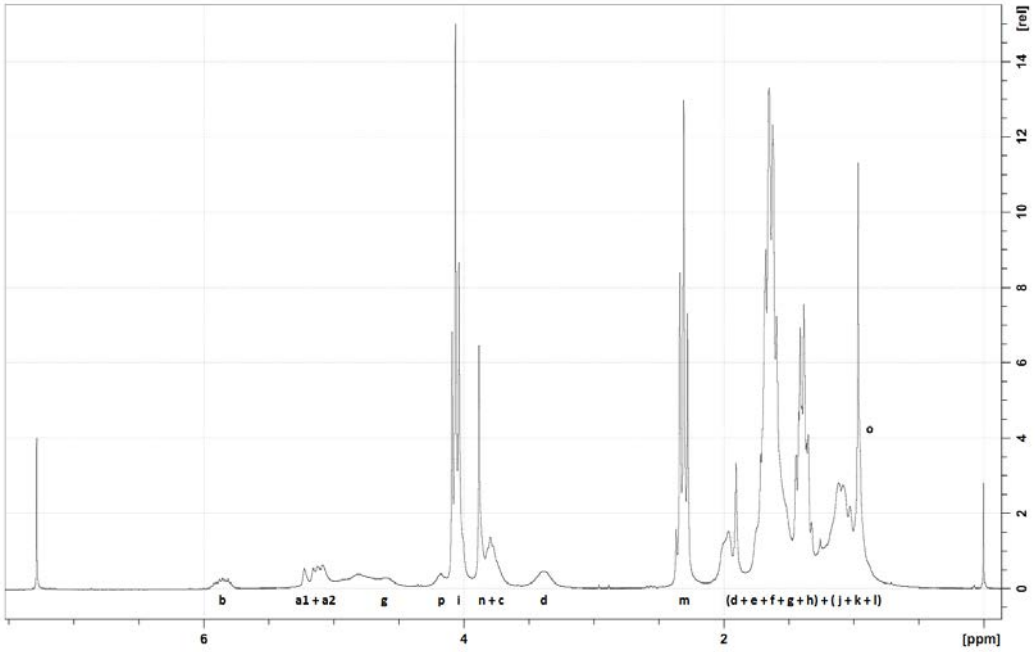

Figure 3. The ^{1}H NMR spectrum of the purified PEU in CDCl3, the synthesis was performed with parameters: [HMDI] : [PCL] : [allylamine] : [Glycerol]=6.62 : 3 : 3 : 1. 0.5 mol% of DBTDL was used as catalyst and the reactions was performed at 80°C for 60mins for the first step, and 0oC for 30mins for the second step.

As can be seen in Table 1, most protons were overlapped by each other at 0.9-2ppm and 4-4.6ppm. However, characteristic protons from each part of the PEU can be clearly observed: Allyl protons from allylamine are located at 5.8ppm and 5.2ppm .α and ε methylene protons (labeled with I and m) from PCL oligomer chains are at 4.0ppm and 2.2ppm respectively. Protons from the PCL co-initiator, 2, 2-dimethyl-1, 3-propanediol, were assigned as j and f.

Table 1. Chemical shift of protons from allyl functionalized and PCL segmented PEUs (all protons were labeled in Scheme 1).

Proton	a1	a2	b	c	d	e1	e2	f1	f2	g
Chemical shift (ppm)	5.22	5.12	5.84	3.83	3.37	1.12	2.00	0.95	1.70	1.25
Proton	h	i	j	k	l	m	n	o	p	q
Chemical shift (ppm)	1.06	4.06	1.62	1.29	1.53	2.31	3.88	0.96	4.20	4.64

The average mole ratio of CL repeat unit to allyl function can be evaluated by comparing the integration of protons b (from allyl proton of allylamine) and e (the α methylene proton from CL). Results are in Table 2. These ratios are in concordance with those expected, confirming that the structure expected by modeling are actually obtained.

Table 2. The average ratio of repeat unit CL to double bond functions in allyl functionalized PCL segmented PEU moles, by idea value and by real value respectively. All polymerization were performed with 0.5 mol% of DBTDL at 80oC for 60mins for the first step, and at 0oC for 30mins for the second step.

Sample Names	U-F3-A3-M1000	U-F5-A7-M1000	U-F7-A11-M1000
Functionality of expected structured PEUs	3	5	7
Expected [double bond function]/[CL] repeat unit, mol : mol	1:8	1:11.2	1:12.6
Calculated [double bond function]/[CL] repeat unit by ^{1}H NMR results, mol : mol	1:8.4	1:10.9	1:14.2

Allyl functionalized PEU syntheses evolution by SEC

To verify the correct evolution of the synthesis when changing the reaction parameters, SEC analyses were also made. The results are summarized in Table 3.

Table 3. Molar mass obtained by SEC tests, and T_g of PCL segmented allyl functionalized PEUs obtained by DSC, synthesized with different parameters, all polymerizations were performed with 0.5 mol% of DBTDL at 80oC for 55mins for the first step, and at 0°C for 30mins for the second step. To remind, U-F3-A1-M1000 means allyl functionalized PCL segmented PEU with expected functionality=3, and average 3 PCL chains owning molar mass 1000 in each PEU mole.

Entry	Sample details	M_n / M_w / MWD	Glycerol content, wt%	T_g of PEU-g-allyl, °C	Double bond content, mmol / g
Run1	U-F3-A1-M1000	6300 / 22400 / 3.56	2.82	-34.1	0.48
Run2	U-F3-A2-M1000	7200 / 17400 / 2.41	1.72	-34.4	0.42
Run3	U-F3-A3-M1000	9410 / 23200 / 2.47	1.20	-38.0	0.32
Run4	U-F3-A3-M2000	15700 / 31200 / 1.99	1.12	-56.2	0.19
Run5	U-F3-A3-M4000	30400 / 53700 / 1.77	0.64	-56.8	0.10
Run6	U-F5-A5-M1000	9100 / 26700 / 2.93	2.21	-34.3	0.55
Run7	U-F5-A7-M1000	11400 / 33100 / 2.90	2.18	-40.2	0.44
Run8	U-F7-A7-M1000	11230 / 28740 / 2.56	2.38	-36.2	0.62
Run9	U-F7-A11-M1000	15320 / 50280 / 3.32	2.30	-40.9	0.46

The molar mass evolutions are coherent with the expected structures of the allyl-terminated PEUs. When comparing Run1, Run2 and Run3, the more PCL segments are introduced into the PEU, the larger the molar mass of the PEU was with narrow molar mass distribution (MWD), which is in accordance with the former report [28]. An increase of the molar mass of the PCL segments from Run3 to Run5 will have the same effect in increasing the molar mass of these polyurethanes, while accompanied by a decrease in the MWD. When investigating the functionality effect on molar mass from Run3 and Run6-Run9, it can be seen that the molar mass of PEUs increased with the increase of their functionality; it is reasonable because the polyurethane having larger functionality or more PCL segments have higher molar mass, as illustrated in Figures 1 and 4.

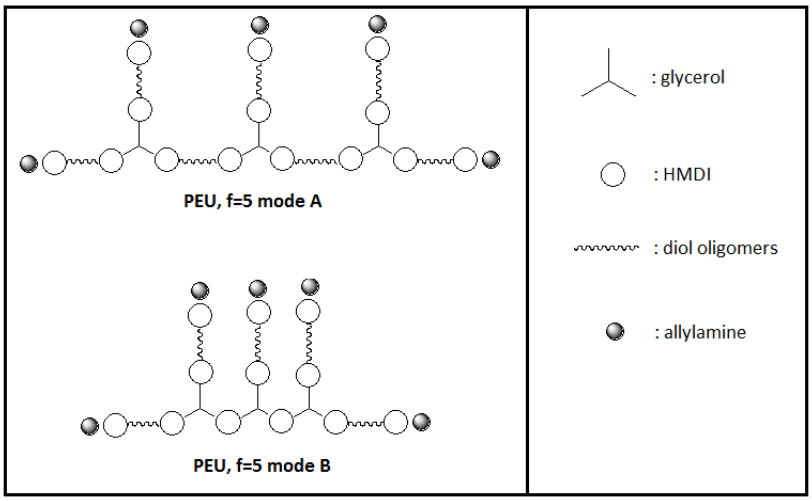

Figure 4. Expected structures of PCL segmented allyl functionalized PEU with functionality equal to 5, correspond with the Run6 and Run7 in Table 3.

Characterization of the PCL segmented poly(ester urethane)s by DSC

DSC was also used to measure T_gs of the obtained PEUs. The results are depicted in Table 3. Throughout the temperature ramping cycles, only one glass transition behavior was observed, which is similar with the H_{12}MDI segmented polyurethanes reported [29], this transition belongs to the PCL segment above its T_g. From Run1 to Run3, the polyurethanes possessing the same PCL segment but a different number of segments have similar glass transition temperatures around -34°C. Run3 shows lower glass transition temperature around -38°C. In this case, PCL chain extension can lead to a PCL having higher molar mass and consequently a lower T_g. Equivalent results were also observed going from Run6 to Run9. Here also the T_gs of the PEUs drop with the increase of their functionality. When increasing the molar mass of the PCL segment, the T_g shifts toward the T_g of the issued PCL: going from Run3 to Run5, the molar mass of PCL increases and consequently the T_g is decreased.

2.3.2 Cross-linking of allyl functionalized PCL segmented and HEMA

The average functionality of a reactive system composed by allyl-functionalized PEUs and HEMA copolymerizing by UV polyaddition is higher than 2. Consequently, cross-linking should occur. In this study, the mass ratio M_{PEUs} : M_{HEMA} was 1 : 1.5 for all the formulas. The PEUs have good solubility in HEMA with this ratio. After polymerization, transparent and flexible films were obtained. As expected these films were not soluble in solvents of the reactive system

such as THF and Chloroform. This is coherent with a cross-linking of the reactive system. Thermomechanical properties of these films are analyzed in this part.

Table 4. The thermomechanical properties of the PEU / HEMA networks. The glass transition temperature of the networks were obtained from the temperature correspond with the Tanδ value. The $Tan\delta_{max}$, working area of damping and storage moduli of rubbery plateau were directly obtained from Figure 5 – 7.

Entry	PEUs adapted in network syntheses	PCL content in the network, wt%	T_g, °C	$Tan\delta_{max}$	Working area of damping (Tanδ > 0.3), °C	Storage moduli at rubbery pateau, (MPa)
Run10	F3A1M1000 (Run1)	14.4	88.9	1.26	58.8 – 122.3	2.50
Run11	F3A2M1000 (Run2)	18.7	76.1	0.74	43.2 – 114.6	2.07
Run12	F3A3M1000 (Run3)	20.7	70.8	0.68	37.8 – 108.5	1.51
Run13	F3A3M2000 (Run4)	25.5	65.2	0.51	43.8 – 111.0	1.45
Run14	F3A3M4000 (Run5)	29.0	65.3	0.69	43.9 – 103.0	0.54
Run15	F5A7M1000 (Run7)	20.8	82.9	0.96	52.3 – 116.1	1.50
Run16	F7A11M1000 (Run9)	20.9	82.8	1.10	53.4 – 118.7	0.79

As shown in Figures 5 - 7, the storage moduli E’ are higher than loss moduli E” throughout all the temperature ranges in all experiments. A rubbery plateau is also obtained at high temperature. All these confirm again the formation of networks. Thermomechanical properties of these networks were obtained from DMA tests and summarized in Table 4.

Effect of oligomer chain number on tri-allyl-functionalized PCL-segmented PEU-based network

For Runs 1-3, Tri-allyl-functionalized PEUs containing respectively 1, 2 and 3 PCL segments were prepared. By copolymerization with HEMA of these PEUs, networks were obtained (runs 10-12). These networks contain respectively 14.4, 18.7 and 20.78 wt% of PCL. The DMA graphs are shown in Figure 5.

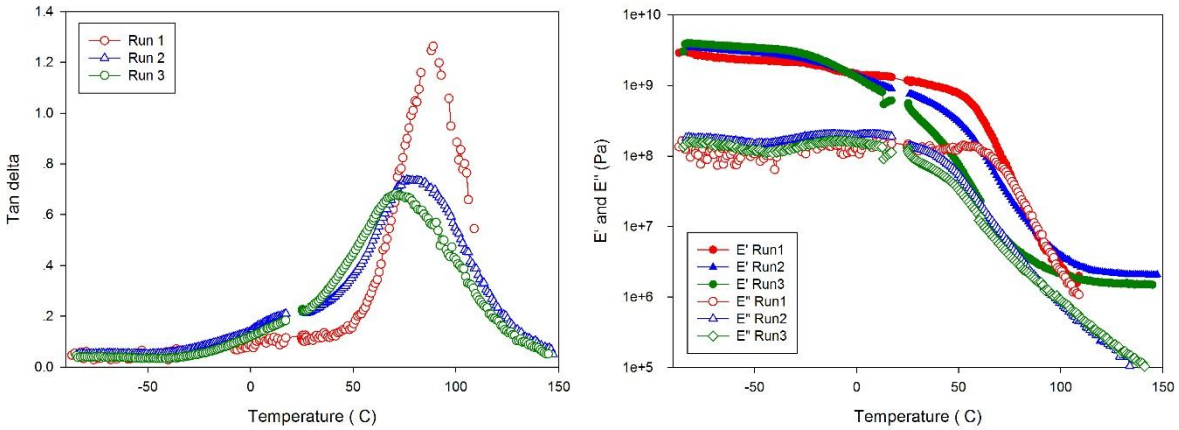

Figure 5. Storage modulus (E'), loss modulus (E") and loss factor Tanδ versus temperature of the PEU/ PHEMA networks 10, 11 and 12 based on Run1, Run2 and Run3 respectively.

As shown in Figure 5, maximum Tanδ shifted toward lower temperature from 89 to 64°C. This is due to the increase of the PCL weight fraction in the copolymer (T_g of the PEUs Run1-Run3 are around -36°C, while the T_g of PHEMA is approximately 87°C). Another attribution of the T_gs change is the double bond concentration of PEUs, which decreases from 0.48 mmol·g^{-1} for Run1 to 0.32mmol·g^{-1} for Run3, which also causes a decrease of the T_g of the network. Tanδ peak becomes broader and decreases its peak value from 1.26 to 0.66 from Run 10 to 12 indicating higher dispersion in the molar mass between cross-links.

Effect of oligomer chain molar mass on networks

The molar mass of the PCL segment (Run 10, 13, and 14) effect on the networks are illustrated in Figure 6.

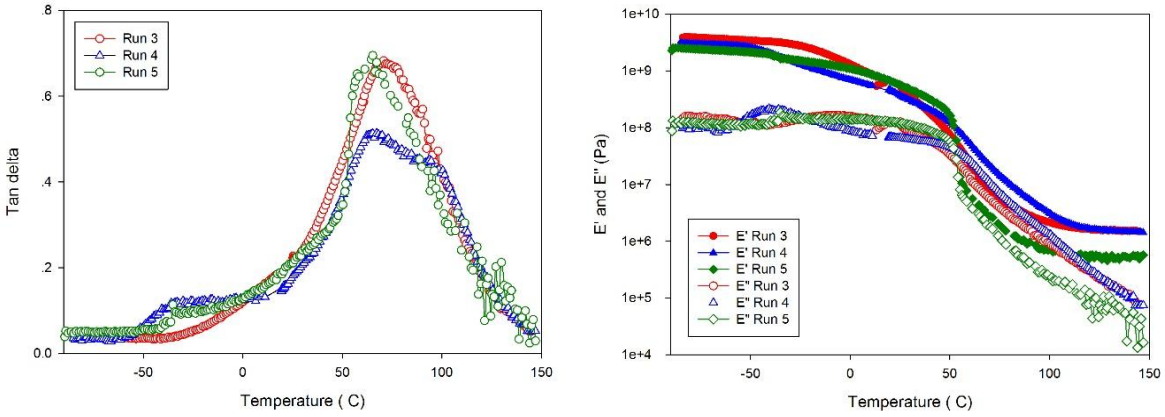

Figure 6. Storage moduli (E'), loss moduli (E") and loss factor Tanδ versus temperature curves of the PEU/ PHEMA networks based on PEUs Run3, Run4 and Run5 with different molar mass of PCL-dialcohol segments,

the structures of PEUs were designed as in Figure 1, f=3.

A reduction in T_g is expected with to the increase of the PCL content (from 14.4 to 25.5 and 29.0 wt%) and also with the increase of the mass between crosslinks (M_c). Noting that the increase of M_c is due to the decrease of double bond functionality of the acrylated prepolymers (from 0.32 to 0.19 and 0.10 mmol·g^{-1}), this decrease of Tg is compensated by the increase of the molar mass of the PCL (from 1000 to 2000 and 4000 Da), which increases the T_g of the network. As a result, there is almost no change in the glass transition of these networks.

Effect of PEU functionality effect on networks

Networks were prepared using PEUs with functionality 3(Run3), 5(Run7) and 7(Run9) in runs 12, 15, 16. Their thermo-mechanical properties are depicted in Figure 7.

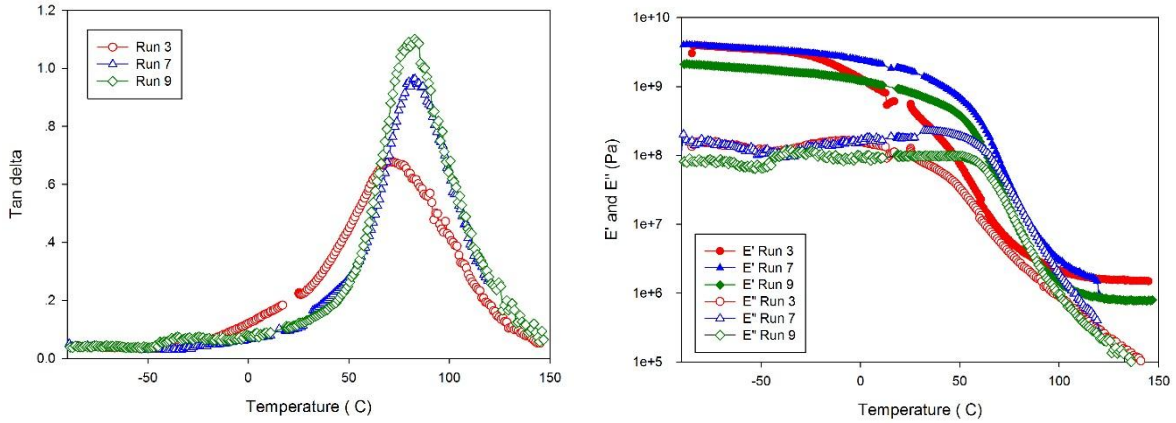

Figure 7. Storage moduli (E'), loss moduli (E") and loss factor Tanδ versus temperature curves of the tri-armed PEU / PHEMA networks based on PEUs Run3, Run7 and Run9 owning different functionalities, the structure of PEUs was designed using modes in Figure 1

Networks based on PEU f=7 (Run9) and PEU f=5 (Run7) seem similar since they contain the same PCL concentration with similar molar mass. In addition, they also have the same double bond concentration. As seen in Figure 7, the thermo-mechanical properties of these two specimens are almost equivalent with only a few differences: networks based on PEU f=7 (Run9) have sharper tangent δ peak and lower rubbery plateau modulus when compared to networks based on f=5 (Run7).

For network based on PEU f=5(Run3), the PCL content is slightly lower than for f=7(Run9) and PEU f=5(Run7). The PEU from run 3 has similar soft/hard segment compositions as those from

runs 7 and 9, but its double-bond concentration is obviously lower than for the other two specimens. This leads to a less dense network that has lower glass transition temperature. This network is more heterogeneous than the other two networks.

2.3.3 Thermogravimetric analysis of the PEU / PHEMA films

The combination of thermogravimetric analysis and FT-IR is a relevant technique for studying the decomposition of the products prepared here. The thermal degradation of the allyl-functionalized PCL-segmented PEU (from Run3) and that of the network prepared by its copolymerization with HEMA are given as examples. Figure 8 (a, b, and c) depicts respectively TGA, Differential TGA and Gram-Schmidt trace of the PEU and the issued network.

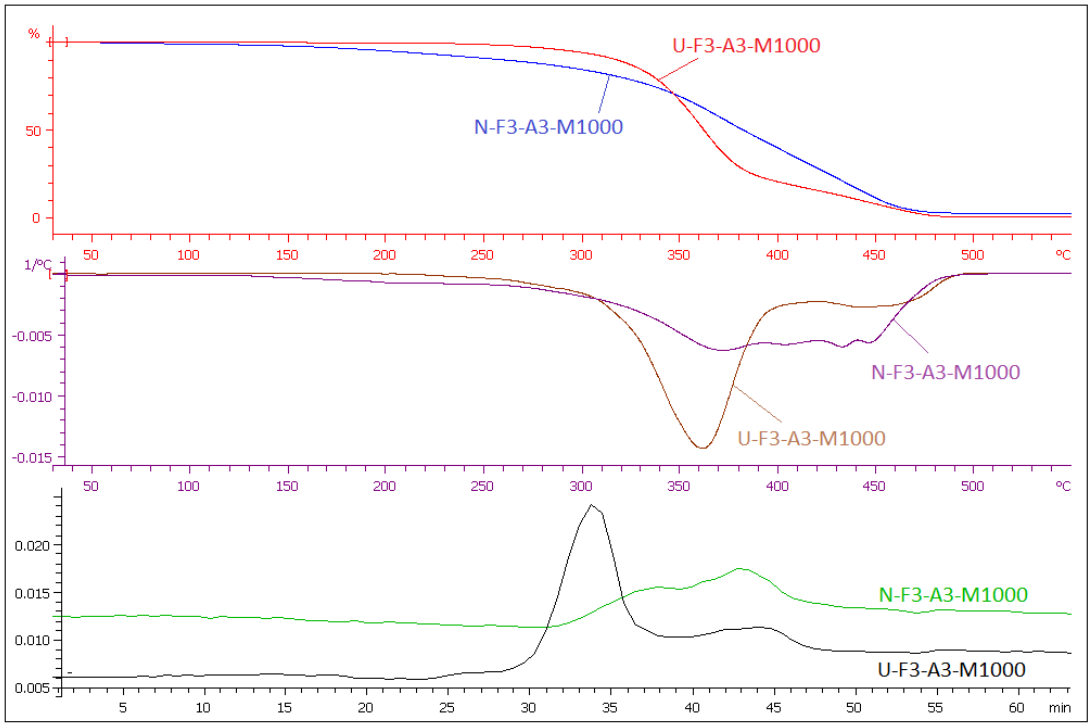

Figure 8. TGA (top), DTGA (middle) and Gram-Schmidt trace curves (bottom) of PEU Run3 and PEU/PHEMA network based on PEU Run3, the thermal degradations were conducted in nitrogen atmosphere from 30°C to 550°C.

For allyl-functionalized and PCL-segmented PEU Run3, its degradation steps were illustrated in Figure 8 and Figure 9. The degradation begins with the decomposition of carbamate linkage to hydroxyl group and isocyanate, with the characteristic absorption of isocyanate group at 2259cm^{-1} in spectra (A) of Figure 9 collected at 26.14min (291°C), which corresponds with the decomposition of PU reported before [30]. However, this step cannot be seen in TGA and DTGA curves because the carbamate decomposition does not cause weight loss. Then, a major

weight loss, with its maximum degradation rate around 362°C, was detected by TGA and DTGA curves. This weight loss is attributed to the degradation of PCL segments and confirmed by the IR spectrum of the gas generated at the same time. The main degradation product of PCL, 5-hexenioc acid, can be identified with its characteristic absorption at 2939cm^{-1} $\gamma_{as}(CH_2)$, 2874 cm^{-1} $\gamma_s(CH_2)$, 1774cm^{-1} $\gamma(C=O)$, 1642cm^{-1} $\gamma(C=C)$, 1448cm^{-1} $\delta(CH_2)$ [31] .

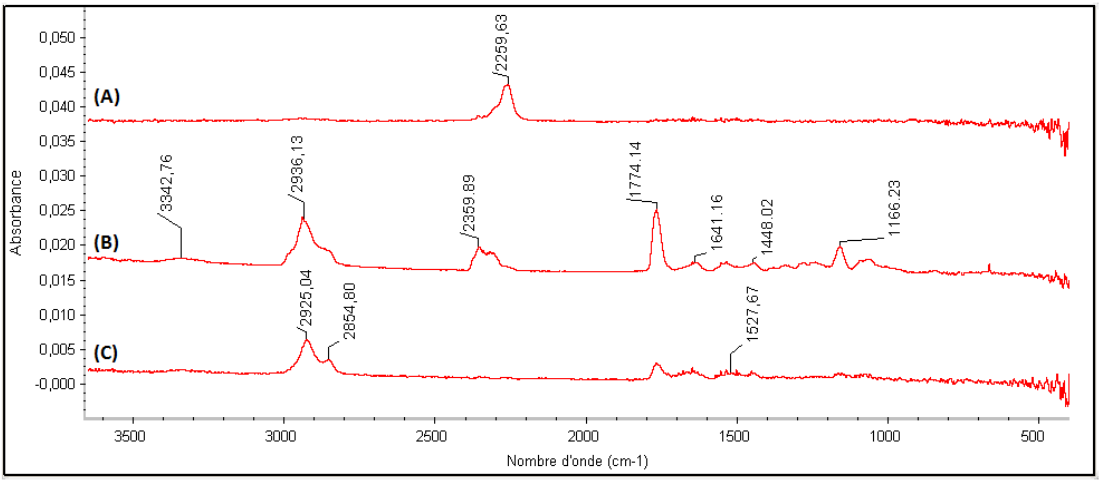

Figure 9. The FTIR spectra of gas collected during PEU Run3, the FTIR spectra was collected at the maximum evolution rate for each decomposition step for degradation at (A) 291°C (B) 367 °C and (C) 470 °C

Compared with the former report, degradation temperature of PCL segment in this PEU is lower, and may be explained by the lower molar mass of the PCL oligomers. At the same time, strong signals of carbon dioxide at 2359cm^{-1} and amine groups at 3340cm^{-1} can be seen. These two peaks were believed to be the degradation products of isocyanate groups and H_{12}MDI fragment [32], or the allylamine fragment. From 430°C to 490°C, another obvious weight loss can be seen from TGA and DTGA curves. This is the further degradation of H_{12}MDI and corresponds to the degradation of H_{12}MDI segmented PU reported by Cervantes with corresponding degradation temperature of H_{12}MDI.[32] Bands at 2931 and 2861 cm^{-1} were still observed and assigned to C-H absorptions. A broad band centered at 1520cm^{-1} was also observed and was related to amine groups [32]. At the same temperature, this degradation is still accompanied by the degradation of remaining PCL segments until the end of the PEU degradation.

The IR spectra of network Run12's degradation product in each degradation stage were shown in Figure 10. Compared to the allyl-functionalized PEU Run3, the network Run12 (based on Run3) is thermally stable below 130°C and has a slight weight loss during the thermal degradation with temperature ramping from room temperature to 550°C. Although the

thermal degradation of network Run12 is more complex with its covalent bonded PHEMA chains, this network has similar degradation steps as its PEU composition Run3.

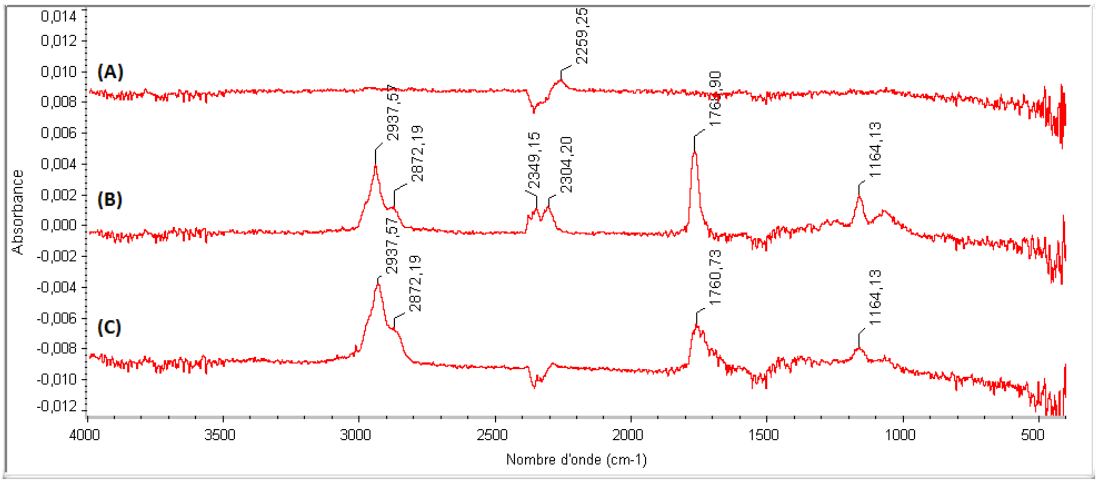

Figure 10. The FTIR spectra of gas collected during PEU Run3, the FTIR spectra was collected at the maximum evolution rate for each decomposition step for degradation at (A) 209°C (B) 388°C and (C) 456 °C

Compared to the PEU degradation TGA curves, the network starts to lose weight above 130°C, which is attributed to the de-polymerization of PHEMA chains into HEMA according to the degradation of homopolymerized HEMA reported before.[33] However the HEMA absorption cannot be detected on the coupled IR. Then, the characteristic isocyanate absorption at 2259cm^{-1} was also found, which is the same as Run13 and corresponds to the decomposition of urethane links, followed by the degradation of PCL segments with coupled IR absorption of 5-hexenioc acid shown in spectrum (B) in Figure 10. Furthermore, from the TGA and DTGA curves of the network, it can be seen that the maximum degradation speed of the PCL segments was delayed from 362°C to 370°C. This delay may be attributed to the restriction of the PCL segment's movement by covalent bond and hydrogen bonds interactions between carbamate group and hydroxyl group from PHEMA before degradation starts.

From 410°C to 490°C, the DTGA curve and especially the Gram-Schmidt trace of the network degradation are different from PEU. Obvious signals are detected around 410°C to 450°C for Gram-Schmidt trace and its intensity is even stronger than the degradation of PCL segments, which can also be seen on DTGA curves. It is believed that this weight loss is caused by the degradation of PHEMA chains, because the PHEMA segments are present in considerable amount (60wt%) in the network, and the second step degradation temperature of homo-polymerized HEMA reported by researchers [34] is similar to this temperature. When

analyzing the gas from degradation of this stage, as shown in spectrum (C) in Figure 10, it can be seen that although the absorption of 5-hexenioc acid decreases, the 2931 and 2861 cm^{-1} band remain strong absorptions. These absorptions come from C-H absorptions of methylene and methine groups, coming from the fragment of the PHEMA chain products.

2.4 Conclusion

The PCL-segmented poly(ester urethane)s were synthesized with H_{12}MDI to strengthen their mechanical properties. The syntheses were performed in 2 steps and double bond functionalized PEUs were obtained. The structure of these PEUs was designed during the syntheses and characterized by HNMR, SEC and DSC tests. Thermogravimetric analysis was conducted to evaluate their thermal stability. These PEUs were cooperated with HEMA to form the network. The result shows that the PEUs have a good compatibility with HEMA and the obtained networks have alterable moduli and damping properties by adapting PEUs with different structures..

Acknowledgement

The authors thank the financial support from China Scholarship Council (state scholarship fund). This work benefited from the international cooperation between Université Jean-Monnet Saint-Etienne (France) and East China University of Science and Technology (China).

Reference:

1. E. Sharmin, et al., *Prog. Org. Coat.*, **73**, 118 (2012).
2. D. Cooke, et al., *Radiation Physics and Chemistry*, **55**, 1 (1999).
3. W. Wang, Y.-l. Guo, and J.U. Otaigbe, *Polymer*, **50**, 5749 (2009).
4. M. Laschke, et al., *Acta Biomaterialia*, **6**, 2020 (2010).
5. C. Boissard, et al., *Acta Biomaterialia*, **5**, 3316 (2009).
6. J. Chen, J.P. Pascault, and M. Taha, *Journal of Polymer Science Part A: Polymer Chemistry*, **34**, 2889 (1996).
7. I. Henry, et al., *Journal of applied polymer science*, **83**, 225 (2002).
8. S. Oprea, *Journal of materials science*, **45**, 1315 (2010).
9. A. Ghaffar, et al., *Journal of Chromatography A*, **1218**, 449 (2011).
10. B.K. Kim and S.H. Paik, *Journal of Polymer Science Part a-Polymer Chemistry*, **37**, 2703 (1999).

11. R.S. Dearth, H. Mertes, and P.J. Jacobs, *Prog. Org. Coat.*, **29**, 73 (1996).
12. A. Alteheld, et al., *Angewandte Chemie International Edition*, **44**, 1188 (2005).
13. Y.K. Feng, et al., *Advanced Materials Research*, **79**, 1431 (2009).
14. L. Zhou, et al., *Macromolecules*, **44**, 857 (2011).
15. P.T. Knight, et al., *Biomacromolecules*, **9**, 2458 (2008).
16. R.Z. Xiao, et al., *Int. J. Nanomed.*, **5**, 1057 (2010).
17. Y. Zhao, et al., *Macromol. Biosci.*, **4**, 901 (2004).
18. L. Liu, et al., *Journal of Applied Polymer Science*, **80**, 1976 (2001).
19. N. Boeree, et al., *Biomaterials*, **14**, 793 (1993).
20. S. Wang, et al., *Polymer Degradation and Stability*, **93**, 1364 (2008).
21. F.J.v. Natta, J.W. Hill, and W.H. Carothers, *Journal of the American Chemical Society*, **56**, 455 (1934).
22. L.S. Nair and C.T. Laurencin, *Progress in Polymer Science*, **32**, 762 (2007).
23. X.J. Loh, K.B.C. Sng, and J. Li, *Biomaterials*, **29**, 3185 (2008).
24. A. Hoglund, M. Hakkarainen, and A.C. Albertsson, *J. Macromol. Sci. Part A-Pure Appl. Chem.*, **44**, 1041 (2007).
25. D.J. Heath, P. Christian, and M. Griffin, *Biomaterials*, **23**, 1519 (2002).
26. M.A. Woodruff and D.W. Hutmacher, *Progress in Polymer Science*, **35**, 1217 (2010).
27. D.R. Miller and C.W. Macosko, *Rubber Chemistry and Technology*, **49**, 1219 (1976).
28. A. Helminen, et al., *Polymer Engineering & Science*, **40**, 1655 (2000).
29. R. Adhikari, et al., *Journal of Applied Polymer Science*, **73**, 573 (1999).
30. Z.S. Petrovic, et al., *Journal of Applied Polymer Science*, **51**, 1087 (1994).
31. C. Vogel and H.W. Siesler, in *Macromolecular Symposia*, Wiley Online Library2008, Vol. 265, pp 183-194.
32. J. Cervantes-Uc, et al., *Polymer Degradation and Stability*, **94**, 1666 (2009).
33. K. Demirelli, M. Coskun, and E. Kaya, *Polymer Degradation and Stability*, **72**, 75 (2001).
34. S.K. Cekingen, et al., *Thermochimica Acta*, **546**, 87 (2012).

Chapter 3

Cross-linkable polylactic acid and polyhydroxybutyrate

Hang SHEN [1, 2, 3], Caroline PILLON [1, 2, 3], Jianding CHEN [1, 4], Mohamed TAHA [1, 2, 3]*

1 Université de Lyon, F-42023, Saint-Etienne, France

2 CNRS, UMR 5223, Ingénierie des Matériaux Polymères, F-42023, Saint-Etienne, France;

3 Université de Saint-Etienne, Jean Monnet, F-42023, Saint-Etienne, France;

4 Laboratory of Advanced Materials Processing, East China University of Science and Technology, 200237 Shanghai, China

*correspondence：Mohamed.Taha@univ-st-etienne.fr

Résumé

Des oligomères PLA et PHB hydroxy téléchéliques de molaire contrôlée ont été synthétisés par polymérisation par ouverture de cycle ou transestérification. Ces oligomères ont été utilisés comme segments souples pour préparer en 2 étapes des polyester-uréthane fonctionnalisés allyle. Les structures attendues ont été confirmées par ^{1}H RMN, SEC et DSC. Les polyuréthanes obtenus ont été copolymérisés avec le HEMA. Les dégradations thermiques des oligomères hydroxy téléchéliques, des polyester-uréthane et des les réseaux émises ont été étudieés par la thermogravimétrie couplée FTIR.

Mots-clés: photo durcissable PLA, PHB, polyuréthane ester, conception de la structure, le réseau, la dégradation thermique

Abstract

Molar mass controlled PLA and PHB dihydroxyl telechelic oligomers were synthesized by ring opening polymerization or transesterification. These oligomers were used as soft segments in 2- step allyl-functionalized polyester-urethane synthesis. The expected structures were confirmed by ^{1}H NMR, SEC and DSC, and the obtained polyurethanes were copolymerized with 2-hydroxylethyl methacrylate. Thermal degradations of the dihydroxyl telechelic oligomers, double-bond functionalized polyester-urethanes and the issued networks were analyzed using thermogravimetry coupled by FTIR analysis.

Keywords: Photo curable, PLA, PHB, poly ester urethane, structure design, network, thermal degradation

3.1 Introduction

Biodegradable polyurethanes have been widely used in biomedical fields [1] such as in blood contact applications, contact lenses, surgical implants, and separation membranes [2-4] based on their good physicochemical and mechanical properties while exhibiting acceptable biological performances. In recent years, these materials have also been extensively studied and used in new applications such as thermo-responsive materials [5] and shape-memory materials [6] because of their contribution in the reduction of environmental issues inherent to non-biodegradable materials.

These polyurethanes, are often synthesized by reaction of a diisocyanate with a mixture of hydrolytically unstable polyester oligomer suitable to obtain multi-phase materials having defined properties [5, 7, 8]. The urethanes constitute the hard segments offering rigid character to the polyurethane while the polyester oligomer part enlarges the molar mass and softens the polymer chains. Among the hydrolytically unstable polyester oligomers, and despite its inevitable drawbacks such as mechanical brittleness, low heat resistance and synthesis costs, polylactic acid (PLA) plays a significant role as a constituent of biodegradable polyurethanes for orthopedic implants as bio-resourced renewable polymers [9]. Several studies concerning PLA-based polyurethanes were reported in literature [10-12]. Naturally synthesized by microorganisms, polyhydroxybutyrate (PHB) has drawn increasing attention during the last decades for its biocompatibility coupled with biodegradability [5, 13]. Even though the biomedical applications of PHB have been investigated for many years [14], the overall results seemed insufficient for practical applications due to its brittleness and a narrow thermo-processing window. Recently, hydroxyl telechelic PHB oligomers were obtained by transesterification [14, 15]. The use of these materials as biomaterials such as blood contact implant materials were reported by Brzeska [16] and Liu [17].

In addition to the intrinsic properties of polyester-urethanes, their functionalization can broaden their scope [1, 18-22]. And the functionality of these polyurethanes can also be altered by designing the structure, which also effect the mechanic properties of the

polyurethanes [23]. In this study, the synthesis of polyester-urethanes containing PLA or PHB segments and end functionalization with double bonds is realized by simple steps. These polyester-urethanes with controlled branched structures and functionalities are used to prepare cross-linked materials having variable properties by copolymerization with 2-hydroxyethyl methacrylate (HEMA).

3.2 Experimental

Materials

Polyhydroxybutyrate PHI002^{TM} (M_n = 4730Da, ^{1}H NMR) was purchased from NaturePLAST$^{@}$. 2-Hydroxyethyl methacrylate was purchased from Röhm GmbH. 3,6-Dimethyl-1,4-dioxane-2,5-dione (L-lactide), 4,4'-Methylenebis(cyclohexyl isocyanate), Glycerol, 1,4-butanediol, Dibutyltin dilaurate, Allylamine, Tin(II) bis (2-ethylhexanoate) were purchased from SIGMA-ALDRICH (France). Anhydrous DMF and diethyl ether were purchased from Carlo Erba Reagents^{TM}. The photo initiator was composed by reagents as follows: 60 wt% of CN381 from Sartomer (containing copolymerizable amine acrylate as synergist), 20 wt% of Benzophenone from Aldrich, and 20 wt% of 2,2-Diethoxyacetophenone from Aldrich. 2-Hydroxyethyl methacrylate was distilled before use. Glycerol was dehydrated by molecular sieves 3 Å (rod shape, size 1/16 inch, Fluka) for 1 week before use. All other reagents were used as received without further purification.

Synthesis of telechelic polylactide (PLA) and polyhydroxybutyrate (PHB) oligomer

The synthesis of the telechelic dihydroxyl PLA oligomer was made as shown in Scheme 1. Typically L-Lactide was added into a 250mL glass batch reactor designed for mixing viscous materials equipped with previously dried nitrogen flow and condenser, and heated at 130^{o}C until all reagents were completely melted. Then a certain amount of 1, 4-butanediol depending on the D_p of the synthesized oligomer and $Sn(Oct_2)$ (1% of the LLA, mol / mol) was injected in. The polymerization was kept under the previously dried nitrogen flow in a silica

column for 3 hours. The synthesized oligomers were immediately characterized and used for the next step syntheses.

For the synthesis of telechelic dihydroxyl polyhydroxybutyrate, PHB (10g) was dissolved in 100mL of chloroform and refluxed for 45mins at 75°C until the system became homogeneous. Then p-toluenesulfonic acid (4.8g) and 1, 4-butanediol (20g) were injected in and mixed. The reaction was carried out at 75°C for 8-24h depending on the required molar mass of PHB. The obtained solution was washed 3 times with distilled water, concentrated and dried under vacuum at 70°C to remove the water. The obtained telechelic dihydroxyl polyhydroxybutyrate was from brown liquid to white solid at room temperature depending on its molar mass.

Syntheses of polyurethane prepolymer and allyl functionalized polyurethanes

A typical synthesis procedure of polyurethanes is as follows (see Scheme 2): glycerol and PLA (or PHB) oligomers were first introduced into a 2-neck flask equipped with previously dried nitrogen flow and condenser. Anhydrous DMF was injected in as the solvent and the system was magnetically stirred until it became homogeneous at room temperature. Then the H_{12}MDI was injected and mixed at room temperature for 5 minutes. Finally the dibutyltin dilaurate was introduced as the catalyst and the whole system was stirred and kept at 80°C in an oil bath for 55 minutes. During the reaction, FTIR was used to monitor the consumption of the isocyanate groups.

The obtained polyurethane solution was diluted with anhydrous DMF and placed in an ice-water bath with magnetic stirring. Then allylamine was dropwise added in to react with the remaining isocyanate groups. The reaction was conducted until the remaining isocyanate groups completely reacted. Then the products were precipitated in ethyl ether, re-dissolved in chloroform and re-precipitate in ethyl ether three times. Then, the obtained solid was collected and dried under vacuum at room temperature for 24 hours and stored at -20°C.

Methacrylate PU network formation by UV irritation

Different allyl-functionalized PCL-segmented polyurethanes were dissolved in HEMA with mass ratio M_{HEMA} : M_{PU} = 1.5 : 1 at room temperature using a shaker until the solution became homogeneous. Then, the photo initiator was fully solubilized in the system by oscillation at room temperature for 3mins. An ultrasonic oscillator was used to remove bubbles before curing.

The mixtures were placed in LDPE moulds (100mm x 10mm x 100µm) and cured in air with a fluorescent lamp, JAD STS-350, equipped with 8W x 3 fluorescent tubes offering λ=250nm UV light. The mixtures were exposed at 3cm for 24hrs. After curing, the samples were collected for analyses.

Instrumentation

FT-IR absorption spectra were recorded on a Nicolet Nexus spectrometer (400-4000 cm^{-1}) using ATR technique.

H-NMR spectra were recorded in a $CDCl_3$ solution at room temperature using a Bruker Avance II spectrometer operating at a frequency of 250 MHz. The chemical shift scales were calibrated on the basis of the TMS peak (0 ppm).

Differential scanning calorimetry (DSC) measurements for the allyl-functionalized PCL-segmented polyurethanes and PU / PHEMA networks were carried out with a Q10 calorimeter from TA Instruments. Samples were transferred to hermetic pans and sealed, and analyzed from -80°C to 210°C with a cooling / heating rate of 10°C·min^{-1}. The glass transition temperatures were evaluated from the data recorded during heating by identifying the inflection points. Each sample underwent two cycles of heating-cooling cycles.

For the analyses of allyl-functionalized PLA-segmented polyurethanes, Size Exclusion

Chromatography (SEC) was conducted using a system equipped with refractive index (Waters 2414) and light scattering (Wyatt MiniDawnTreos) detectors. Two columns HR1 and HR3 from Waters were used. The eluent was tetrahydrofuran (THF) with a flow rate of 1 $mL \cdot min^{-1}$ and the elution temperature was 35°C. The molar mass of copolymers were determined using a calibration curve established on a set of polystyrene standards. For the analyses of allyl-functionalized PHB-segmented polyurethanes, Size Exclusion Chromatography (SEC) was conducted using a system equipped with UV detector (Waters 486, wavelength = 280 nm), light scattering detector (Wyatt TREOS) and RI refractometer detector (Schimadzu RID 10A). Two columns PLgel 5µm MIXED-C and PLgel 20mm Guard from Organic GPC were used. The eluent was chloroform with a flow rate of 1 $mL \cdot min^{-1}$ and the elution temperature is 22°C. The samples tested were prepared with a concentration of 2$mg \cdot mL^{-1}$.

A thermogravimetric analyzer (TGA) from Mettler Toledo, TGA/DSC 1, was used to perform the thermogravimetric analysis. Thermal degradation experiments were done under nitrogen purge with a flow rate of 80 $mL \cdot min^{-1}$ for all experiments. Samples ranging from 15 to 20 mg were heated at a heating rate of 10°C$\cdot min^{-1}$ from ambient temperature to 550°C.

For the TGA–FTIR study, the TGA was interfaced with a Thermoscientific Nicolet™ Fourier transform infrared (FTIR) spectrometer using TGA / FTIR interface. The IR cell and the heated line transferring evolved gases from the TGA to the FTIR were maintained at 225°C and 215°C respectively. IR spectra were recorded in the spectral range of 4000–500 cm^{-1} with a 4 cm^{-1} resolution throughout the degradation analyses.

3.3 Results and discussions

3.3.1 Syntheses and characterizations of multi-allyl functionalized polyurethanes

Properties of the polyurethanes mainly depend on their soft / hard segment properties and compositions and their structure. In this study, PLA and PHB oligomers, having well-defined molar masses soft segments were used in polyurethane syntheses.

Hydroxy telechelic PLA and PHB oligomers were first synthesized and characterized.

Syntheses and characterizations of PLA / PHB dihydroxy telechelic oligomers

The syntheses of PLA (or PHB) dihydroxy telechelic oligomers are illustrated in Scheme 1. Dihydroxyl-terminated PLA oligomers were obtained by Tin (II) 2-ethylhexanoate catalyzed lactide ring opening polymerization with 1,4-butanediol as dialcohol co-initiator. Dihydroxyl-terminated PHB was prepared by transesterification between a commercially available PHB and 1,4-butanediol using p-toluene sulfonic acid as catalyst.

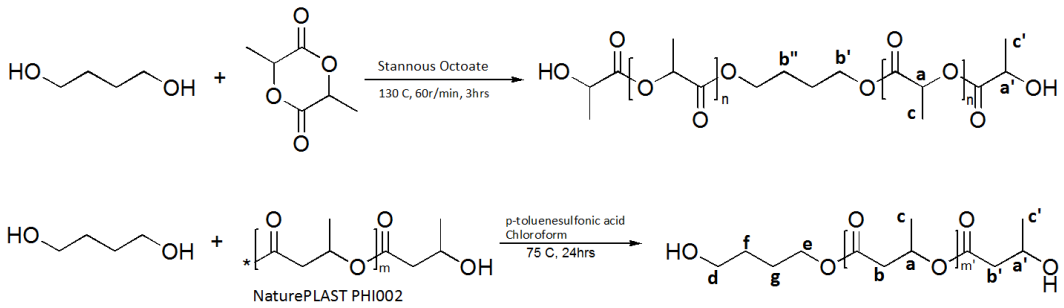

Scheme 1. Synthesis of dihydroxyl telelic polylactide and polyhydroxybutyrate

The obtained products were analyzed by ^{1}H NMR and depicted in Figures 1, 2 and Table 1, 2:

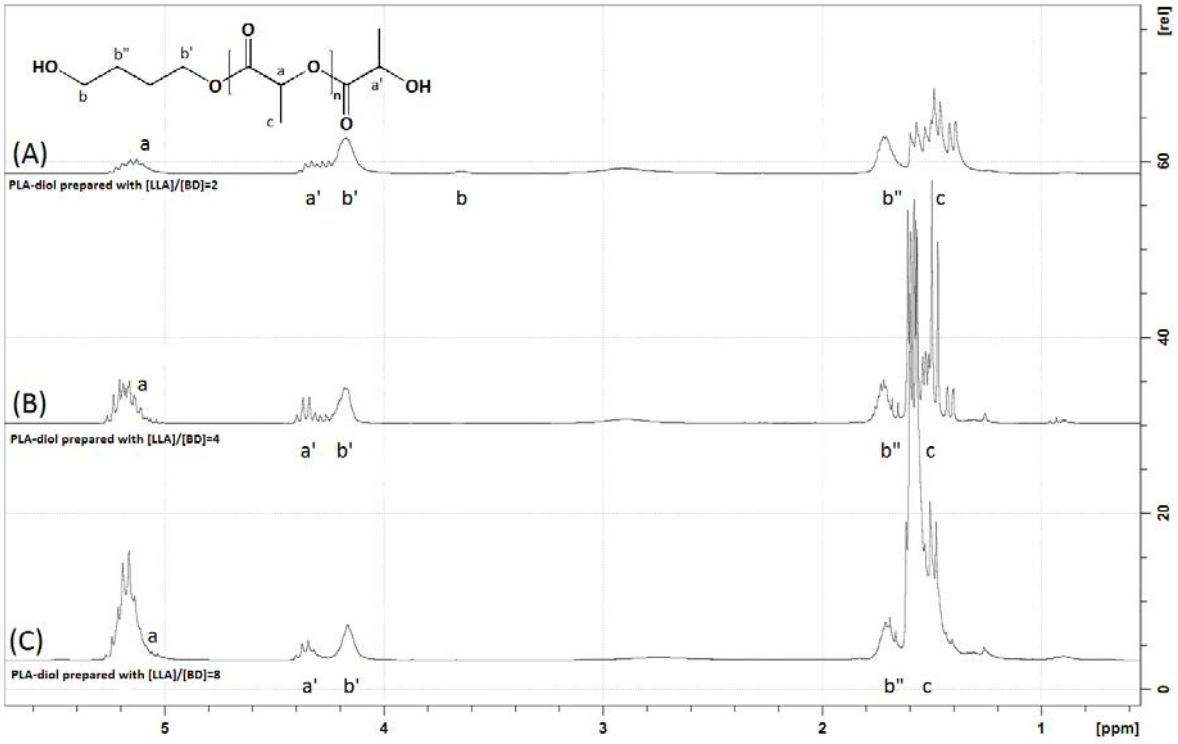

Figure 1. The ^{1}H NMR spectrum of telechelic hydroxylated PLA oligomer with different [LLA] : [BD] feeding ratios in $CDCl_3$, from 3.0ppm to 5.5ppm: (A) [LLA] : [BD] =2; (B) [LLA] : [BD] =4; (C) [LLA] : [BD] =8.

Figure 1 shows the possible structure and the ^{1}H NMR spectra of the telechelic dihydroxyl PLA synthesized with different [PLA] / [1, 4-butanediol] mole ratios. The quartet at 4.35ppm and the multiplet at 5.2ppm correspond to protons a and a' from main / end chain methines of PLA repeat units. The ratio (a+a') / a represents the polymerization degree of the oligomer. It is clear that this ratio decreased when the [LLA] / [1, 4-butanediol] ratio decreased. The molar mass of the oligomers calculated from ^{1}H NMR spectra listed in Table 1 is in accordance with SEC results. Furthermore, if the ratio of [LLA] / [1, 4-butanediol] is less than 4, some hydroxyl group from 1, 4-butanediol did not initiate the ROP and generated adjacent methylene proton b in Figure 1. The obtained PLA oligomers were used for the polyurethane synthesis immediately after the polymerization because of its hydrophilicity [24].

Table 1 Molar mass and T_g of hydroxyl telechelic PLA oligomers synthesized with different [LLA] / [BD] ratios, polymerizations were performed at 130°C for 3hrs.

ratio of [LLA]/[BD] (mol/mol)	8	4	2
Theoretical M_n (g/mol)	1387	811	622.51
M_n by SEC (g/mol)	2242	1060	681
M_n by ^{1}H NMR (g/mol)	1684	860	537
T_g by DSC (°C)	4.67	-14.6	-28.8

The ^{1}H NMR spectra of the telechelic dihydroxyl PHB oligomer prepared by transesterification with dialcohol are shown in Figure 1. The molar mass of a PHB oligomer can be controlled by adjusting the transesterification reaction time.

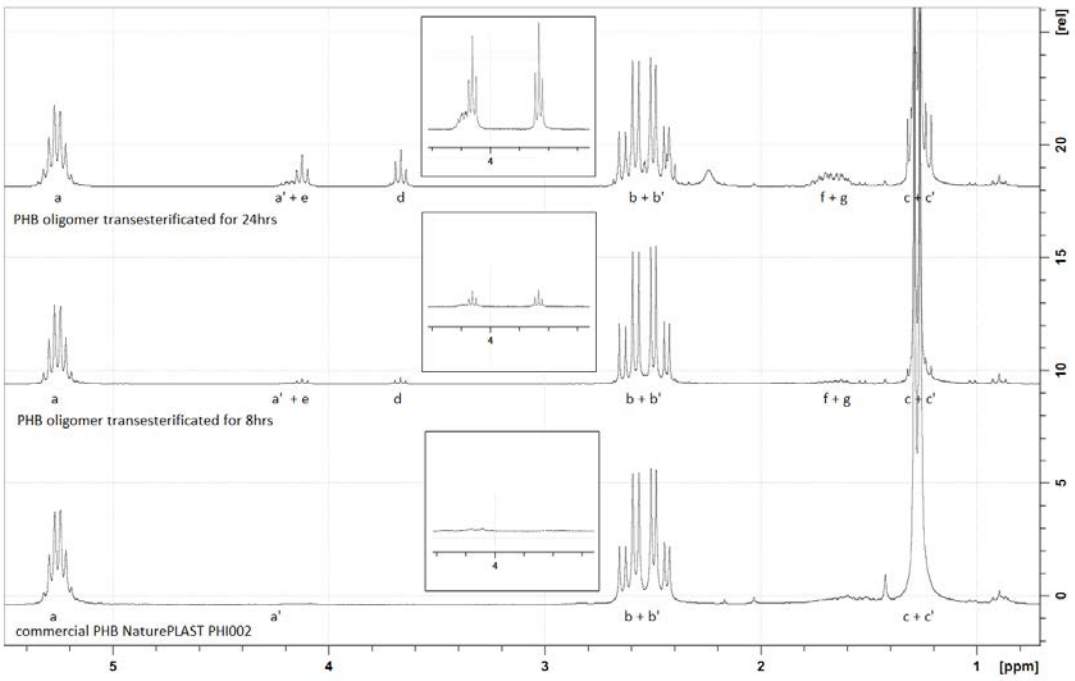

Figure 2. The ^{1}H NMR spectrum of purified telechelic hydroxylated PHB oligomer from 1ppm to 5ppm, the experiment was performed at 70°C with chloroform reflux

Transesterification of PHB and 1, 4-butanediol led to the formation of mass-reduced telechelic oligomers. Their structures are shown in Scheme 1. Comparing the commercial PHB and the prepared PHB oligomers, new protons belonging to 1,4-butandiol attached on the oligomer end chain are obtained: d (triplet), e (triplet), f and g (multiplets). The sextets a and a' represent the methine proton of the PHB repeat unit. Therefore, the polymerization degree can be calculated as the ratio 2(a+a') / e. As expected, the Dp_n decreased with reaction time. ^{1}H NMR results are depicted in table 2:

Table 2 Molar mass and T_g of hydroxyl telechelic PHB oligomers synthesized with esterification temperatures, transesterifications were performed for 24hrs.

Samples	PHB (PHI002)	PHB oligomer 1	PHB oligomer 2
M_n by ^{1}H NMR (g/mol)	4230	1470	980
T_g by DSC (°C)	1.9	1.4	-0.8
Reaction time (h)	0	16	26

Syntheses and characterizations of multi allyl functionalized polyurethanes

By designing the structures of the telechelic PLA or PHB segmented polyurethanes, structures including hard / soft segment composition, double bond functionality of the polyurethanes

could be changed as well as the methacrylated networks based on these polyurethanes. Different structures were designed; an example is given in Figure 3:

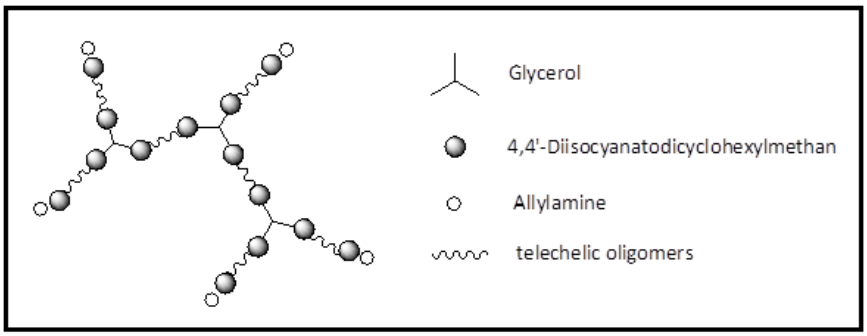

Figure 3. Polyurethane structure with double bond functionality equal to 5 the mole ratio of each component is [H12MDI] : [Glycerol] : [telechelic oligomer] : [allylamine] = 17.65 : 3 : 7 : 5

Miller – Macosko equations 1-3 [25] mentioned in chapter 2 were used again to avoid cross-linking of the reactive system fixing gel conversion to a higher value than one (typically 1.05). Formulae of polyurethanes synthesized in this study were listed in Table 3:

$$P^2_{gel} = \frac{1}{(\overline{f}_A - 1)(\overline{f}_B - 1)} \times \frac{1}{r} \quad \text{Eq.1}$$

$$\overline{f}_i = \frac{\sum n_i f_i^2}{\sum n_i f_i} \quad \text{Eq.2}$$

$$r = \frac{n_A f_A}{n_B f_B} \quad \text{Eq.3}$$

Table 3. Formula and compound details for polyurethane syntheses

Entry	Expected double bond functionality	Degradable segment numbers in expected structures	M_n of degradable segment (Da)	Mole ratio of the reagents (H_{12}MDI : glycerol : PLA (or PHB) : allylamine)
Run 1	3	1	PLA / 870	4.41 : 1 : 1 : 3
Run 2	3	2	PLA / 870	5.52 : 1 : 2 : 3
Run 3	3	3	PLA / 870	6.62 : 1 : 3 : 3
Run 4	3	3	PLA / 530	6.62 : 1 : 3 : 3
Run 5	3	3	PLA / 1680	6.62 : 1 : 3 : 3
Run 6	5	7	PLA / 870	17.65 : 3 : 7 : 5
Run 7	7	11	PLA / 870	28.7 : 5 : 11 : 7
Run 8	3	1	PHB / 980	4.41 : 1 : 1 : 3
Run 9	3	2	PHB / 980	5.52 : 1 : 2 : 3
Run 10	3	3	PHB / 980	6.62 : 1 : 3 : 3

Run 11	3	3	PHB / 1470	6.62 : 1 : 3 : 3
Run 12	5	7	PHB / 980	17.65 : 3 : 7 : 5
Run 13	7	11	PHB / 980	28.7 : 5 : 11 : 7

As shown in Table 3, from Run1 to Run3 (or Run 8, 9 and 10 for PHB system), the tri-functionalized polyurethane was segmented with a different number of the same degradable oligomers. The group including Runs 3, 4 and 5 (or Run 10 to Run 11 for the PHB system) is designed by using the same number of degradable segments but with different molar masses in synthesizing tri-functionalized polyurethanes. When comparing Runs 3, 6 and 7 (or Runs 8, 12 and 13 for the PHB system), different functionalities of these polyurethanes were expected. These 3 groups were designed to alter the hard / soft segment compositions and the double bond functionalities of the polyurethanes.

Synthesis monitoring of multi allyl functionalized polyurethanes synthesis by FTIR

Syntheses of polyurethanes were monitored by FTIR as illustrated in Figure 4. C-H stretching absorption of methyl groups around 3000 cm^{-1} was used as the constant peak. The first step of the synthesis was performed at 80° C. After 55mins, the absorption at around 2263 cm^{-1} (assigned to the N=C=O group) stopped decreasing and became constant. The elimination of the absorption at 3476 cm^{-1} (assigned to the -OH group) and the appearance of the absorption peak at around 3350 cm^{-1} (assigned to the -NH group) confirmed the consumption of the alcohols. Then allylamine was added to the reactive system. When the N=C=O absorption at 2263 cm^{-1} completely disappeared, the second step was achieved.

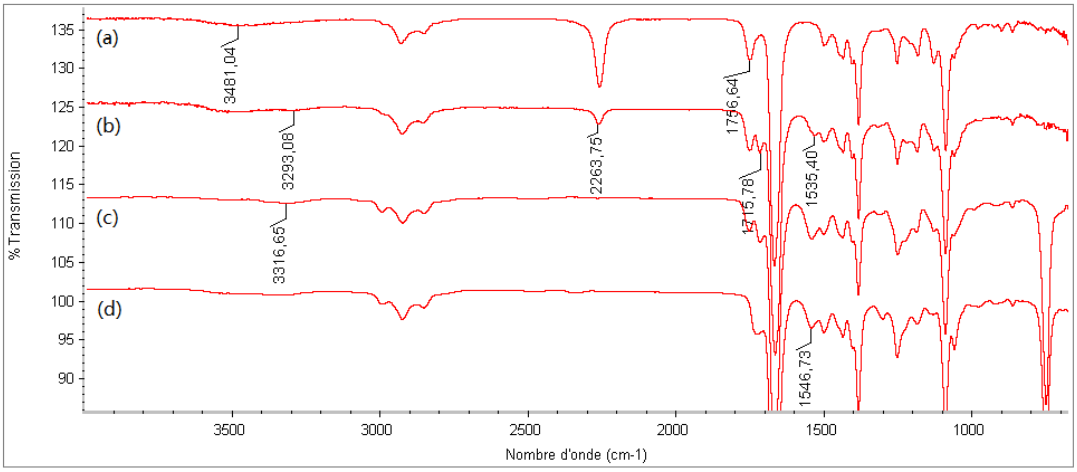

Firgure 4. FTIR spectra for the monitoring of the allyl-functionalized polyurethane syntheses. For PLA-segmented PU Run3: (a) reagents at initial time, (b) PLA-segmented PU prepolymer after the first step of synthesis, (c) allyl-functionalized PLA-segmented PU after the second step; for PHB-segmented PU Run10: (d) allyl-functionalized PHB PU after the second step

Qualitative characterizations of multi-allyl functionalized polyurethanes by ^{1}H NMR

The obtained polyurethane was purified twice with large amount of diethyl ether to remove the unreacted small moles and catalysts. Then they were dried under vacuum and analyzed by ^{1}H NMR. An example is shown in Figure 5.

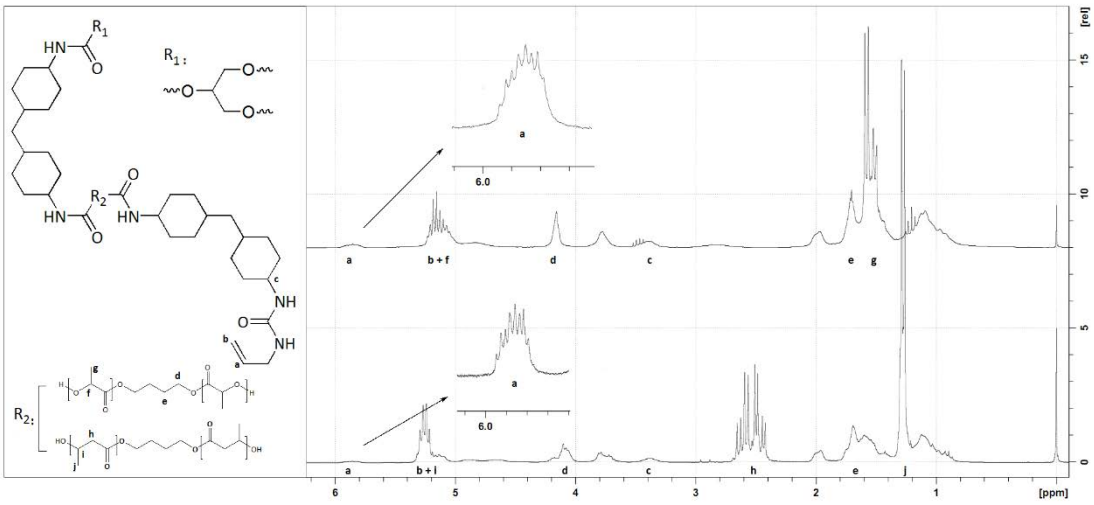

Figure 5. The expected structure of allyl functionalized polyurethane (left) and their ^{1}H NMR spectra (right): PLA based PU for Run3 (upper) and PHB based PU for Run11 (lower) in $CDCl_3$. All the samples are purified before the analyses.

^{1}H NMR spectra of polymers are presented in Figure 5 to confirm the polyurethane structures. Each component of the Polyurethanes can be easily recognized. For PLA-segmented

polyurethane, the methyl and methine protons from lactide repeat unit can be located as g and f at 1.5 and 5.2ppm respectively. For PHB-segmented polyurethane, protons from methyl and methylene as well as methine protons from its hydroxybutyric repeat unit can be recognized at 1.2, 2.5 and 5.2ppm, labeled as j, h and I respectively. For both systems, the methylene proton of 1, 4-butanediol segments can also be found as d and e on the spectra. The intensive multiplet from 0.8 to 2.1ppm is attributed to the protons of H_{12}MDI cyclohexyl rings, with the methine proton c adjacent to the urethane linkage that can be found at 3.4ppm. Protons from allyl functions can also be found at 5.2 and 5.8ppm as b and a.

For the PLA-based PU, the PLA protons f and g were overlapped by other protons, so the 1,4-butandiol methylene proton d was used to evaluate the mole ratio [LA] / [allyl].

r_{PLA} = [LA] /[allyl]= d / 4a * N

Where N is the Dp_n of PLA;

For the PHB-based PU, the mole ratio of PHB repeat units to allyl functions can be evaluated as the ratio of methylene protons of PHB to allyl protons:

r_{PHB} = [PHA] / [allyl] = j / 2a

Some results are listed in Table 4:

Table 4. The average ratio of repeat unit to double bond functions in allyl functionalized polyurethane moles, by idea value and by real value respectively. All polymerization were performed with 0.5 mol% of DBTDL at 80°C for 60mins for the first step, and at 0°C for 30mins for the second step.

Samples	Run3	Run6	Run7	Run11
Functionality of expected structured PEUs	3	5	7	3
Expected [allyl function]/ [LA (or HB)] repeat unit , mol : mol	1 : 4N	1 : 5.6N	1 : 6.2N	1 : 48.0
Calculated [allyl function]/ [LA (or HB)] repeat unit by ^{1}H NMR results, mol : mol	1 : 3.8N	1 : 5.3N	1 : 6.4N	1 : 46.4

Comparing the expected ratio to the real ratio from the obtained product by ^{1}HNMR analyses, the values are very close to each other, proving the expected structure by formula design.

SEC and DSC analyses of multi-allyl functionalized polyurethanes

To further evaluate the structures of the products, these allyl-polyurethanes were analyzed by SEC. The results are listed in Table 5. The molar mass of the polyurethanes can be affected by 3 factors: functionality, number of the degradable segments and molar mass of these segments. As expected, the molar mass of the polyurethanes increased when each of these factors increased.

Table 5. Molar mass obtained from SEC analyses and glass transition temperature by DSC analyses for the mulit-allyl functionalized polyurethanes. All polymerization were performed with 0.5 mol% of DBTDL at 80°C for 55mins for the first step, and at 0°C for 30mins for the second step. All samples were purified before the analyses.

Entry	[NCO] / [OH], mol / mol	M_n / M_w	degradable segment content, wt%	Glycerol content, wt%	Double bond content, mmol/g	T_g °C
Run 1	1.60	7620 / 14620	37.9	3.69	1.31	53.9
Run 2	1.43	7160 / 15060	50.3	2.52	0.87	47.4
Run 3	1.33	9730 / 25020	56.6	1.32	0.65	49.2
Run 4	1.33	7520 / 22350	44.6	2.41	0.83	59.0
Run 5	1.33	11780 / 32620	71.6	1.27	0.42	27.5
Run 6	1.22	11500 / 35670	53.9	2.37	0.44	46.1
Run 7	1.19	16800 / 47400	53.2	2.50	0.39	46.0
Run 8	1.60	3972 / 10270	40.8	3.53	1.25	18.5
Run 9	1.43	4880 / 11100	53.4	2.38	0.81	7.8
Run 10	1.33	5185 / 9502	59.5	1.79	0.61	13.2
Run 11	1.33	13470 / 37870	68.7	1.39	0.46	1.7
Run 12	1.22	5926 / 10429	56.9	2.23	0.41	2.7
Run 13	1.19	6868 / 14860	56.2	2.34	0.36	2.6

Glass transition temperatures of these allyl-functionalized polyurethanes were measured by DSC (Table 5). The PLA segmented polyurethanes have the same T_gs. These T_gs are, as expected, higher than the T_g of PLA oligomers used in the PU synthesis (Table 1) because of the presence of urethane functions that harden the polymer chains and also induce hydrogen bonds. The product obtained in Run5 (PU with PLA M_n=1680) has a T_g obviously lower than the others. This difference is the result of longer PLA chain and PCL content that decrease the hard segment content and consequently result in fewer hydrogen bonds. For PHB-segmented polyurethanes as well, the T_gs of the poly ester-urethanes shift towards the T_g of PHB when PHB content increases.

3.3.2 Methacrylated PU copolymer networks syntheses and thermal characterizations

2-hydroxyl ethylmethacrylate was used as co-monomer and also as reactive solvent of the prepolymers prepared in section 3.1 (scheme 2). The mass ratio M_{HEMA} : M_{PU} = 1.5 : 1 was used for all samples and the copolymerizations were UV initiated. The obtained products became insoluble in THF and chloroform as a result of cross-linking.

PU / PHEMA networks by DSC

The obtained PU / PHEMA networks were analyzed by DSC. Results are given in Table 6. For all samples, only one glass transition was observed, indicating the homogeneity of the networks and the good compatibility of the polyurethanes and PHEMA.

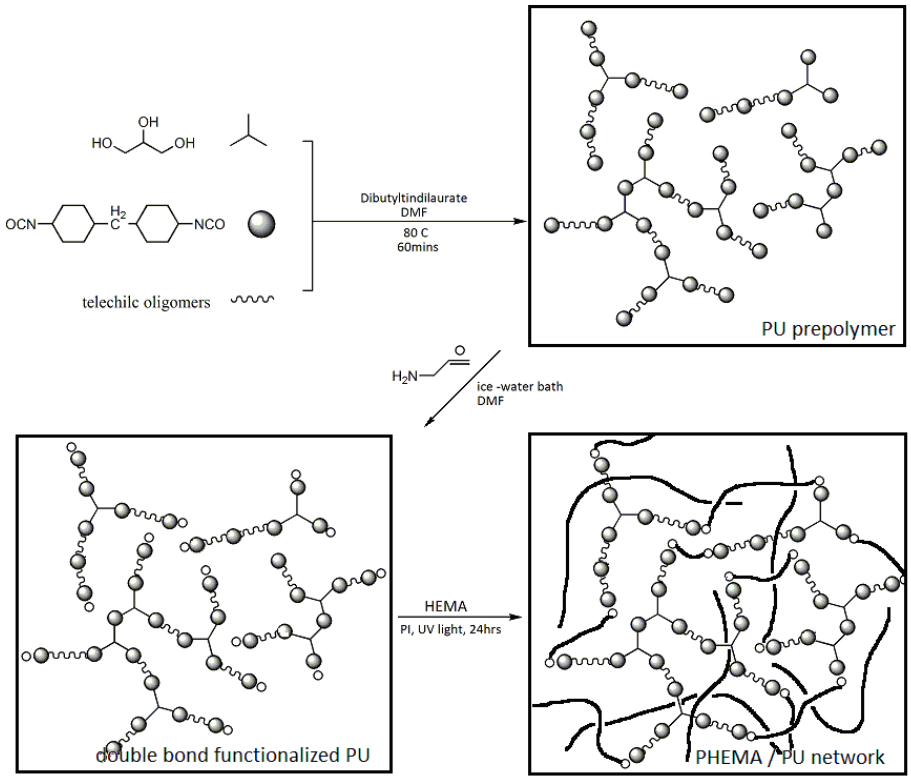

Scheme 2. 2-step syntheses of PLA / PHB segmented, double bond end functionalized polyurethanes and the following networks prepared by PU copolymerized with HEMA

Table 6. The polyurethane composition in the network and the Tg of the network obtained by DSC tests. All networks were performed with 3 wt% of photo initiator and the mass ratio M_{HEMA} : M_{PEU} = 1.5 : 1, the mixtures were irradiated by UV exposure for 24hrs

Entry	Polyurethane adapted in network formation	degradable segment concentration, wt%	T_g of the PEU or the network, °C
Run14	Run1	PLA, 15.2	62.3
Run15	Run2	PLA, 20.1	61.5
Run16	Run3	PLA, 22.6	59.6
Run17	Run4	PLA, 17.8	68.5
Run18	Run5	PLA, 28.6	28.0
Run19	Run6	PLA, 21.6	60.3
Run20	Run7	PLA, 21.3	62.9
Run21	Run8	PHB, 16.3	36.3
Run22	Run9	PHB, 21.4	18.7
Run23	Run10	PHB, 23.8	16.0
Run24	Run11	PHB, 27.5	6.7
Run25	Run12	PHB, 22.8	7.9
Run26	Run13	PHB, 22.5	5.7

For all the data illustrated in Table 6, it can be seen that the cross linking ability of the polyurethane obviously affects the glass transition of the network.

Investigating networks formed by PLA-segmented polyurethanes, samples from Runs 17, 16 and 18 were based on the polyurethanes from Run 4 (PLA, M_n=530), Run 3 (PLA, M_n=870) and Run 5 (PLA, M_n=1680). In this group, Run 4 has the lowest PLA content and the highest double bond concentration, so the network based on Run 4 has the highest T_g when compared with other networks. On the contrary, Run 5 has more PLA content which leads to its lower T_g and lower double bond concentration. When synthesizing the network with this polyurethane, the obtained network shows almost no increase of its glass transition temperature. Similar trends can be observed when comparing Run14, Run15 and Run16 based on polyurethanes from Run1 (1 PLA segment), Run2 (2 segment) and Run3 (3 segment). Though these 3 polyurethanes have similar T_g, the network from Run14 based on polyurethane from Run1 with more cross-linkable double bonds shows higher glass transition temperature than the network from Run16 based on Run3. When comparing polyurethanes with different functionalities, polyurethanes from Run6 (f=5) and Run7 (f=7) have similar composition and double bond concentration, so the networks based on these have the same T_g.

The PHB-segmented polyurethane-based networks illustrate more clearly the conclusion drawn just above: network from Run21 composed of Run8 (1 PHB segment) shows completely different T_g, higher than in other networks, while the network from Run23 and polyurethane from Run10 have almost the same T_g due to a low double bond quantity in the polyurethane from Run10. Networks from Run25 and Run26 have even lower T_g because the polyurethanes from Run12 (f=5) and Run13 (f=5) have the lowest double bond concentration among all polyurethanes. From the data listed above, it can be seen that the T_g of the network mainly depends on the crosslinking density provided by polyurethanes with different double bond concentration, and the T_g of the polyurethane.

3.3.3 Thermal degradation of the UV irradiated polyurethane / PHEMA networks monitored by TGA-FTIR

Thermal Degradation should be considered when a biomaterial must be processed at high temperature such as in extrusion or injection molding. Representative specimens were analyzed in this part.

a. Thermal degradation of telechelic PLA and PHB oligomers

Figure 6 shows the thermal degradation process of the PLA oligomer with molar mass 870 (resulted from ^{1}H NMR analysis in Table 1). From TGA and DTGA curves, it can be seen that the degradation of the PLA oligomer starts at 180^{o}C and reaches its maximum degradation rate around 300^{o}C

Correspond with the TGA and DTGA curve, Gram-Schmidt trace shows the degradation product of PLA oligomers. According to the spectra of the coupled FTIR, lactide is discovered as the main degradation product during the degradation by bands at 3006cm^{-1} (γCH_3), 2949cm^{-1}($\gamma_{as}CH_3$), 2891cm^{-1} (γ_sCH_3), 1790cm^{-1} (γC=O), 1236cm^{-1} and 1116cm^{-1} (γ_sC-O-C). Besides, the ring skeletal vibration at 932cm^{-1} is a characteristic absorption for the cyclic oligomer that is also shown in lactide FTIR spectra. By contrast with the former research [26],

the characteristic absorption of acetaldehyde at 3475 (γC=O) and 2740 (γCHO) was not detected, indicating that aldehyde wasn't generated during the degradation, and neither was the generation of carbon monoxide or dioxide with absorptions at 2350cm^{-1} and at 2170 / 2115cm^{-1}. The γO-H band at 3576cm^{-1} is believed to originate from the hydroxyl group of lactide and 1,4-butanediol, the co-initiator that ROP the LLA.

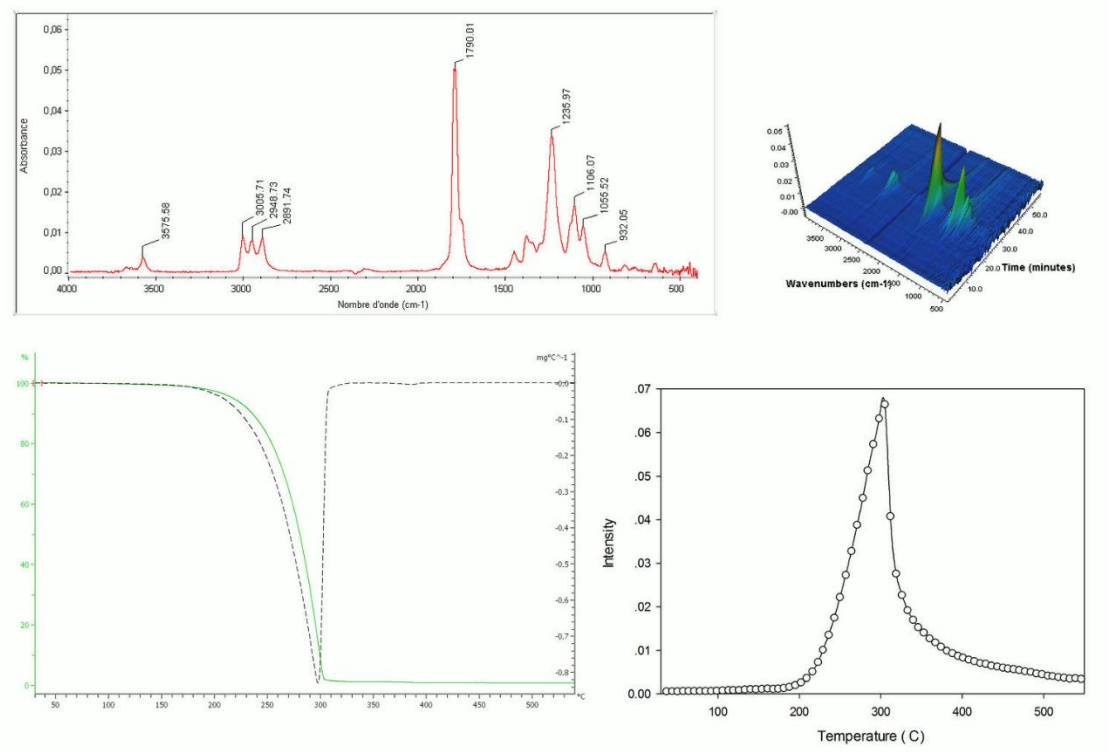

Figure 6. TGA, DTGA curves and 3D FTIR spectra for degradation of PLA oligomer. The PLA oligomer was prepared with mole ratio [LA] : [BD]=8 at 130°C for 3hrs. The IR spectrum top left was collected at 305°C

Compared to PLA oligomers, PHB-diol has a higher starting degradation temperature but a narrower degradation range around 310 °C, as shown in Figure 7. Degradation of the PHB generates crotonic acid as the main product with absorption at 3576cm^{-1} (γO-H), 3056 to 2882cm^{-1} (γC-H), 1768 and 1752cm^{-1} (γC=O), 1660cm^{-1} (γC=C), 1451cm^{-1} (γC-H), 1357cm^{-1}(γCH$_3$), 1144 and 1093cm^{-1}(γC-O), 964cm^{-1}(γ trans C=C). The absorption at 694 cm^{-1} is characteristic for the cis-configuration of crotonic acid, which corresponds with the former researches [27, 28].

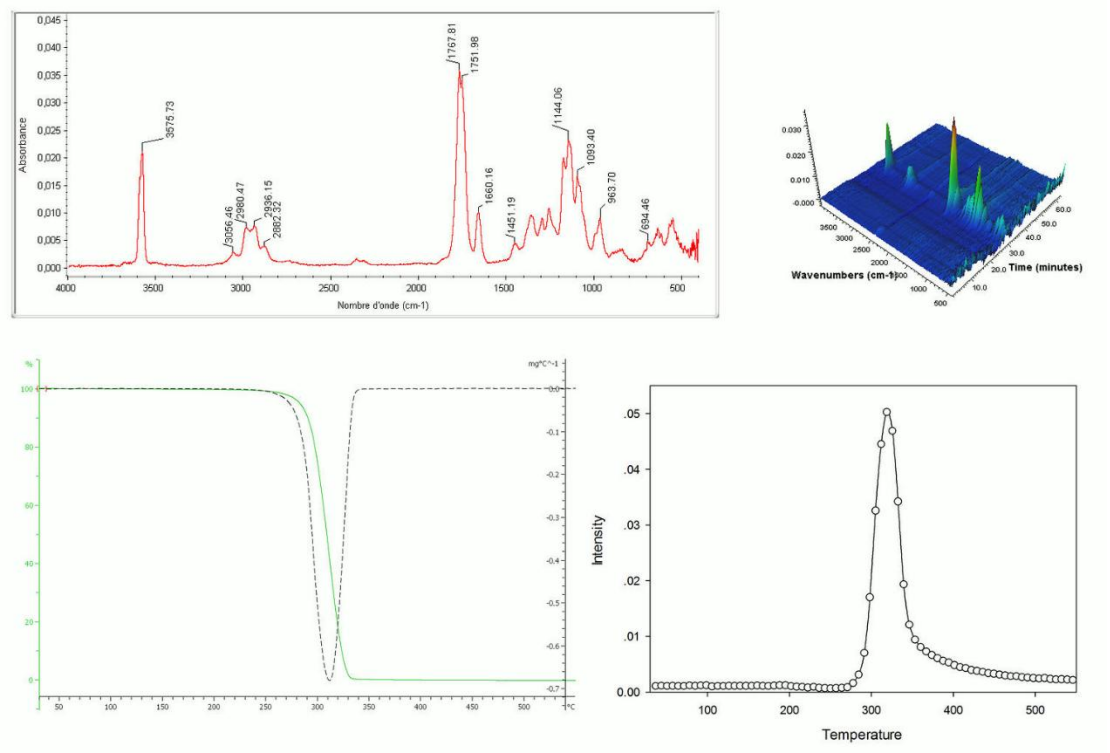

Figure 7. TGA, DTGA curves and 3D FTIR spectra for degradation of PHB oligomer. The PHB oligomer with Mn=980 was prepared with chloroform reflux at 70°C for 24hrs, as shown in Table 2. The IR spectrum top left was collected at 312°C

b. Thermal degradation of allyl functionalized PLA or PHB segmented polyurethanes

The thermal degradations of allyl-functionalized polyurethanes were investigated based on their degradable segment degradation mechanism illustrated above. In this study, Run 1 from PLA and Run 8 for PHB systems were chosen for their higher isocyanate content. The degradation of the isocyanate of these polyurethanes can be more clearly shown on the curves. Results were illustrated in figure 8 and 9.

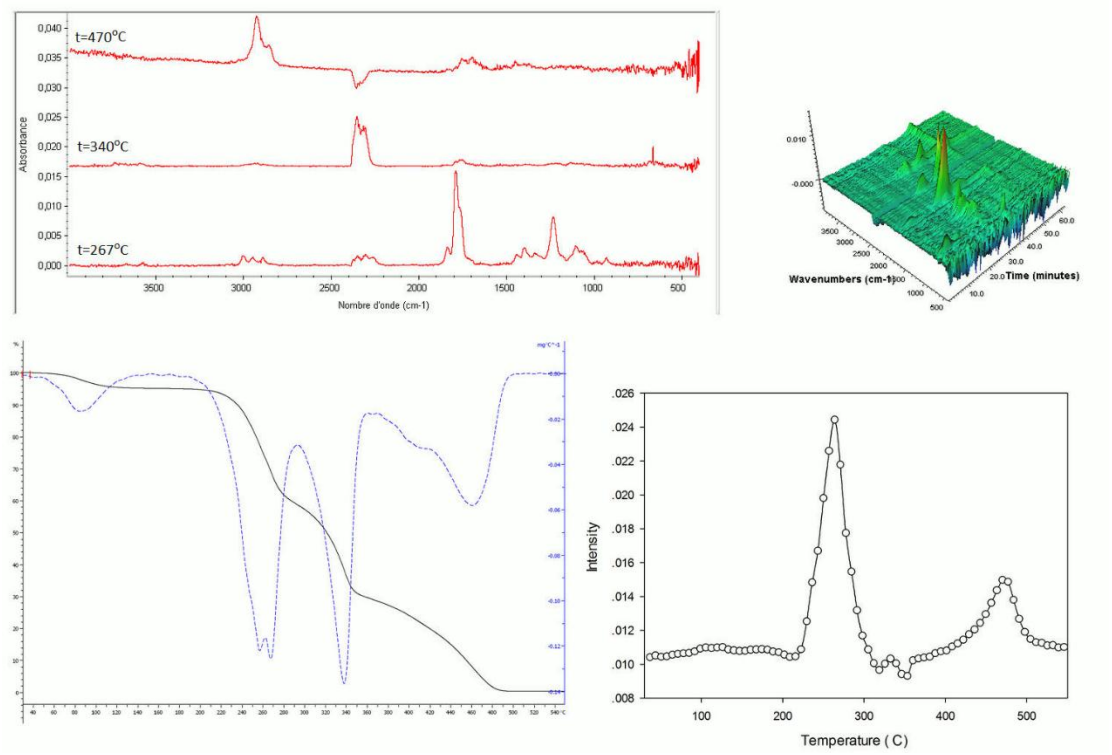

Figure 8. TGA, DTGA curves and 3D FTIR spectra for degradation of PLA-segmented purified polyurethane Run1. The FTIR spectra were obtained at the maximum evolution rate for each decomposition step.

Figure 8 shows the thermal degradation of the PLA segmented polyurethane Run1. For TGA and DTGA and Gram-Schmidt curves, the weight loss below 150°C is the evaporation of the remaining solvent (DMF).

Compared with the degradation of PLA oligomers, 3 new degradation steps were shown by DTGA curve and Gram-Schmit traces around 260°C, 340°C and 460°C. Moreover, the degradation step at 260°C overlaps the PLA degradation step at similar temperature range (270°C). According to the research of Cervantes et al. [29], these 3 new degradations belong to the degradation of H_{12}MDI, including the decomposition of urethane linkage, the continuous degradation of cyclohexyl rings around and finally the generation of fragments containing amino groups. FTIR spectra shown in Figure 8 are the yielding gaseous products collected at the maximum evolutions in each decomposition step. The spectrum of the product collected at 257°C in Figure 8 corresponds to the lactide monomer. At 340°C, the increase of isocyanate absorptions at 2260cm^{-1} is due to carbamate groups' decomposition

which happened simultaneously during the degradation of PLA segments, corresponding to the DTGA curve. At 470°C, the increase of C-H absorption around 2900cm^{-1} is attributed to the hydrocarbons generating from further degradation of isocyanate fragments, and absorption centered at 1520cm^{-1} is believed to be the hydrocarbon with amino groups, according to Cervantes's reports. By contrast with Cervantes's research, the carbon dioxide absorption at 2349cm^{-1} continues to increase, shown by IR spectrum collected at 340^{o}C. It comes from the decomposition of isocyanate groups (N=C=O) with considerable amounts in the composition of polyurethane. The degradation of PLA segments was completing, with only a few of lactide detected at this stage.

Figure 9 shows the PHB segmented polyurethane thermal degradation. Different from the thermal degradation of PLA segmented polyurethanes, the decomposition of the carbamate happened before the degradation of the PHB segment. As shown by IR spectrum at 257^{o}C in Figure 9, isocyanate absorption was detected with trace absorption of crotonic acid - the degradation product of PHB that appeared at higher temperature (260-335^{o}C). The 3-step degradation of H_{12}MDI can also be seen in DTGA curve and IR spectra at 278^{o}C, 345 / 367^{o}C and 470^{o}C respectively.

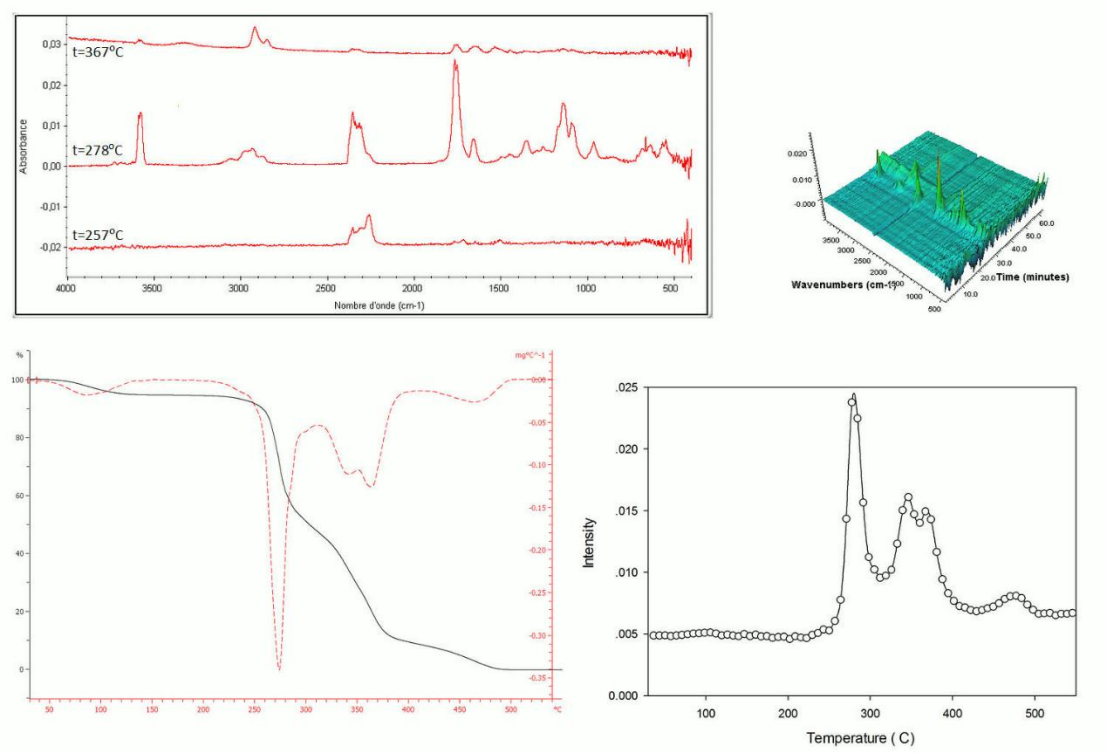

Figure 9. TGA, DTGA curves and 3D FTIR spectra for degradation of PHB segmented polyurethane Run8 and the FTIR spectra were obtained at the maximum evolution rate for each decomposition step.

To further investigate the degradation behavior of PLA and PHB segmented polyurethanes with different compositions, all polyurethanes synthesized in Table 3 were characterized with TGA and compared with each other with results listed in Figure 10.

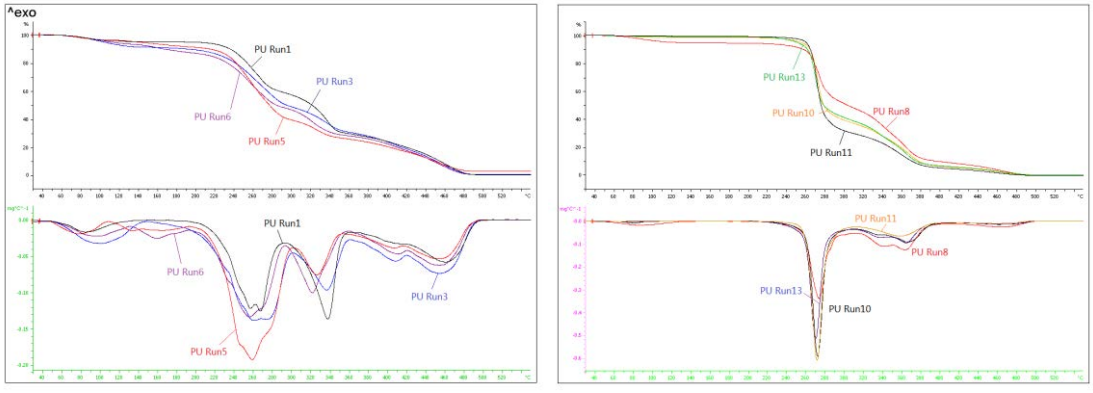

Figure 10. TGA and DTGA curves of polyurethanes synthesized in Table 3, left: PLA Polyurethanes, right: PHB based Polyurethanes

When comparing the TGA curves of the PLA segmented polyurethane Run5 and Run3 on the left graph, it can be seen that PU having longer degradable segments are more stable than

those with shorter chains, but intend to lose more weight in their first degradation step. This point was also confirmed by comparing Run3 to Run1 for PLA systems or Run10 to Run8 for PHB systems. Furthermore, Polyurethanes with more H_{12}MDI seem more stable than those with fewer content. It can be explained because a higher H_{12}MDI content means more carbamate groups in the polyurethanes. Therefore the more rigid structure and stronger hydrogen bond interaction between carbamate group and carbonyl or hydroxyl groups make the system more thermal-stable. These curves indicate that the stability of the polyurethanes depend mainly on the H_{12}MDI content and the molar mass of the degradable segments.

For DTGA curves of both systems, polyurethanes having more degradable contents, for example Run5 and Run13, are expected to lose weight faster (with the maximum degradation rate shown by DTGA curve) during the first degradation step. On the contrary, the polyurethanes having more H_{12}MDI content showed similar trends during their degradation step around 450°C. This result corresponds to the conclusion of the syntheses part, which proves that the expected structure was obtained through structure design. The functionality of Polyurethanes have little effect on their stability since it does not dramatically change the ratio of hard / soft segment composition, shown as the TGA graph above.

c. Thermal degradation of polyurethane / PHEMA networks

Based on the thermogravimetric analysis of the multi-allyl functionalized polyurethanes, these polyurethanes were cooperated with HEMA to form a biocompatible network through UV-induced radical polymerization with a mass ratio M_{HEMA} : $M_{polyurethane}$ = 1.5 : 1. Thermal degradation of these networks was also performed with TGA-FTIR technology and the result was also listed from Figure 11 to Figure 13.

Figure 11 shows the TGA and DTGA curves of the polyurethane / PHEMA network based on polyurethane from Run3. Compared with the DTGA curve of the polyurethanes from Run3, the DTGA curve of the network Run16 (based on PU Run3) only shows 2 maximum degradation peaks on the Gram-Schmidt trace at 260°C and 420°C. The former one is due to

the degradation of PLA segments and urethane link decomposition, while the later one is believed to be caused mainly by the decomposition of the PHEMA chains (also including degradation of H_{12}MDI). The strong weight loss in this stage is coherent with the particularly high content of PHEMA in the network: 60 wt%. Though thermal degradation behavior of PHEMA was discussed with different results [30-34], only one degradation step around 420°C was detected and recognized as the main degradation of PHEMA chains in the polyurethane, which should generate $CH_2=C(CH_3)CO$, $CH_2=C(CH_3)$- and $(CH_3)_2CHCO_2$ fragments by decomposition [34].

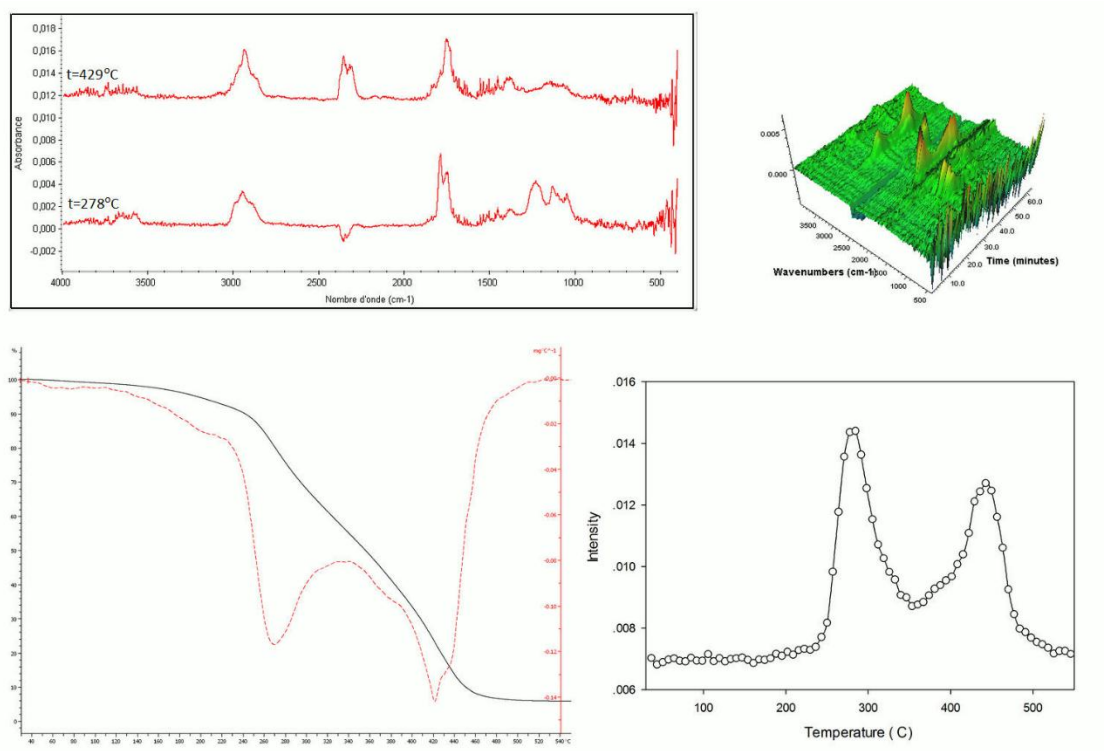

Figure 11. TGA, DTGA curves and 3D FTIR spectra collected during the degradation of networks based on PU Run3. The FTIR spectra were obtained at the maximum evolution rate for each decomposition step.

Compared with the IR spectra of PLA segmented polyurethanes in Figure 8, bands at 1738cm^{-1}(-C=O), 1400-1380cm^{-1}(-CH_2) in Figure 11 can be recognized as the absorption of HEMA – the degradation product of PHEMA chains and correspond with the result with the former results mentioned above. However, peaks at 1637, and 816 cm^{-1} corresponding to double-bond absorptions for HEMA are not obvious in the polymer spectrum.

Similar trends can be found in Figure 12 concerning the degradation of PHB-polyurethane-based networks. Contrarily to the degradation of PHB-based polyurethane shown in Figure 9,

in Figure 12 (the degradation of PHB-polyurethane-based network), the DTGA curve shows fast weight loss around 450°C with its degradation rate at 0.2mg/°C, and the Gram-Schmidt trace shows far larger degradation intensity at 463°C with HEMA characteristic absorptions shown in the top left spectra. These two pieces of evidence are good proof for PHEMA degradation around 450°C.

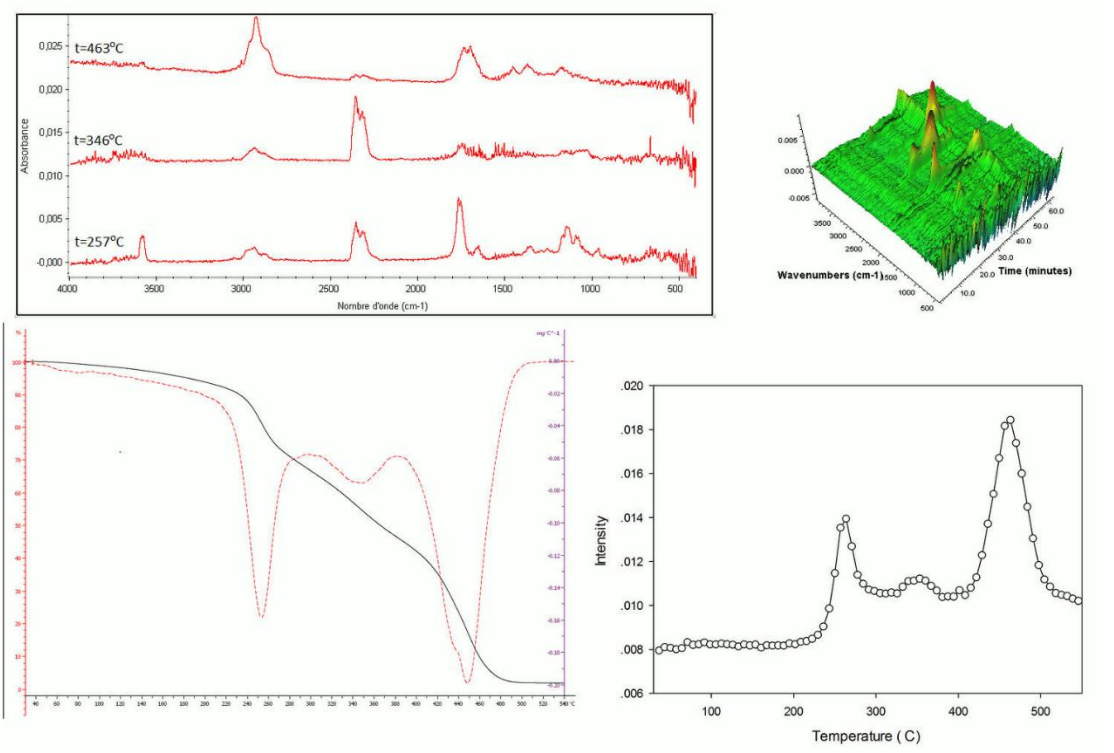

Figure 12. TGA, DTGA curves and 3D FTIR spectra collected during the degradation of network based on Run8.

The FTIR spectra were obtained at the maximum evolution rate for each decomposition step.

Moreover, the PHEMA segment in polyurethane networks has a 40°C higher average than its starting degradation temperature and maximum degradation temperature when compared to the pure PHEMA reported before (300°C or 400°C, [30-33]). It can be explained by the crosslink effect from multi-double-bond functionalized Polyurethanes and the hydrogen bond interactions between hydroxyl/ester groups of HEMA and carbamate groups from Polyurethanes.

To investigate the properties of polyurethane systems that affect the network, polyurethanes synthesized in Table 3 were also used to build up the network, and these networks were compared with each other for their thermal degradation by TGA and DTGA curves, as shown

in Figure 13.

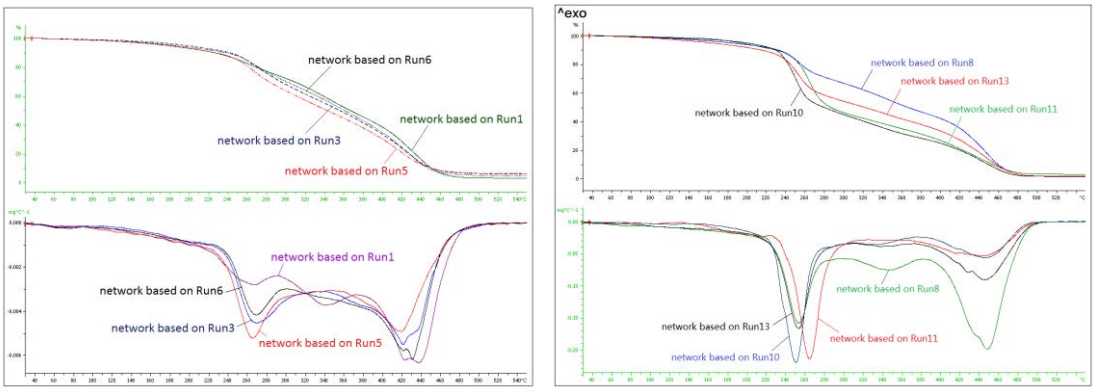

Figure 13. TGA and DTGA curves of Polyurethane / PHEMA networks synthesized with different parameters, up: PLA-based networks; bottom: PHB-based networks

Figure 13 clearly shows the effect the polyurethanes bring to the network. First, the degradation temperature of the soft segments in the network increases with the increasing crosslink density of the network. For example, the network based on Run5 has its first maximum degradation temperature at 262°C, which is lower than its Run3 counterpart at 265°C. This can be explained by the fact that the network based on Run3 has higher crosslink density than the network based on Run5.

For the network based on PHB systems, the thermal stability depends on the molar mass of the PHB segment. As shown on Figure 12, Run 11 with higher molar mass PHB segments has higher degradation temperature than other networks. The crosslinking effect is not obvious for PHB-based networks because the disassociation of carbamate group happened earlier than the degradation of PHB segment, which destroyed the network structure. It can also be seen that networks with polyurethanes having higher H_{12}MDI content and longer degradable segments show more stability in thermal degradation, which also corresponds with the conclusion drawn from polyurethane thermal degradation.

3.4 Conclusion

The poly(ester urethane)s segmented with prepared PLA and PHB oligomers were synthesized

with H_{12}MDI to strengthen their mechanic properties. The syntheses were performed through 2 steps and the double-bond functionalized Polyurethanes were obtained. The structure of these Polyurethanes was designed during the syntheses and characterized by ^{1}H NMR, SEC and DSC tests. These Polyurethanes were cooperated with HEMA to form the networks. Thermogravimetric analysis - Fourier transform spectroscopy copolymerization was adapted to characterize the thermal degradation behavior of the telechelic dihydroxyl oligomers, Polyurethanes and the networks. Through this method, designed structures of Polyurethanes were also evaluated.

Acknowledgement

The authors thank the financial support from China Scholarship Council (state scholarship fund). This work benefited from the international cooperation between Université Jean-Monnet Saint-Etienne (France) and East China University of Science and Technology (China).

Reference

1. Kim BK and Paik SH. Journal of Polymer Science Part a-Polymer Chemistry 1999;37(15):2703-2709.
2. Lai YC and Baccei LJ. Journal of Applied Polymer Science 1991;42(12):3173-3179.
3. Zulfiqar M, Quddos A, and Zulfiqar S. Journal of Applied Polymer Science 1993;49(12):2055-2063.
4. Zdrahala RJ and Zdrahala IJ. Journal of biomaterials applications 1999;14(1):67-90.
5. Loh XJ, Sng KBC, and Li J. Biomaterials 2008;29(22):3185-3194.
6. Wang WS, Ping P, Chen XS, and Jing XB. Journal of Applied Polymer Science 2007;104(6):4182-4187.
7. Eceiza A, Larranaga M, de la Caba K, Kortaberria G, Marieta C, Corcuera MA, and Mondragon I. Journal of Applied Polymer Science 2008;108(5):3092-3103.
8. Moravek SJ and Storey RF. Journal of Applied Polymer Science 2008;109(5):3101-3107.
9. Garlotta D. Journal of Polymers and the Environment 2001;9(2):63-84.
10. Michell RM, Muller AJ, Boschetti-de-Fierro A, Fierro D, Lison V, Raquez JM, and Dubois P. Polymer 2012;53(25):5657-5665.

11. Cooper TR and Storey RF. Macromolecules 2008;41(3):655-662.

12. Gu S, Yang M, Yu T, Ren T, and Ren J. Polymer International 2008;57(8):982-986.

13. Chen C, Yu CH, Cheng YC, Yu PHF, and Cheung MK. Biomaterials 2006;27(27):4804-4814.

14. Chen GQ and Wu Q. Biomaterials 2005;26(33):6565-6578.

15. Hirt TD, Neuenschwander P, and Suter UW. Macromolecular Chemistry and Physics 1996;197(5):1609-1614.

16. Brzeska J, Dacko P, Janeczek H, Kowalczuk M, Janik H, and Rutkowska M. Polimery 2010;55(1):41-46.

17. Liu QY, Cheng ST, Li ZB, Xu KT, and Chen GQ. Journal of Biomedical Materials Research Part A 2009;90A(4):1162-1176.

18. Mallek H, Jegat C, Mignard N, Abid M, Abid S, and Taha M. Journal of Applied Polymer Science 2013;129(3):954-964.

19. Henry I, Pascault JP, Taha M, Vigier G, and Flat JJ. Journal of Applied Polymer Science 2002;83(2):225-233.

20. Chen J, Pascault JP, and Taha M. Journal of Polymer Science Part A: Polymer Chemistry 1996;34(14):2889-2907.

21. Coudray S, Pascault J, and Taha M. Polymer Bulletin 1994;32(5-6):605-610.

22. Mallek H, Jegat C, Mignard N, Taha M, Abid M, and Abid S. Journal of Macromolecular Science, Part A 2013;50(7):728-737.

23. Unal S, Ozturk G, Sisson K, and Long TE. Journal of Polymer Science Part A: Polymer Chemistry 2008;46(18):6285-6295.

24. Nakayama Y, Yamaguchi R, Tsutsumi C, and Shiono T. Polymer Degradation and Stability 2008;93(1):117-124.

25. Miller DR and Macosko CW. Rubber Chemistry and Technology 1976;49(5):1219-1231.

26. Vogel C and Siesler HW. Thermal Degradation of Poly (ε ‐ caprolactone), Poly (L ‐ lactic acid) and their Blends with Poly (3 ‐ hydroxy ‐ butyrate) Studied by TGA/FT ‐ IR Spectroscopy. Macromolecular Symposia, vol. 265: Wiley Online Library, 2008. pp. 183-194.

27. Nishida H, Ariffin H, Shirai Y, and Hassan MA.

28. Chen C, Fei B, Peng S, Zhuang Y, Dong L, and Feng Z. Journal of Applied Polymer Science 2002;84(9):1789-1796.

29. Cervantes-Uc J, Espinosa J, Cauich-Rodríguez J, Ávila-Ortega A, Vázquez-Torres H, Marcos-Fernández A, and San Román J. Polymer Degradation and Stability 2009;94(10):1666-1677.

30. Pielichowski K and Njuguna J. Thermal degradation of polymeric materials: iSmithers

Rapra Publishing, 2005.

31. Caykara T, Özyürek C, Kantoğlu Ö, and Erdoğan B. Polymer Degradation and Stability 2003;80(2):339-343.

32. Çaykara T and Güven O. Polymer Degradation and Stability 1998;62(2):267-270.

33. Demirelli K, Coşkun M, and Kaya E. Polymer Degradation and Stability 2001;72(1):75-80.

34. Vargün E and Usanmaz A. Journal of Macromolecular Science, Part A: Pure and Applied Chemistry 2010;47(9):882-891.

Chapter 4

Ring opening Copolymerization of caprolactone and glycidyl methacrylate and cross-linking of the issued methacrylated polycaprolactone

Hang SHEN [1, 2, 3], Jianding CHEN [4], Mohamed TAHA [1, 2, 3]*

1 Université de Lyon, F-42023, Saint-Etienne, France;

2 CNRS, UMR 5223, Ingénierie des Matériaux Polymères, F-42023, Saint-Etienne, France;

3 Université de Saint-Etienne, Jean Monnet, F-42023, Saint-Etienne, France;

4 Laboratory of Advanced Materials Processing, East China University of Science and Technology, 200237 Shanghai, China

*correspondence：Mohamed.Taha@univ-st-etienne.fr

Résumé

Des copolymères statistiques du caprolactone et du méthacrylate de glycidyle ont été préparés par copolymérisation par ouverture de cycle dans un procédé sans solvant. Les produits obtenus ont été analysés par ^{13}C RMN. Avec les paramètres de copolymérisation utilisés, il n'y a pas de monomère caprolactone résiduel. Le TBD, le dioctoate d'étain et l'acide 4-hydroxybenzènesulfonique ont été utilisés comme amorçeurs et l'alcool benzylique en tant que co–amorçeurs. Le TBD a été particulièrement efficace. Des analyses MALDI-TOF des produits obtenus confirment la copolymérisation. La composition des produits obtenus n'est pas uniforme: des macro cycles et des chaînes linéaires ont été détectés.

Des réseaux P (CL-co-GMA) ont été préparés en utilisant le méthacrylate de 2 -hydroxyéthyle et / ou des agents de couplage multi- mercaptans. Les réseaux obtenus ont été étudiés par analyse thermomécanique. L'attention a été accordée à la relation entre la composition du système réactif et les propriétés amortissantes des réseaux obrenus. Des amortissements dans une large gamme de températures ont été obtenus pour certains matériaux.

Mots-clés: copolymérisation de l'anneau d'ouverture, méthacrylate glycidyle, acrylate polycaprolactone, réseau, réaction thiol-ène, l'amortissement, polyhydroxyéthylméthacrylate.

Abstract

P(caprolactone-co-glycidyle mathacrylate) copolymers were prepared by ring opening copolymerization in a one-step solvent-free process. Under the used copolymerization parameters, there is no residual caprolactone monomer. TBD, Stannous Octoate and 4-hydroxybenzenesulfonic acid were used as initiators with benzyl alcohol as co-initiator. TBD was particularly efficient. MALDI-TOF analysis of the obtained products confirms the copolymerization. The composition of the obtained product is not uniform: macro cycles and linear chains were detected. P(CL-co-GMA) networks were prepared using 2-hydroxyethyl methacrylate and/or multi-mercapto coupling agents. Thermomechanical analyses of the obtained networks were made. Particularly important damping in a wide range of temperatures was obtained for some materials.

Keywords: Ring opening copolymerization, glycidyl methacrylate, acrylated polycaprolactone, network, thiol-ene reaction, damping, poly hydroxyethyl methacrylate.

4.1 Introduction

Biocompatible and biodegradable Poly (ε-Caprolactone), PCL, is recognized as an important synthetic biodegradable polymer [1-3] and can be processed by classical polymer processing techniques [4-6]. When well defined, it can be used for a variety of applications in the medical field such as sutures, bone fixation, and also as drug release carriers [7-10]. CL ring opening polymerization with suitable organometallic catalysts or initiators has been well studied [11, 12]. Among catalysts and initiators, tin carboxylates or titanium and aluminum alkoxides were often used. Organic reagents [13, 14] containing hydroxyl groups are often used as co-initiators [15, 16]. Besides ionic and insertion-coordination mechanism based catalysts, 1,5,7-Triazabicyclo [4, 4, 0]dec-5-ene (TBD), a nonionic guanidine base, is reported to be capable of inserting a cyclic ester monomer into a propagating polymer. Subsequently it can hydrogen bind the adjacent nitrogen to alcohol to complete a transesterification cycle from a polyester [17, 18]. This particular mechanism was recently used to modify polymers with pendant ester groups to endow new functions or grafts [19-21]. For ring opening copolymerizations, TBD/benzyl alcohol were claimed to be capable of catalyzing the synthesis of crystalline poly(lactic acid-co-CL) random copolymers [22].

To broaden it's scope of application, different functions have been deliberately introduced into PCL as precursors for networks elaboration. Two strategies were principally used for this goal. For the first strategy, PCL main chains were activated by UV or plasma irradiation under oxidant environments (O_2 or H_2O_2) to generate reactive centers that can lead by combination to the cross-liking of the reactive system [23, 24]. The second way relies on the synthesis of acrylated PCL oligomers [25, 26]. Mecerreyes reported the synthesis and copolymerization of 6-allyl ε-caprolactone and 4-(acryloyloxy)-ε-caprolactone [27, 28]. The ROP of these monomers with caprolactone led to new allyl-functionalized copolymers. Comonomers other than those derived from caprolactone were also used. For example, acryloyl cyclic carbonate monomers were prepared and copolymerized with ε-CL giving acryloyl functionalized copolymers.

Glycidyl methacrylate (GMA), is generally polymerized or copolymerized with vinyl monomers

by radical initiation to synthesize polymers or copolymers with pendant epoxy groups [29-32]. GMA can also polymerize or copolymerize by ring opening of the epoxy group. In this case, the methacrylate function remains available for further modification. Almost all literature reporting this possibility concern the copolymerization of GMA with other epoxides [33-36]. Concerning the ROP between lactone and epoxide, the literature is rare. Bednarek copolymerized CL with ethylene oxyde by cationic copolymerization in order to prepare hydroxy-telechelic PCL [37]. Uenishi and coworkers also reported the copolymerization of lactone and GPE, an epoxide [38].

The present study concerns the synthesis of methacrylated PCL and it's copolymerization with2-hydroxyethyl methacrylate (HEMA). The studies reported in literature on the synthesis of double bond functionalyzed PCL are based on the copolymerization of CL with a modified CL. Even if this method is very efficient, the modified CL is not commercially available and its preparation in high quantity is relatively complicated. In this study, instead of using functionalyzed CL, an original and simple method for the synthesis of methacrylated PCL by direct ring opening copolymerization of CL and GMA is evaluated and optimized. The obtained methacrylated PCL will be copolymerized with HEMA and the properties of the obtained networks will be analyzed. Multi-thiols were also introduce to alter the mechanical properties of the networks by thiol-ene click and telomerizations.

4.2 Experimental Part

Materials

The ε-caprolactone was purchased from Solvay. 2-Hydroxyethyl methacrylate was purchased from Röhm GmbH. Hydroquinone (99%), Benzyl alcohol, 1,5,7-Triazabicyclo[4.4.0]dec-5-ene, Tin(II) bis(2-ethylhexanoate), 4-Hydroxybenzenesulfonic acid solution (65%, in H_2O), Trimethylolpropane tris(3-mercaptopropionate) and Glycidyl methacrylate (97%) were purchased from SIGMA-ALDRICH (France).

The photo initiator was composed by reagents as follows: 60 wt% of CN381 from Sartomer, 20 wt% of Benzophenone (99%) from Aldrich, and 20 wt% of 2,2-Diethoxyacetophenone from Aldrich. ε-caprolactone and 2-Hydroxyethyl methacrylate were distilled before use. All the other reagents were used as received.

Synthesis

The copolymerization between CL and GMA was made in a 250mL glass reactor (62 mm diameter) with a 3-necked steel cover. A steel anchor stirrer operating with a RW 28 W IKA motor at 60 rpm, a condenser and a T-type thermocouple probe were fixed to the cover. A nitrogen flow, previously dried in a silica column, allowed the air elimination from the reactor. The reactor was heated by an IKA HBR4 bath with silicon oil.

Copolymerization of CL and GMA

The CL, benzyl alcohol and hydroquinone were mixed and introduced in the reactor heated at 110°C. The GMA was introduced into the reactor 10mins later. When the system was completely homogeneous and thermally stabilized, TBD was introduced and the reaction was kept for 45-180mins. The product was dissolved in chloroform, precipitated in large amount of cold ethyl ether, filtered and dried under vacuum at room temperature for 48 hours than stored at -20^{o}C.

Radical polymerization of the P(CL-co-GMA) and HEMA by photo irritation

The copolymer of CL and GMA was dissolved simultaneously in HEMA with different mass ratios and in Trimethylolpropane tris(3-mercaptopropionate) by oscillation at room temperature for 3mins. Then the photo initiator was added and mixed. The mixture was placed in an ultrasonic oscillator to remove the air bubbles before curing. To initiate the UV irritation, reagent mixtures were placed in Teflon molds (40mm*10mm*0.1mm) and cured in air with a fluorescent lamp, JAD STS-350, equipped with 8W*3 fluorescent tubes offering λ=250nm UV light. The mixtures were exposed at a distance of 3cm from the lamps for 24hrs. After the curing, the sample bars were collected for mechanical analyses.

Instrumentation

IR

FT-IR absorption spectra of the polymer were recorded on a Nicolet Nexus spectrometer (700-3500 cm^{-1}) using attenuated total reflectance (ATR) technique.

NMR analysis

NMR analyses were performed with a Bruker Advance III spectrometer operating at 400 MHz for ^{1}H NMR analyses and 100.6 MHz for ^{13}C NMR analyses. The analyses were performed with 10mm diameter tubes containing about 400 mg of polymer in 0.6mL of chloroform-D, with tetramethylsilane as the internal reference at 0 ppm.

MALDI-TOF Spectroscopy

MALDI-TOF analysis was performed on a BRUKER Daltonics Ultraflex III. The polymer samples were dissolved in DMSO. The cationization agent used was sodium iodide dissolved in acetone at a concentration of 10 mg mL^{-1}. The matrix used was dithranol and was dissolved in DMSO at a concentration of 10 mg mL^{-1}. Solutions of matrix, salt, and polymer were mixed in a volume ratio of 10:1:1, respectively.

DSC

Differential scanning calorimetry (DSC) measurements were carried out with a Q10 calorimeter from TA Instruments. Samples were transferred to hermetic pans and sealed, and analyzed from -80 °C to 150 °C with a cooling/heating rate of 10 °C·min^{-1}. The glass transition temperatures were evaluated from the data recorded during heating by identifying the inflection points. Each sample underwent two heating-cooling cycles.

SEC

Size exclusion chromatography (SEC) was conducted using a system equipped with refractive index (Waters 2414), viscosimeter (Wyatt ViscoStar) and light scattering (Wyatt

MiniDawnTreos) detectors. Three columns HR 0.5, HR1 and HR3 from Waters were used. The eluent was tetrahydrofuran (THF) with a flow rate of 1 mL·min^{-1} and the elution temperature was 35°C. The copolymer molecular weights were determined using a calibration curve established with a set of polystyrene standards of different molecular weights ranging from 500 to 700 000.

Dynamic Mechanical Analysis

The rheologic measurements in solid state were made with a Rheometric Scientific ARES N2. Specimens prepared with a predetermined shape (30 mm x 2 mm x 10 mm) were subjected to a sinusoidal microstrain with a fixed autotension at a constant frequency of 1.0 rad·s^{-1}. Dynamic temperature sweep tests were chosen with strain amplitudes of 0.01 %, to keep the measured torque at a sufficient level, and a heating rate of 3 °C·min^{-1} from -85 °C to 100 °C.

4.3 Results and discussion

In order to verify the copolymerization between the GMA and CL, and furthermore the use of the obtained products in thiol-ene reactions, the synthesis and characterization of the copolymers was firstly performed.

4.3.1 Synthesis and characterization of the P(CL-co-GMA) copolymer

P(CL-co-GMA) copolymers were prepared by ring opening copolymerization of caprolactone and the epoxy function of glycidyle methacrylate. In this study, TBD, Stannous Octoate and 4-hydroxybenzenesulfonic acid were used as initiators with benzyl alcohol as co-initiator. No solvent was used in this synthesis. The obtained copolymer is expected to contain unreacted pendant double bonds on the backbone as illustrated in Scheme 1.

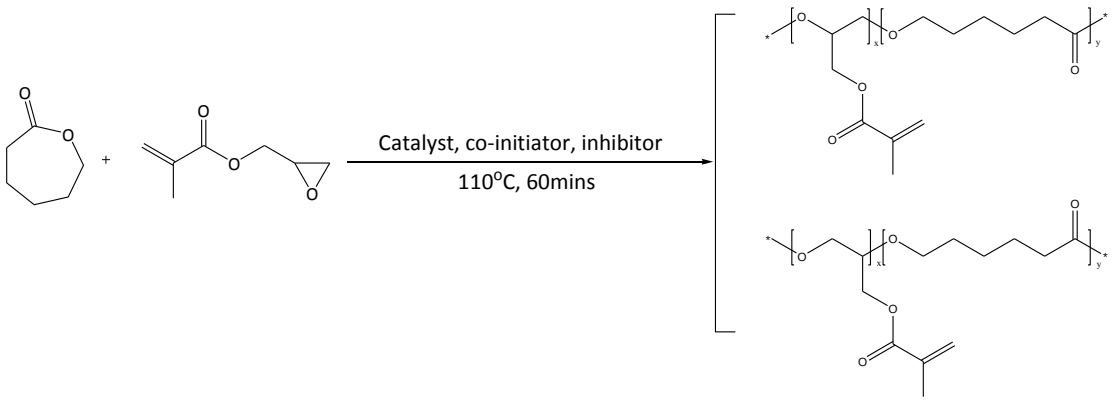

Scheme 1. Ring opening copolymerization of caprolacotne and glycidyl methacrylate

Qualitative analysis of the obtained copolymers

The obtained products were analyzed by ^{13}C NMR. Figure 1 shows, as an example, a ^{13}C NMR spectrum of a non-purified copolymer. The resonances attributions of the different carbons of the copolymer are given in Figure 1. Under the used copolymerization parameters, there is no residual caprolactone monomer in the system. The carbons of the caprolactone repeat unit can be easily located, labeled from 1 to 6 in the spectrum, as well as GMA repeat unit carbons, from 7 to 13. The presence of few unreacted epoxy cycles is detected by the persistence of unreacted epoxy ring carbons at 44.6 and 49.4ppm. Moreover, the methanetriyl carbon expected at 84ppm for GMA homopolymer is not presented, showing that GMA only copolymerized with CL.

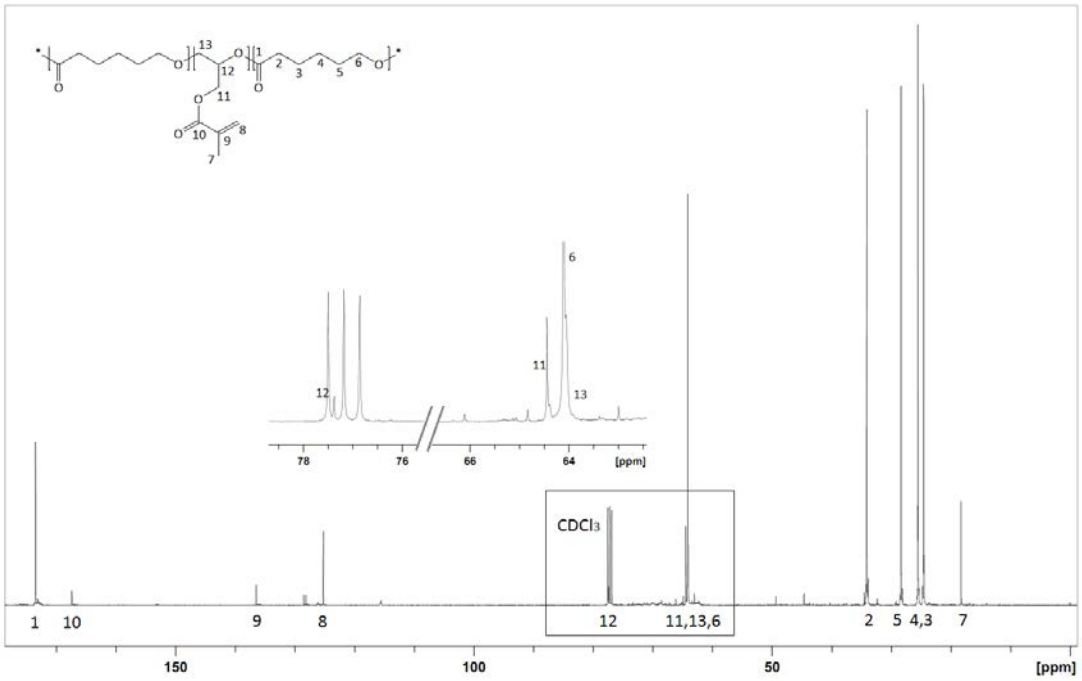

Figure 1. ^{13}C NMR spectrum of a P(glycidyl methacrylate-co-caprolactone) in $CDCl_3$. The sample was synthesized with [CL]:[GMA]=5, [CL]:[TBD]:[Benzyl alcohol]:[Hydroquinone]=100:1:1:1, at 110°C for 60mins

To confirm that CL and GMA copolymerized by ROP, MALDI-TOF analyses of the obtained products were made. Figures 2-a and 2-b give an overview of the obtained polymer composition with molecular weights ranging from 600 to 3000, which is in accordance with the results from GPC that will be given below. Several series of macromolecules containing different GMA units can be identified showing that the composition of the obtained product is in fact not uniform. As expected, all the series contain principally CL repeat unit as seen by a molecular weight increment of 114.06 g/mol. Series containing two, one and zero GMA units are those having the highest intensities. All the easily detectable series contain only CL and GMA units showing that they are macro cycles. Linear chains with lower intensities were also detected; they also contain GMA.

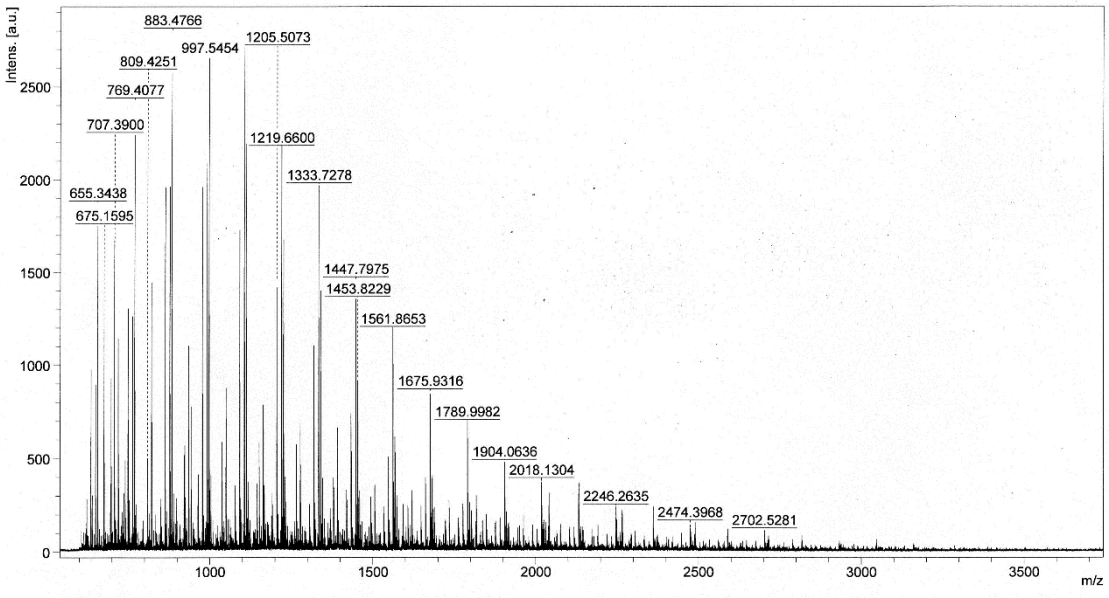

Figure 2-a. MALDI-TOF spectrum of the P(glycidyl methacrylate-co-caprolactone) with m/z from 600 to 2500. The sample was synthesized with [CL]:[GMA]=5, [CL]:[TBD]:[Benzyl alcohol]:[Hydroquinone]=100:1:1:1, performed at 110°C for 60mins

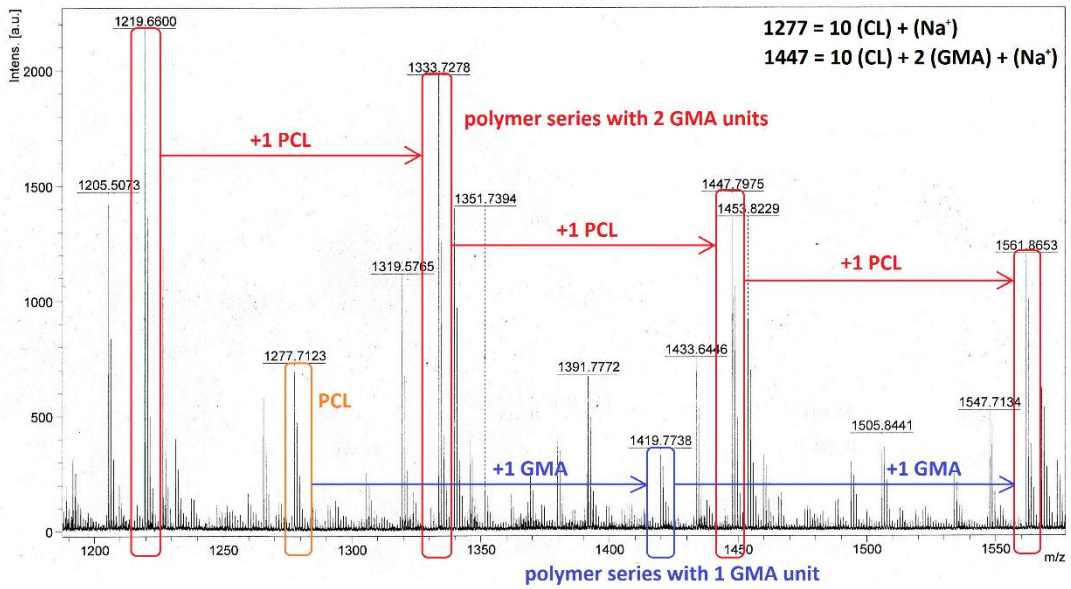

Figure 2-b. MALDI-TOF spectrum of the P(glycidyl methacrylate-co-caprolactone) with m/z from 1200 to 1600. The sample was synthesized with [CL]:[GMA]=5, [CL]:[TBD]:[Benzyl alcohol]:[Hydroquinone]=100:1:1:1, performed at 110°C for 60mins.

From these analyses, conclusion can be drawn that a copolymer containing CL and GMA repeat units can be obtained by ring opening copolymerizations of GMA and CL. The product also contains homopolymerized PCL as macro rings, but the homopolymerization of GMA was not found by the qualitative analysis.

Quantitative analysis of the obtained polymers

Based on the qualitative results above, quantitative analyses were also carried out. The expected structure of a poly(caprolactone-co-glycidyl methacrylate) prepared by ROP is shown in Scheme 1. The obtained polymer was purified to remove the unreacted monomer, catalyst and initiator, and analyzed by ^{1}H NMR to evaluate the structure of the polymer, shown in Figure 3.

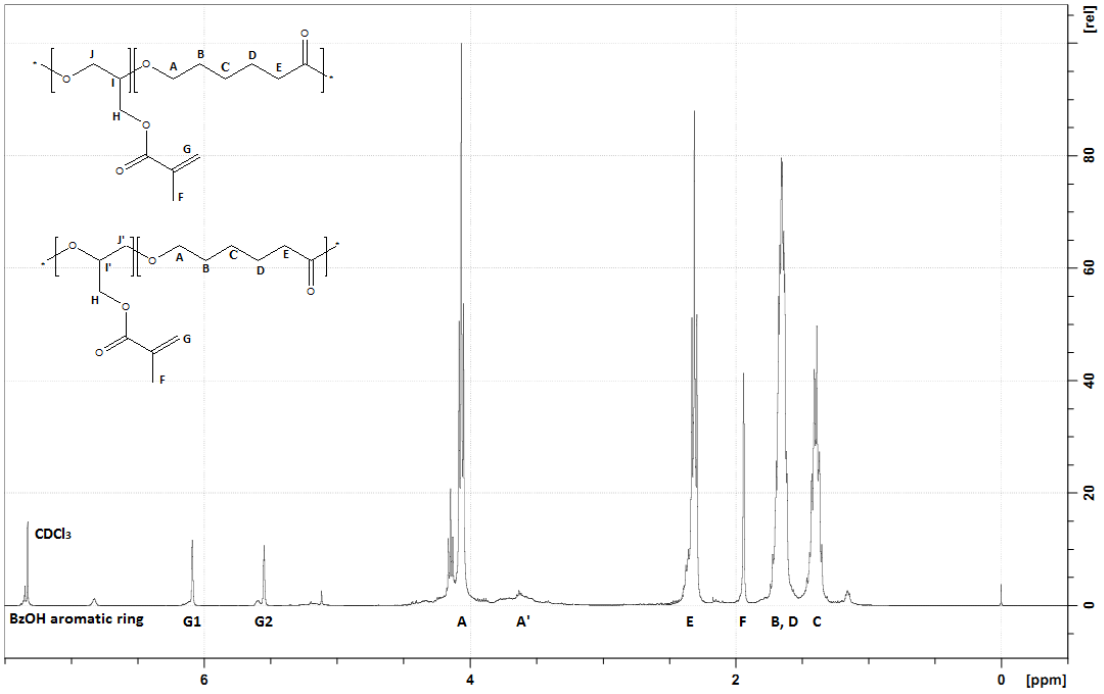

Figure 3 ^{1}H NMR spectrum of purified P(glycidyl methacrylate-co-caprolactone) in $CDCl_3$. The sample was synthesized with [CL]:[GMA]=5, [CL]:[TBD]:[Benzyl alcohol]:[Hydroquinone]=100:1:1:1, at 110°C for 60mins.

Presence of GMA and caprolactone repeat units was clearly observed in ^{1}H NMR spectra. It can be observed that the epoxy ring reacted (with no epoxy ring protons at 2.6, 2.8 and 3.2ppm) while the double bond remained in the system with proton chemical shifts at 5.6ppm and 6.1ppm. Besides there is no residual caprolactone monomer. Proton A' is the end chain ε proton of the caprolactone repeat unit. It should be noticed that the triplet A of ε proton from caprolactone split into 2 parts, which is believed to have been caused by the CL connected with different repeat units, CL or GMA. This proves again the copolymerization of CL and GMA because the area ratio of these two peaks is close to the feed ratio and the sum of these two peaks is always equal to the area of α or ε protons from caprolactone repeat units for all the samples with different monomer feeding rates. Due to the mechanism of epoxy ring opening, there may be two ways to propagate the chain: the nucleophile attacks either the least substituted carbon, in accordance with standard SN_2 nucleophilic addition reaction process, or the most substituted carbon by steric effects and by carbocationic stability [39], shown in scheme 1. For the obtained products, the backbone protons I, I', J, J' generated by the epoxy ring cannot be quantified because they are overlapped by protons A and A', and also overlap each other around 3.7-4.5ppm. E and F correspond to respectively the α-methylene group

from the CL repeat unit and the methyl group from the GMA repeat unit.

Consequently, the average ratio of these two repeat units can be calculated by the integration ratio

r=3E / 2F

and the average functionality f can be obtained using the M_n from SEC.

$f= M_n / (114.04 \times r) + (142.15)$

Furthermore, the conversion of the GMA into repeat units can also be calculated by:

$p= ([GMA] / [CL]) / ([GMA]_0 / [CL]_0)$

where [GMA] and $[GMA]_0$ correspond to GMA concentrations in the obtained polymer and the GMA initial concentration. (The CL conversion was total)

Following the equations above, the quantitative analyses of the samples synthesized with different parameters are listed in table 1.

Table 1. Caprolactone and glycidyle methacrylate copolymerization at 110°C for 60mins

Sample	Feeding ratio [CL] : [GMA]	Repeat unit ratio [CL] : [GMA]	[TBD] : [BzOH] amount, mol% : mol%	GMA conversion (as repeat unit) %	Molecular weight by SEC, Mw/Mn/WMD	Average functionality
run1[a]	1:1	/	1:1	/	/	/
run2[b]	2.5:1	4.4:1	1:1	56.8	4550 / 2430 / 1.87	3.2
run3	5:1	6.5:1	1:1	76.95	7660 / 4100 / 1.87	4.6
run4	10:1	14:1	1:1	70.56	10860 / 5790 / 1.79	3.1
run5	20:1	43:1	1:1	47.21	11950 / 6100 / 1.96	1.2
run6[b]	5:1	7.5:1	0.5:1	35.6	2700 / 1330 / 2.03	1.3
run7[b]	5:1	10:1	0.2:1	11.4	171.6 / 583.0 / 3.40	0
run8	5:1	6.5:1	1:0.5	61.69	6730 / 3700 / 1.82	4.2
run9	5:1	6.3:1	1:2	67.21	4640 / 2540 / 1.82	2.9
run10	5:1	6.8:1	0.75:1.5	45.15	6310 / 3190 / 1.97	3.5

a: sample cannot be analyzed due to gelation at 60mins

b: reactions were not finished, with considerable residual GMA and CL at 60mins by result of ^{1}H NMR

Synthesis optimization

Different parameters can be used to investigate and optimize the copolymerizations, including the kind and amount of initiators, the ratio of initiator to co-initiators and the monomer feeding ratios. The obtained polymers are quantified by characterizations to investigate the conversion of the monomers, the molecular weight of the copolymers and the average functionalities, through which the best synthesis parameters were obtained as follows:

Catalyst efficiency

Stannous octoate, TBD and 4-Hydroxybenzenesulfonic acid were used as catalysts. Reactions were monitored by FTIR .GMA conversion was evaluated by epoxy ring absorption in Figure 4 and NMR analysis.

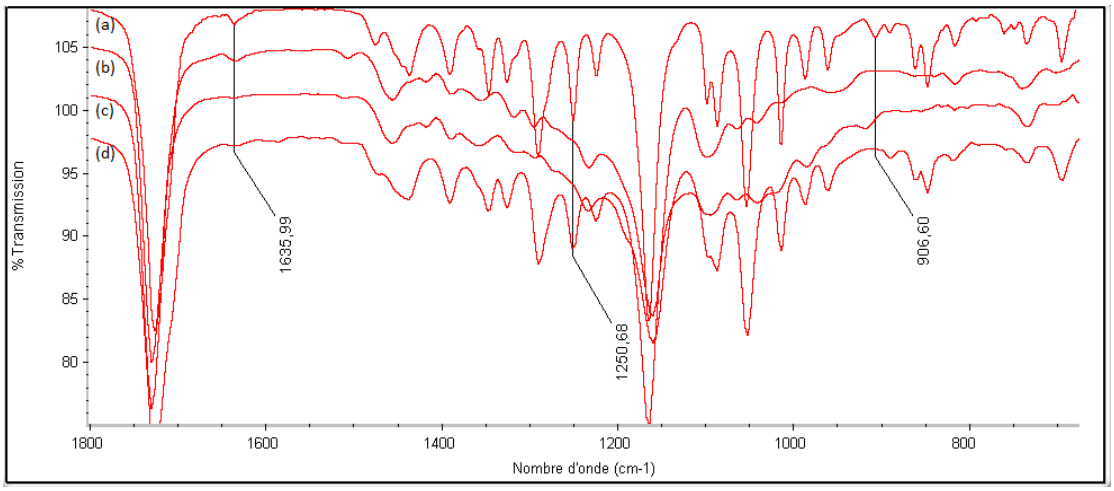

Figure 4. FTIR spectra of the: (a) monomer mixtures, and products synthesized by catalysis of (b) TBD, (c) Sn(Oct)2 and (d) 4-hydroxylbenzensulfonic acid, all the copolymerizations were performed with [CL]:[Cata.]:[Benzyl alcohol]:[Hydroquinone]=100:1:1:1, at 110°C for 60mins

From the result of IR spectra, when taking carbonyl absorption (1726cm^{-1}) as constant peak, the epoxy ring was almost consumed in systems with TBD or $Sn(Oct)_2$, while there is still a lot of GMA in the 4-HBSA systems, illustrated by the change of epoxy ring absorption (915cm^{-1} and 1250cm^{-1}, $\gamma_{c\text{-}o}$) [22, 40]. However, a decrease of double bound absorption at 1635cm^{-1} [41] in $Sn(Oct)_2$ systems indicated that $Sn(Oct)_2$ was not a suitable catalyst for this copolymerization. This result corresponded with the data obtained for NMR analysis, shown in table 2.

Table 2. Conversion of CL and GMA from systems with different catalyst, all the copolymerizations were

performed by [CL]:[GMA]=5, [CL]:[Cata.]:[Benzyl alcolhol]:[Hydroquinone]=100:1:1:1 at 110°C for 60mins.

Catalyst and amount	Reaction time	Conversion of CL to repeat unit, % By NMR, %	Conversion of GMA to repeat units, by NMR, %	Consumption of GMA double bonds, by NMR, %
TBD, 1% of CL	60mins	100	76.95	0
4-HBSA, 1% of CL	120mins	46.62[a]	44.13[a]	93.10
Tin octoate, 1% of CL	120mins	100	24.58	51.86

a: result is not precise due to the gelation during the reaction.

Conversion of CL and GMA to repeat units were also investigated by ^{1}H NMR to get precise results. With 4-hydroxylbenzensulfonic acid as catalyst, considerable amounts of CL were not consumed after 60mins and gelation happened in the system while lots of double bonds were lost in $Sn(Oct)_2$ catalyzed systems. TBD acted better for its higher GMA conversion and no double bond were lost in the copolymerizations.

Effect of TBD / Benzyl alcohol amount and ratios on GMA/CL copolymerization

When using TBD as the catalyst, its amount greatly affects the reaction speed of the polymerization from seconds to several hours. Six conversion-time kinetic curves concerning conversion of GMA and caprolactone were obtained by varying catalyst concentration at 110°C. The conversion of the monomers was calculated by ^{1}H NMR spectroscopy using the ratio between integrals of double bond proton resonance of GMA monomer and repeat unit at 6.10ppm and 6.16ppm respectively, and α methylene proton chemical shifts for CL monomer and repeat unit at 2.0ppm and 2.4ppm. The obtained results are listed in table 1 (Run 3, 6-10) and illustrated by figure 5 and 6:

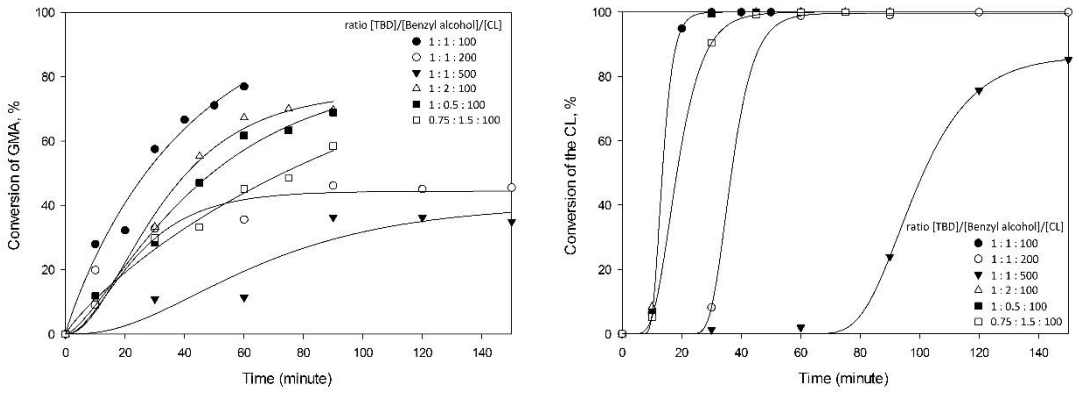

Figure 5 and 6. GMA (left) and CL (right) conversion versus reaction time curves of CL-GMA copolymerization

with different [TBD]/[Benzyl alcohol] concentrations, all the copolymerizations were performed with feeding ratio $[CL]_0$:$[GMA]_0$=5:1 at 110°C

From figures 5 and 6 it can be seen that the amount of the TBD greatly affects the rate of the reaction and the conversion of GMA. With a higher content of TBD, 80% of the GMA was consumed within 1 hour, compared to those with only 0.2 mol% of the TBD, for which the GMA total conversion was no more than 50% even after 2.5hrs. However, more TBD (>2 mol% of CL) will lead to an uncontrollable reaction and generate insoluble products in seconds due to the radical polymerization of GMA.

Benzyl alcohol reacts with the intermediate generated from nucleophilic reaction of the TBD with the loactone. So, the concentration of benzyl alcohol affects the consumption of the GMA. Nevertheless; its effect is not as important as that of the catalyst. (Table 1 , run 8-10) (amidine imine nitrogen to the ester carbonyl) [18]. The ratio of [CL] / [Benzyl alcohol] affects the molecular weight of the product, shown in table 1 (Run 8-10)

As for the copolymerization of CL, the monomer consumption rate depends mainly on the amount of catalyst in the system. The copolymerization works efficiently when the amount of catalyst is higher than 0.5 mol% of the CL, upon which the reaction of the CL will be completed in 60 minutes. The conversion of GMA remains stable after the consumption of CL, meaning that the homopolymerization of GMA will not happen when using TBD as catalyst, which is proved again by individual experiments mixing TBD, hydroquinone and GMA at 110C for 1.5hrs.

Effect of monomer feeding ratio [CL]/ [GMA] on their copolymerization

In order to increase the functionality of the copolymer and endow more pendant double bonds on the chains, the feeding ratio [GMA] / [CL] was changed to investigate the effects on polymer contents. The obtained polymer was characterized by SEC and HNMR as well and the results are as listed in table 1.

From the results shown in table 1 and figure 9, increasing amount of GMA will bring the

decrease of the molecular weight and larger molecular weight distribution to the samples, therefore decreasing the melting point and recrystallization temperatures of the copolymers by DSC results in Figure 7 and 8. Dual melting endotherms and recrystallization cannot be observed when the feeding ratio is 2.5. It can be explained by the different reactivity of GMA and CL. On the other hand, with a lower content of GMA, caprolactone inclines to homopolymerize and yield polymers with a high molecular weight, whereas a higher content of the GMA will result in an insoluble gel from radical polymerization crosslinking even in the existence of the inhibitor. Quantitative results are listed on table 1. It is clear that the sample with feed ratio [GMA] / [CL] = 1 : 5 has better GMA conversion and molar mass, and therefore higher functionality, which is suitable for copolymer synthesis.

DSC was used to characterize the thermal behavior of the P(GMA-co-CL) synthesized with different monomer feeding ratios. Results are shown in Figures 7 and 8. Glass transition temperature was found around -60°C corresponding to a caprolactone-rich phase. The products exhibit dual endotherms at 18.5°C and 32.3°C corresponding to a melting-recrystallisation-remelting often observed in PCL [42, 43]. These endotherms as well as the crystallization are switched to lower temperatures with the incorporation of epoxy units into the PCL chains [37].

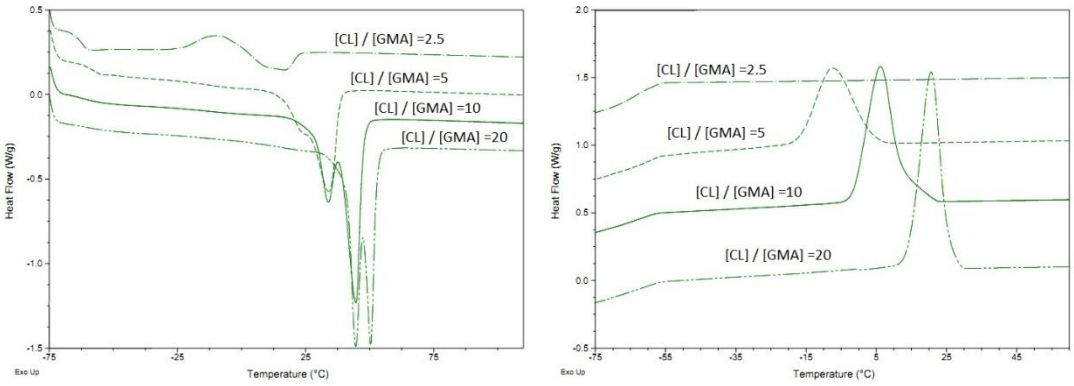

Figure 7 and 8 DSC thermographs of copolymers synthesized with different [CL]/[GMA] feeding ratios, left: melting transition of the copolymer chains, right: recrystallization of the copolymer chains. All the samples were obtained from copolymerization with parameters [CL]:[Cata.]:[Benzyl alcohol]:[Hydroquinone]=100:1:1:1 at 110°C for 60mins.

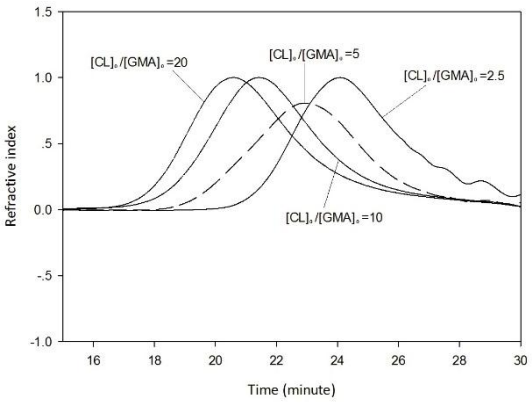

Figure 9. The SEC graph of copolymers synthesized with different [CL]/[GMA] feeding ratios. All the samples were obtained from copolymerization with parameters [CL]:[Cata.]:[Benzyl alcohol]:[Hydroquinone]=100:1:1:1 at 110°C for 60mins.

4.3.2 Network formation using P(GMA-co-CL)

P(GMA-co-CL) with pendant methacrylate functions can be used to prepare different networks. In the first part of this study, the use of a multi-mercapto reagent in thiol-ene click reactions is expected to build networks by coupling P(GMA-co-CL) chains. Secondly, P(GMA-co-CL) copolymerized with 2-hydroxyethyle methacrylate, leading to the formation of networks in which P(GMA-co-CL) are expected to be linked by PHEMA chains that have molar mass distributions.

P(CL-co-GMA) network using multi-mercapto coupling agents

P(GMA-co-CL) was reacted with Trimethylolpropane tris(3-mercaptopropionate) with different double bond/mercapto stoichiometric ratios to form networks by thiol-ene reactions through UV initiation. In this case, a photo initiator was not necessary. The evolutions of thermo-mechanical properties of the obtained products were obtained by DMA. Figure 10 shows the moduli and loss tangent of cured samples with different [double bond] / [thiol] mole ratios.

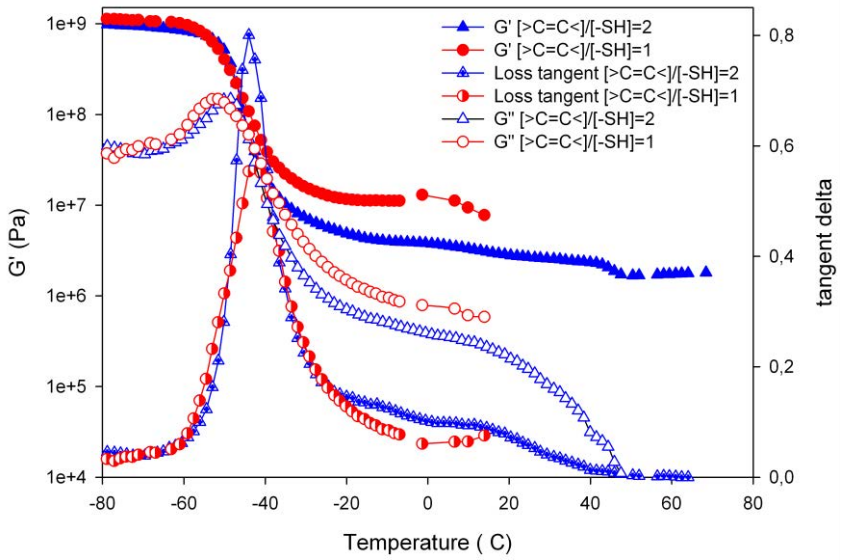

Figure 10. Storage moduli (G'), loss moduli (G") and loss factors of the networks formed by P(GMA-co-CL) and trimethylolpropane tris(3-mercaptopropionate) with different mole ratios after UV irritation. The P(GMA-co-CL) used is sample Run3 in Table 1. Round spot curves: polymer with mole ratio [>C=C<]/[-SH]=1; Triangle spot curves: polymer with mole ratio [>C=C<]/[-SH]=2

These spectra indicate that networks were obtained, since the storage moduli are higher than loss moduli in the whole temperature range analyzed and also because of the appearance of a rubbery plateau. Moreover, the narrow tanδ peak with maximum value at -40°C indicates that a PCL homogeneous network was prepared. As expected, using an equivalent [methacrylate] / [thiol] mole ratio (=1) lead to a network having a higher storage modulus plateau and a lower mass between crosslinks, M_c, than when this ratio was 2.

Co-crosslinking of P(CL-co-GMA) and Poly 2-hydroxyethyl methacrylate (PHEMA)

Based on the previous results, P(GMA-co-CL) and HEMA copolymerization through UV initiation was studied. The effects of different reaction parameters (listed in table 3) were analyzed.

Table 3. Syntheses parameters of P(CL-co-GMA) / Poly 2-hydroxyethyl methacrylate / Trimethylolpropane tris(3-mercaptopropionate) cooperated networks.

Sample	Feeding ratio of [P(GMA-co-CL)] / [HEMA], wt / wt	Tri-thiol amount introduced in networks, mol%	Functionally of P(GMA-co-CL) in network establishment
Run11	1.5 / 1	0	4.6
Run12	1.25 / 1	0	4.6
Run13	1 / 1	0	4.6
Run14	1 / 2	0	4.6
Run15	1.25 / 1	0	3.1
Run16	1.25 / 1	0	1.3
Run17	1.25 / 1	10	4.6
Run18	1.25 / 1	20	4.6
Run19	1.25 / 1	30	4.6
Run20	1 / 1.5	10	4.6
Run21	1 / 2	10	4.6

a. [P(GMA-co-CL)] / [HEMA] mass ratio

Copolymerization of P(GMA-co-CL) (Sample Run3 in table 1) and HEMA with different mass ratios were made. Reactions were conducted until the total consumption of the double bonds detected by their absorption at 1630cm^{-1} in FTIR spectra. Thermo-mechanical property evolutions with temperature of these products are depicted in Figure 11.

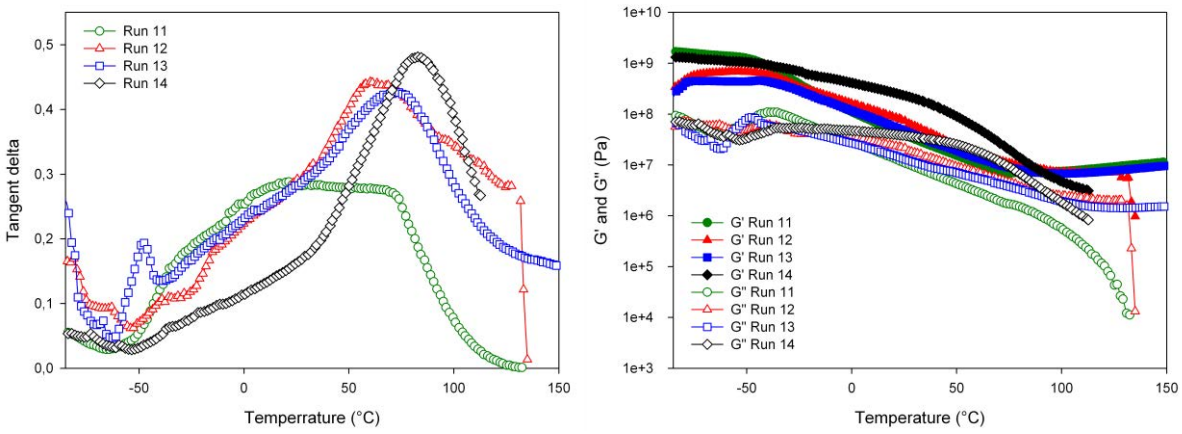

Figure 11. Loss factor tanδ (left), modulus G' and G" (right) versus temperature curves of networks composed of different P(GMA-co-CL) / HEMA mass ratios. Run11-[P(GMA-co-CL)]:[HEMA]=1.5:1, Run12-1.25:1, Run13-1:1, Run14-1:2

Higher G' value than G" throughout the temperature range confirms again the crosslinking of

the products. For P(GMA-co-CL)] / [HEMA] = 1:2 (Run14), the PHEMA rich phase is predominant and clear with a distinct tanδ peak although broadened towards lower temperature, while the T_g of the PCL rich phase is almost undetectable. By reducing the quantity of HEMA ([P(GMA-co-CL)] / [HEMA] =1:1, Run13), two different tanδ peaks and an intermediate region with high tanδ are observed. Two different phases are separated out. The one at lower temperature corresponds to the PCL-rich phase and the one at higher temperature corresponds the PHEMA rich phase. Two tanδ peaks corresponding to these phases shift towards each other (table 4) indicating interactions with each other. The intermediate tanδ region indicates that several network structures are formed by linking PCL backbones with PHEMA segments that have different chain lengths. This structural evolution continues with [P(GMA-co-CL)] / [HEMA] = 1.25:1.

For [P(GMA-co-CL)] / [HEMA] = 1.5: 1 (Run11), the PCL or PHEMA rich phases are no longer distinguishable. A wide relaxation transition between the initial PCL and PHEMA rich phases is obtained with a tanδ peak reduction. The tanδ curve was broadened and almost rectangular in a wide temperature zone. In these multi-component systems, the effective damping temperature range was broadened. All the networks showed expanded dumping peaks with tanδ peak values higher than 0.3, as shown in table 4:

Table 4. glass transition temperature and tanδ peak value of GMA and CL phase in copolymers, and their working area for damping. The networks were synthesized without the introduction of thiols, Run11-[P(GMA-co-CL)]:[HEMA]=1.5:1 P(GMA-co-CL) f=4.6, Run12-1.25:1 f=4.6, Run13-1:1 f=4.6, Run14-1:2 f=4.6, Run15-1.25:1 f=3.1, Run16-1.25:1 f=1.3

Samples	P(GMA-co-CL) phase		PHEMA phase		Δtanδ>0.3, °C
	T_g, °C	$Tan\delta_{max}$	T_g, °C	$Tan\delta_{max}$	
Run11	16	0.29	68	0.28	/
Run12	-38	0.10	60	0.44	30~117
Run13	-49	0.19	74	0.42	34~97
Run14	-55	0.04	84	0.48	53~108
Run15	-28.1	0.12	53	0.52	23.0~73.7
Run16	-32.5	0.14	71	0.50	32.1~90.4

b. Functionality of P(CL-co-GMA)effects on the P(CL-co-GMA) / HEMA network

P(GMA-co-CL) with different functionalities were copolymerized with HEMA. The [P(CL-co-GMA)] / [HEMA] mass ratio was kept constant and equal to 1.25. DMA results of the obtained samples were illustrated in Figure 12.

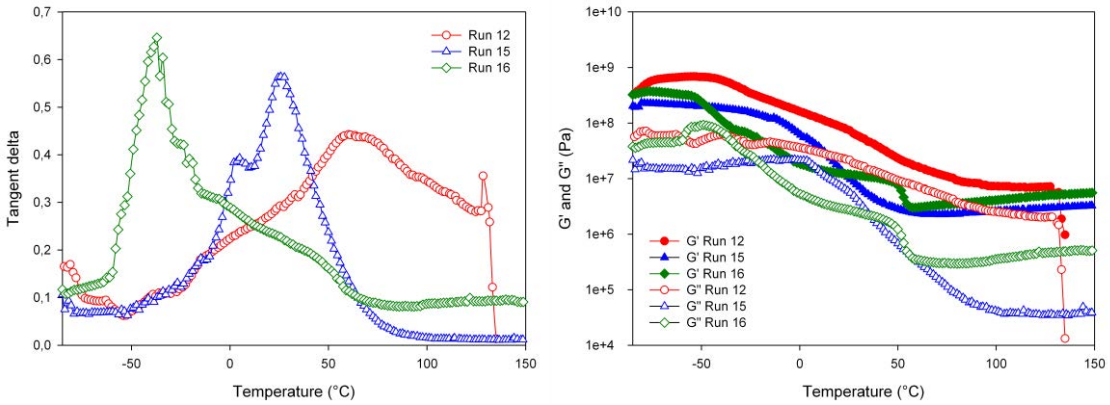

Figure 12. Loss factor tanδ (left), modulus G' and G" (right) versus temperature curves of the networks built of HEMA and P(GMA-co-CL) with different P(GMA-co-CL) functionalities, the mass ratio [copolymer]:[HEMA]=1.25:1, Run12-P(GMA-co-CL) f=4.6, Run13-f=3.1, Run14-f=1.3

For the network built with P(GMA-co-CL) that had the lower mean functionality (f=1.3, Run16), the tanδ peak was obtained at low temperature. This peak is attributed to the P(GMA-co-CL) containing lower GMA quantities. The copolymerization of these P(GMA-co-CL) with HEMA is relatively low. In this network, the more functionalized P(GMA-co-CL) which copolymerized with HEMA can be seen with broadened tanδ peaks observed at higher temperature with damping effects ranging from -15 to 60 °C.

A network built with highly functionalized P(GMA-co-CL) (f=4.6, Run12) shows the reverse effect. The more functionalized P(GMA-co-CL) part was largely grafted and modified, giving network relaxations similar to those of the PHEMA. The less functionalized part was the less modified part and led to networks having glass transitions at lower temperature. A particular damping effect between -15 and 140°C was obtained.

For the network built using the intermediate functionalized P(GMA-co-CL) (f=3.1, Run15), two transitions were obtained. The tanδ corresponding to the PCL and PBMA rich phases had a

very important shift approaching each other showing an important compatibility effect. These peaks became relatively high and narrow, which indicates a growing mobility in the region of relaxation transition (0-60°C).

c. Effects of the addition of multi-thiols on the P(CL-co-GMA)/HEMA network

Multi-thiols act not only as cross linkers but also as efficient chain transfer agents in radical polymerizations and directly affect the polymerization degree of the polymers, as proved by our labs [44, 45]. They also reduce oxygen inhibition in radical photo-polymerizations [46]. In this study, tri-thiols were added during the P(CL-co-GMA)/HEMA copolymerization. Figure 13 gives the plots of loss factors (tanδ) versus temperature curves of networks obtained with different contents of multi-thiols.

Three cases should be considered according to the number of mercapto groups that have reacted per tri-thiol molecule. For the first case, only one mercapto group reacted. The interruption of the PHEMA chain growth resulted in a pendant PHEMA segment with two ending mercapto functions on P(GMA-co-CL) chains. This is equivalent to a loss of a methacrylate function on the PCL backbone that will not participate in the formation of bridges between the P(GMA-co-CL) chains. For the second case, two mercapto groups reacted, thanks to which the growth of PHEMA chain was maintained leading to a segment connecting two chains and bearing one residual mercapto function. For the last case, all mercapto functions reacted, so an additional crosslinking point was obtained. Actually, the three cases occured in parallel with a predominance of a particular case depending on the stoichiometry of the various reagents.

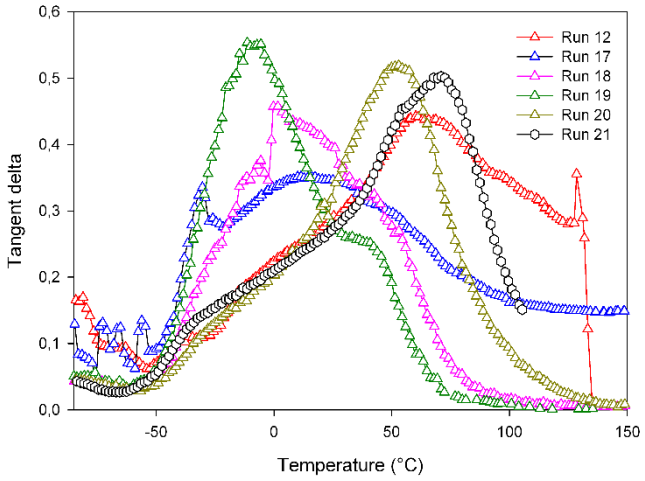

Figure 13. Loss factor tanδ versus temperature curves of networks synthesized with HEMA, P(GMA-co-CL) and thiol by different parameters, Run12-[P(GMA-co-CL)]:[HEMA]=1.25:1, without thiol, Run17-1.25:1, 10%mol thiol, Run18-1.25:1, 20%mol thiol, Run19-1.25:1, 30%mol thiol, Run20-1:1.5, 10%mol thiol, Run21-1:2, 10%mol thiol

For all experiments, networks were obtained (G' higher than G" for all the temperature ranges). The shape of the tanδ curve corresponding to the run12 is only maintained for run21. In this case the addition of thiol is compensated by the addition of important quantities of HEMA. When the quantity of HEMA is lower, a small shift of Tanδ toward lower temperature is obtained for run20 and much more important for run17.

As expected, the addition of thiols in run17 results in an effect equivalent to the decrease of P(GMA-co-CL) functionality. This results in an important transfer reaction leading to pendant chains with residual mercapto groups. When quantities of mercaptans increased in runs 18 and 19 this effect was enhanced. Damping properties of these networks are shown below in table 5.

Table 5. glass transition temperature and tanδ peak value of GMA and CL phase in copolymers, and their working area for damping. The networks were synthesized with the introduction of thiols, Run12-[P(GMA-co-CL)]:[HEMA]=1.25:1, without thiol, Run17-1.25:1, 10%mol thiol, Run18-1.25:1, 20%mol thiol, Run19-1.25:1, 30%mol thiol, Run20-1:1.5, 10%mol thiol, Run21-1:2, 10%mol thiol

Samples	P(GMA-co-CL) phase		PHEMA phase		Δtanδ>0.3, °C
	T_g, °C	$Tan\delta_{max}$	T_g, °C	$Tan\delta_{max}$	
Run12	-38	0.10	60	0.44	30~117

Run17	-30.4	0.34	11.5	0.35	-34~ -29, -13 ~ 48
Run18	1.6	0.45	42.6	0.32	-16~45
Run19	-11.4	0.55	40.30	0.26	-31~23
Run20	-28.1	0.12	53.0	0.52	-28
Run21	-34.1	0.13	71.0	0.50	33-90

4.4 Conclusion

An efficient and easy novel way to synthetize acrylated PCL by ring opening copolymerization of glycidyl methacrylate with caprolactone was proposed. These P(GMA-co-CL) copolymers are able to be altered in their molecular weight and functionality by changing reaction parameters such as nature and ratio of catalyst/co-initiator and monomers stoichiometry. The obtained copolymers can lead by thiol-ene reactions with trimethylolpropane tris(3-mercaptopropionate) to homogeneous transparent networks. When P(GMA-co-CL) copolymerized with HEMA, the network obtained had original and tailorable damping properties that can be adapted by changing curing parameters such as monomers ratios and functionalities. Furthermore, the addition of multi-thiols can lead to networks with supplementary cross linking points.

Acknowledgement

The authors thank the financial support from the China Scholarship Council (state scholarship fund). This work benefited from the international cooperation between the Université Jean-Monnet, Saint-Etienne (France) and the East China University of Science and Technology (China).

Reference:

1. Albertsson AC and Varma IK. Biomacromolecules 2003;4(6):1466-1486.
2. Jerome C and Lecomte P. Advanced Drug Delivery Reviews 2008;60(9):1056-1076.
3. Okada M. Progress in Polymer Science 2002;27(1):87-133.
4. Yeh CC, Chen CN, Li YT, Chang CW, Cheng MY, and Chang HI. Cellular Polymers 2011;30(5):261-276.
5. Tay BY, Zhang SX, Myint MH, Ng FL, Chandrasekaran M, and Tan LKA. Journal of Materials Processing Technology 2007;182(1-3):117-121.
6. Baji A, Wong SC, Srivatsan TS, Njus GO, and Mathur G. Materials and Manufacturing Processes 2006;21(2):211-218.
7. Yoshimoto H, Shin YM, Terai H, and Vacanti JP. Biomaterials 2003;24(12):2077-2082.
8. Diba M, Kharaziha M, Fathi MH, Gholipourmalekabadi M, and Samadikuchaksaraei A. Composites Science and Technology 2012;72(6):716-723.
9. Rai B, Teoh SH, Hutmacher DW, Cao T, and Ho KH. Biomaterials 2005;26(17):3739-3748.
10. Ebersole GC, Buettmann EG, MacEwan MR, Tang ME, Frisella MM, Matthews BD, and Deeken CR. Surgical Endoscopy and Other Interventional Techniques 2012;26(10):2717-2728.
11. Stridsberg KM, Ryner M, and Albertsson AC. Controlled ring-opening polymerization: Polymers with designed macromolecular architecture. In: Albertsson AC, editor. Degradable Aliphatic Polyesters, vol. 157, 2002. pp. 41-65.
12. Majoumo-Mbe F, Smolensky E, Lonnecke P, Shpasser D, Eisen MS, and Hey-Hawkins E. Journal of Molecular Catalysis a-Chemical 2005;240(1-2):91-98.
13. Hua C, Dong CM, and Wei Y. Biomacromolecules 2009;10(5):1140-1148.
14. Mishra AK, Patel VK, Vishwakarma NK, Biswas CS, Raula M, Misra A, Mandal TK, and Ray B. Macromolecules 2011;44(8):2465-2473.
15. Becquart F, Chalamet Y, Chen J, Zhao Y, and Taha M. Macromolecular Materials and Engineering 2009;294(10):643-650.
16. Becquart F, Taha M, Zerroukhi A, Kaczun J, and Llauro M-F. European Polymer Journal 2007;43(4):1549-1556.
17. Lohmeijer BG, Pratt RC, Leibfarth F, Logan JW, Long DA, Dove AP, Nederberg F, Choi J, Wade C, and Waymouth RM. Macromolecules 2006;39(25):8574-8583.
18. Simon L and Goodman JM. Journal of Organic Chemistry 2007;72(25):9656-9662.
19. Sadik T, Massardier V, Becquart F, and Taha M. Polymer 2012;53(21):4585-4594.
20. Chevallier C, Becquart F, Majeste JC, and Taha M. Designed Monomers and Polymers 2013;16(6):564-577.
21. Okhay N, Jegat C, Mignard N, and Taha M. Reactive & Functional Polymers 2013;73(5):745-755.

22. Bouyahyi M, Pepels MPF, Heise A, and Duchateau R. Macromolecules 2012;45(8):3356-3366.

23. Zhu YB, Gao CY, and Shen JC. Biomaterials 2002;23(24):4889-4895.

24. Riva R, Lenoir S, Jerome R, and Lecomte P. Polymer 2005;46(19):8511-8518.

25. Coudray S, Pascault J, and Taha M. Polymer Bulletin 1994;32(5-6):605-610.

26. Mallek H, Jegat C, Mignard N, Taha M, Abid M, and Abid S. Journal of Macromolecular Science, Part A 2013;50(7):728-737.

27. Mecerreyes D, Humes J, Miller RD, Hedrick JL, Detrembleur C, Lecomte P, Jerome R, and San Roman J. Macromolecular Rapid Communications 2000;21(11):779-784.

28. Mecerreyes D, Miller RD, Hedrick JL, Detrembleur C, and Jerome R. Journal of Polymer Science Part a-Polymer Chemistry 2000;38(5):870-875.

29. Abdyev OB. Polymer Science Series B 2011;53(5-6):278-282.

30. Horak D and Shapoval P. Journal of Polymer Science Part a-Polymer Chemistry 2000;38(21):3855-3863.

31. Sha K, Li D, Li Y, Liu X, Wang S, and Wang J. Polymer International 2008;57(2):211-218.

32. Zhang B, Li Y, Ai P, Sa Z, Zhao Y, Li M, Wang D, and Sha K. Journal of Polymer Science Part a-Polymer Chemistry 2009;47(20):5509-5526.

33. Ahmetli G, Kocak A, and Yazicigil Z. Journal of Applied Polymer Science 2007;106(6):3710-3715.

34. Bicak N and Karagoz B. Polymer Bulletin 2006;56(1):87-93.

35. Fernandez X, Salla JM, Serra A, Mantecon A, and Ramis X. Journal of Polymer Science Part a-Polymer Chemistry 2005;43(15):3421-3432.

36. Labbe A, Brocas A-L, Ibarboure E, Ishizone T, Hirao A, Deffieux A, and Carlotti S. Macromolecules 2011;44(16):6356-6364.

37. Bednarek M and Kubisa P. Journal of Polymer Science Part a-Polymer Chemistry 2005;43(17):3788-3796.

38. Uenishi K, Sudo A, and Endo T. Journal of Polymer Science Part a-Polymer Chemistry 2009;47(14):3662-3668.

39. Odian G. Principles of Polymerization, Fourth Edition 2004:544-618.

40. Nikolic G, Zlatkovic S, Cakic M, Cakic S, Lacnjevac C, and Rajic Z. Sensors 2010;10(1):684-696.

41. Sato T, Oki T, Seno M, and Hirano T. Journal of Polymer Science Part a-Polymer Chemistry 2001;39(9):1269-1279.

42. Meng YF, Li HF, Wen HY, Jiang SC, and An LJ. Acta Polymerica Sinica 2007(2):198-202.

43. Lezcano EG, Coll CS, and Prolongo MG. Polymer 1996;37(16):3603-3609.

44. Boutevin B, Snoussi MH, and Taha M. European Polymer Journal 1985;21(5):445-447.

45. Boutevin B, Mouanda J, Pietrasanta Y, and Taha M. Journal of Polymer Science Part A: Polymer Chemistry 1986;24(11):2891-2902.

46. Shin J, Nazarenko S, and Hoyle CE. Macromolecules 2009;42(17):6549-6557.

Chapter 5

Multi mercapto-functionalized PLA, PHB and PCL segmented polyurethanes

Hang SHEN [1, 2, 3], Jianding CHEN [4], Mohamed TAHA [1, 2, 3]*

1 Université de Lyon, F-42023, Saint-Etienne, France

2 CNRS, UMR 5223, Ingénierie des Matériaux Polymères, F-42023, Saint-Etienne, France;

3 Université de Saint-Etienne, Jean Monnet, F-42023, Saint-Etienne, France;

4 Laboratory of Advanced Materials Processing, East China University of Science and Technology, 200237 Shanghai, China

*correspondence：Mohamed.Taha@univ-st-etienne.fr

Résumé

Le polymére de type polyuréthanne fonctionnalisé multi-mercapto ont été synthétisé en deux étapes suivies par FTIR, ce qui est une nouvelle voie de synthése polyuréthanes dégradables porteurs de fonctions mercapto. Les structures de ces polyuréthanes ont été conçus pour doter les polyuréthanes avec de compositions différentes de de segments hard / soft et fonctionnalités mercapto.

Les produits obtenus ont été évalués par leurs structures par analyses RMN ^{1}H. Les composés identifiés confirment les structures attendues. La masse molaire obtenue par SEC augmente avec l'augmentation de la masse molaire et du nombre de segmentsdes diols introduits dans le polyuréthane, et de la fonctionnalité de ces polyurethanes. La température de transition vitreuse des polyuréthanes par DSC est proche de cette diols lorsque l'on augmente la quantité de diol, ce qui confirme aussi les structures attendues. Après la caractérisation et la purification de ces polyuréthanes les monoméres HEMA et MMA ont été télomérisés fonctions mercaptan. Les analyses SEC et RMN ^{1}H confirment les telomerization.

Mots-clés: Mercapto fonctionnalisation, polyuréthane dégradable, télomérisation, PCL, PLA et PHB.

Abstract

Multi-mercapto functionalized poly ester urethanes were synthesized using PLA, PHB and PCL segments. The structures of these poly ester urethanes were designed to endow oligomers with different hard / soft segment compositions and mercapto functionalities. The effects of the different reactions parameters on the structure, molar mass and glass transition temperature of these oligomers were evaluated. The mercapto groups were used as chain transfer agents during the radical polymerization of 2-hydroxylethyl methacrylate and methyl methacrylate leading to new original structures.

Keywords: Mercapto functionalization, degradable polyurethane, telomerization, PCL, PLA AND PHB

5.1 Introduction

Bio-based poly ester urethanes are used in many fields such as thermo-responsive and shape-memory materials for their physico-chemical and mechanical properties while exhibiting acceptable biological performance [1-5]. They were used as biomaterials like contact lenses and surgical implants in medical fields [6-8]. These polyurethanes were normally synthesized between dialcohols and diisocyanates yielding linear products. For their telechelic groups, most of them were converted from hydroxyl functions into double functions by acyltaion and used to radical copolymerize with methacrylates [9, 10]. Among these poly ester urethanes, non-linear architectures like star, comb shape and dendrimers [11-13] have attracted considerable interest recently owing to their possibility of post modification. The introduced branches result in more compact structure that dramatically affects crystalline, mechanical and viscoelastic properties. Moreover, versatile terminal groups endows these polyurethanes with application possibilities in catalysis, drug delivery, anion binding, and biomimetics [14-18]. Concerning these terminal groups, mercapto functions are efficient chain transfer functions in radical polymerization for regulating polymer length and telomers synthesis of telomers [19-22].

Mercapto functionalized polymers were often obtained by the aminolysis of dithioester or xanthate functions [23-25]. These xanthate functions are from the reversible addition–fragmentation chain transfer (RAFT) polymerization initiators [26, 27]. The aminolysis procedure may produce side products in oxidizing atmosphere [28]. Few attentions has been devoted to the degradable polyester-urethanes bearing such functions. Syntheses of polyurethanes bearing mercapto groups were described decades ago, the procedures were complex with low yields [29, 30]. Recently synthesis of polyurethanes bearing protected mercapto groups was reported [31], but the de-protection of the mercapto group were not mentioned.

The aim of this study is to prepare PLA, PHB and PCL segmented com-shape poly ester-urethanes bearing mercapto groups at the chain-ends using simple reaction procedures.

These polymers will be used as chain transfer or clicked with different monomers, for example, grafting PMMA branches. The covalent C-S bond of the PMMA branch to the polyurethanes may make the PMMA / PCL system more stable compared with the PMMA / PCL physical blends, which has recently gained significant interests as an economical and scalable route to achieve degradation and mechanical properties. On the other hand, hydrophilic 2-hydroxyethyl methacrylate (HEMA) can improve the hydrophilicity and cell adhesion of the polymer, which can also be grafted from the mercapto functionalized polyurethanes, and these PHEMA chains will also improve the mechanical properties of the polyurethane matrix due to its high T_g and pendant hydroxyl groups allowing for further modifications. In this study, to synthesize these polyurethanes, molar mass controlled polyhydroxybutyrate (PHB) diols and polylactide (PLA) diols were prepared and used for synthesizing PEUs with isocyanate end-groups. While Experiments reacting 2-aminothiopehnol with H_{12}MDI as model were first conducted to confirm reactions of isocyanate with the amine rather than with the mercapto function of the 2-aminothiopehnol. So by reaction 2-aminothiophenol and isocyanate terminated PEU, PEUs with mercapto end-groups can be prepared.

5.2 Experiment

Materials

2-Hydroxyethyl methacrylate was purchased from Röhm GmbH. Dihydroxyl terminated polycaprolactone oligomers CAPA@ 2100A, 2200A and 2402 were purchased from Solvay and their molar masses are 1000, 2000 and 4000 Da respectively as indicted by the supplier and confirmed by ^{1}H NMR. Polyhydroxybutyrate PHI002™ was purchased from NaturePLAST with its molecular weight of 4730Da determined by ^{1}H NMR analysis. 3,6-Dimethyl-1,4-dioxane-2,5-dione (lactide), 4,4'-Methylenebis(cyclohexyl isocyanate) (H_{12}MDI), Glycerol, 1,4-butanediol, 2-propanol, 2-Aminothiophenol, Methyl methacrylate, Acrylamide, p-toluenesulfonic acid, Hydrochloric acid solution (0.1N), Dibutyltin dilaurate, Tin(II) bis (2-ethylhexanoate) were purchased from SIGMA-ALDRICH (France). Anhydrous DMF and diethyl ether was purchased from Carlo Erba Reagents™. Methyl methacrylate and 2-Hydroxyethyl methacrylate were distilled before use. Glycerol was dehydrated by molecular sieves 3 Å (rod

shape, size 1/16 inch, Fluka) for 1 week before use. Other reagents were used as received without further purification.

Model reaction of H_{12}MDI and 2-aminothiophenol

The reaction of 2-aminothiophenol and 4,4'-Methylenebis (cyclohexyl isocyanate) was performed with mole ratio $N_{2\text{-aminothiophenol}} : N_{HMDI} = 2 : 1$, and DMF was used as the solvent. At 0°C (ice-water bath), the DMF diluted 2-aminothiophenol was dropwise added into the H_{12}MDI DMF solution, and the reaction was kept for 30mins. After the reaction, the product was collected for titration to calculate the remaining amino groups, and also characterized by ^{1}H NMR to evaluate the structure of the product.

The titration of the product was done monitored by electric pH meter. Typically 1.255g (2.4mmol) of the product was dissolved in 2-propanol / water mixture with volume ratio 40mL / 10mL, and 0.1N hydrochloric acid was used to titrate the residual amino group. Thymol blue was also used as the indicator of the end point during the titration.

Synthesis of isocyanate terminated prepolymer with degradable polyester segments

Molar mass controlled PLA and PHB dihydroxyl telechelic oligomers were prepared according to according to Harri [32] and Loh's [4] work. The PLA telechelic oligomer was synthesized through 1, 4-butanediol initiated ring opening polymerization, PHB telechelic oligomers were prepared by p- toluenesurfonic acid catalyzed transesterification of PHB with 1, 4-butanediol. In this study, the PLA telechelic oligomers were prepared with molar mass 530, 870 and 1680 Da, and PHB telechelic oligomers with molar mass 980 and 1470 Da.

A typical synthesis procedure of isocyanate terminated degradable polyester segmented prepolymer is illustrated in Scheme 2: certain amount of glycerol and the oligomer diol were firstly added into the 2-neck flask equipped with previously dried nitrogen flow and condenser, then the anhydrous DMF was injected in as solvent, and the system was magnetically stirred

until homogeneous at room temperature. Then, H_{12}MDI was added and completely dispersed into the system, followed by the injection of dibutyltin dilaurate as catalyst. The whole system was placed in the oil bath at 80°C for 55 minutes. During the reaction, the FTIR was used to monitor the consumption of isocyanate group in the system.

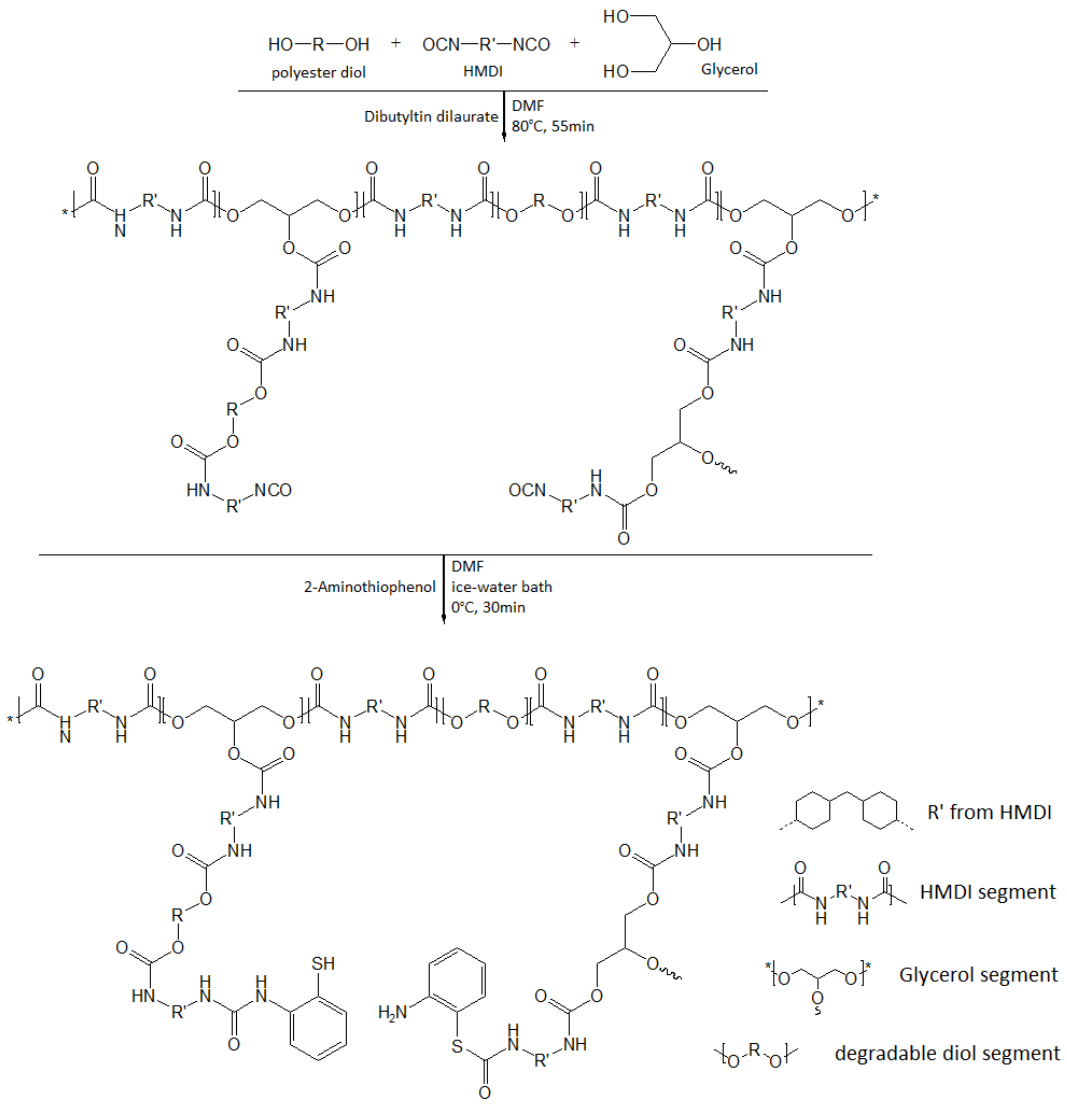

Scheme 2. Syntheses of mercapto / amino functionalized polyurethanes with degradable segments

Mercapto functionalization of the prepolymer by 2-aminothiophenol

Illustrated in Scheme 2, the obtained prepolymer solution above was diluted with anhydrous DMF and magnetic stirred in ice-water bath to decrease its temperature to 0-5°C. Then, 1.1 times of the stoichiometric 2-aminothiophenol was dropwise added to react the remaining isocyanate group. From the model experiment, conclusion can be drawn that the amino group

have priority to react with isocyante when compared with mercapto functions, as the result, the mercapto group will remain as the end function of the polyurethane. The reaction was kept for 30mins till the remaining isocyanate groups completely reacted, monitored by FTIR. The products was collected through three times the dissolve-precipitate process by precipitation with large amount of ethyl ether to remove the DMF in the system. Then, the product was dried in vacuum at room temperature for 24 hrs and kept at -20°C.

PEU structure design

In order to obtain poly ester urethanes with different properties, different structures of the PEUs are designed with different functionalities. An example is shown in Figure 1:

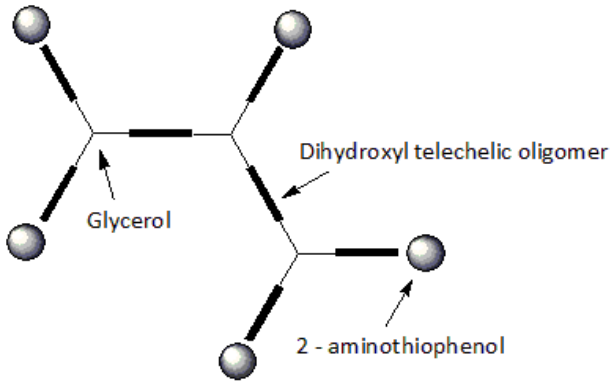

Figure 1. Expected structure model of the designed PEUs with functionality =5 (Run6 in Table 1), the linkage among glycerol, oligomer and 2-aminothiophenol were realized by diisocyanate H_{12}MDI.

The ratio of the monomers was decided by the expected structure above and the gel point was calculated by Macosko - Miller theory based equations [33], all formulae are listed in table 1:

Table 1. Formula of the PCL/PLA/PHB segmented mercapto functionalized PEUs, all polymerization were performed with 0.5 mol% of DBTDL at 80°C for 55mins for the first step, and at 0°C for 30mins for the second step. All samples were purified before the analyses.

Entry	Expected total functionality (-SH + NH_2)	Degradable segment numbers in expected structures	M_n of degradable segment / Da	Mole ratio of the reagents (H_{12}MDI : glycerol : PLA (or PHB) :2-aminothiophenol)
PCL based Pus				
Run 1	3	1	PCL / 1000	4.41 : 1 : 1 : 3
Run 2	3	2	PCL / 1000	5.52 : 1 : 2 : 3
Run 3	3	3	PCL / 1000	6.62 : 1 : 3 : 3
Run 4	3	3	PCL / 2000	6.62 : 1 : 3 : 3
Run 5	3	3	PCL / 4000	6.62 : 1 : 3 : 3
Run 6	5	7	PCL / 1000	17.65 : 3 : 7 : 5
Run 7	7	11	PCL / 1000	28.7 : 5 : 11 : 7
PLA based PUs				
Run 8	3	1	PLA / 870	4.41 : 1 : 1 : 3
Run 9	3	2	PLA / 870	5.52 : 1 : 2 : 3
Run 10	3	3	PLA / 870	6.62 : 1 : 3 : 3
Run 11	3	3	PLA / 530	6.62 : 1 : 3 : 3
Run 12	3	3	PLA / 1680	6.62 : 1 : 3 : 3
Run 13	5	7	PLA / 870	17.65 : 3 : 7 : 5
Run 14	7	11	PLA / 870	28.7 : 5 : 11 : 7
PHB based PUs				
Run 15	3	1	PHB / 980	4.41 : 1 : 1 : 3
Run 16	3	2	PHB / 980	5.52 : 1 : 2 : 3
Run 17	3	3	PHB / 980	6.62 : 1 : 3 : 3
Run 18	5	7	PHB / 980	17.65 : 3 : 7 : 5
Run 19	7	11	PHB / 980	28.7 : 5 : 11 : 7
Run 20	3	3	PHB / 1510	6.62 : 1 : 3 : 3

The structure design of these polyurethanes was mainly focused on their degradable segments, hard / soft segment compositions and average functionalities of these polyurethanes. By the formula listed in Table 1, polyurethanes with different properties can be obtained, characterized, evaluated for their structures and used for further post-modifications.

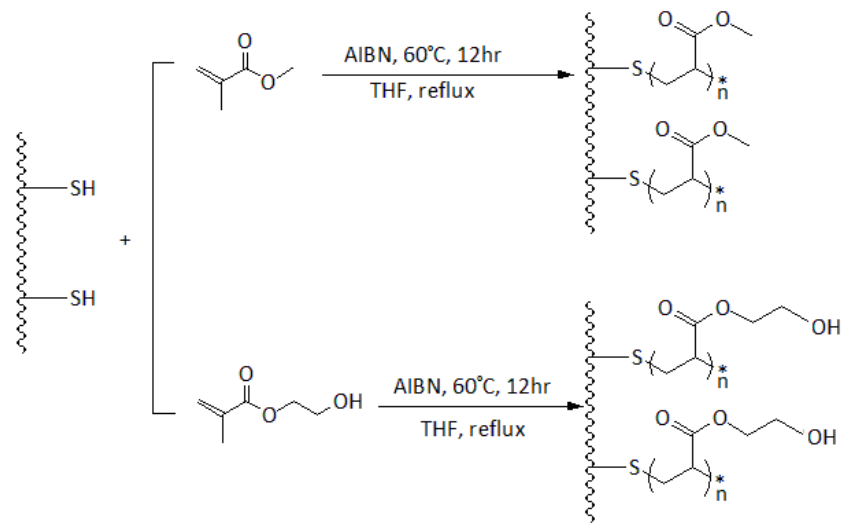

Scheme 3. Comb shaped polymers prepared by polymethacrylates grafted from mercapto functionalized polyurethanes

Shown on Scheme 3, the prepared mercapto functionalized polyurethanes were dissolved in THF at room temperature, then the certain amount of methacrylates were add into the solution. After the completely disperse of these monomers, the polymerization was initiated by 0.5 wt% AIBN at 60°C with the refluxing THF or 12hours. After the reaction, the obtained solutions were diluted in THF and precipitated in large amount of diethyl ether, and the samples were dried and collected in vacuum at room temperature.

Instrumentation

FTIR spectroscopy

FT-IR was used to monitor the reaction of isocyanate group and quantitatively characterize the PEUs. The absorption spectra of the polymer were recorded on a Nicolet Nexus spectrometer (700-3500 cm^{-1}) using attenuated total reflectance (ATR) technique.

Hydrogen nuclear magnetic resonance

NMR analyses were performed with a BRUKER Advance II spectrometer operating at 250MHz for ^{1}H NMR. The analyses were performed with 5mm diameter tubes containing about 25mg of polymer in 0.5mL chloroform-D with tetramethylsilane as internal reference at 0ppm. And

each sample was scanned for 64 times at 300K.

Differential scanning calorimetry

Differential scanning calorimetry (DSC) measurements for the allyl functionalized PCL segmented PEUs and PEU / PHEMA networks were carried out with a Q10 calorimeter from TA Instruments. Samples were transferred to hermetic pans and sealed, and analyzed from -80°C to 210°C with a cooling / heating rate of 10°C·min^{-1}. The glass transition temperatures were evaluated from the data recorded during heating by identifying the inflection points. Each sample underwent two cycles of heating-cooling cycles.

Size Exclusion Chromatography

For the analyses of mercapto functionalized PCL (or PLA) segmented polyurethanes, Size exclusion chromatography (SEC) was conducted using a system equipped with refractive index (Waters 2414) detectors. Two columns HR1 and HR3 from Waters were used. The eluent was tetrahydrofuran with a flow rate of 1 mL·min^{-1} and the elution temperature is 35^{o}C. The copolymer molecular weights were determined using a calibration curve established on a set of narrow polystyrene standards of different molecular weights ranging from 500 to 700 000.

For the analyses of mercapto functionalized PHB segmented polyuethanes, Size exclusion chromatography (SEC) was conducted using a system equipped with UV detector (Waters 486, wavelength = 280 nm), Light Scattering Detector (Wyatt TREOS) and RI refractometer detector (Schimadzu RID 10A). Two columns PLgel 5µm MIXED-C and PLgel 20mm Guard from Organic GPC were used. The eluent was chloroform with a flow rate of 1 mL·min-1 and the elution temperature is 22^{o}C. The samples tested were prepared with concentration 2mg·mL^{-1}.

5.3 Results and discussions

5.3.1 Model reaction of H12MDI and 2-aminothiophenol

To investigate the priority of amino group or mercapto group to the isocyanate function, the

model reaction was performed between H_{12}MDI and 2-aminothiophenol, the obtained product was titrated to determine the remaining amino amounts, with titration curves shown in Figure 2:

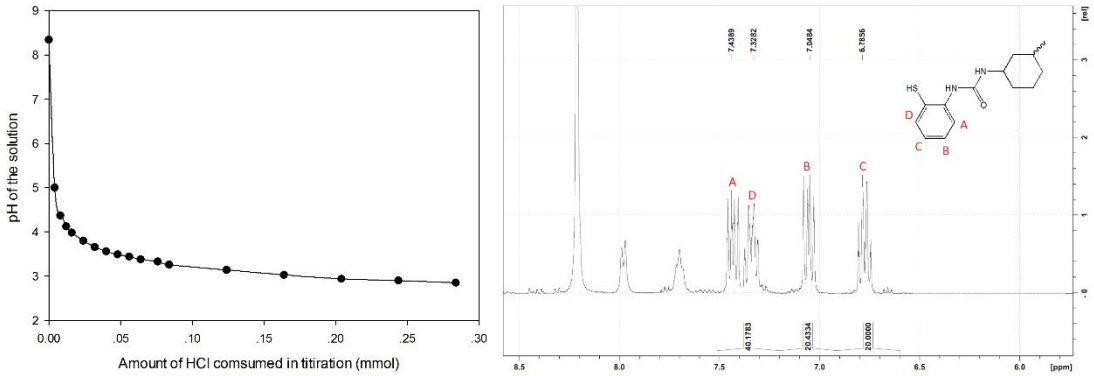

Figure 2. Left: pH versus HCl consumption curve for amino quantitative titration. Right: 1H NMR spectrum of the obtained product in DMF-D at 300K, form 6.5ppm to 8.5ppm

From Figure 2, the solution of the product is weak alkaline before titration (pH = 8.34), indicating the existence of few amino groups in the system. For the stoichiometric reaction of H_{12}MDI and 2-aminothiophenol, existence of these amino groups can be explained by the reaction of mercapto group of 2-aminothiophenol to the H_{12}MDI, but with very small amount. By interpolate calculating, 98.9 mol% of the amino group react with the isocyanate, proving the priority of amino-isocyanate reaction. To further confirm this conclusion, the obtained product was also analyzed with ^{1}H NMR, with spectrum also shown in Figure 2. Compared with the standard spectrum of 2-aminothiophenol (SDBS), the mercapto adjacent proton D stay still, while the animo function adjacent proton A shift from 6.64ppm to 7.44ppm, the corresponding chemical shift of protons B and C, and the integration of all protons proves the estimated structure, and priority of amino-isocyanate reaction to mercapto -isocyanate reaction..

5.3.2 Synthesis of functionalized poly (ester urethane)s

Mercapto functionalized poly ester urethane were prepared in two steps: hydroxyl terminated polyester oligomer (PLA, PHA or PCL) reacts with an excess of diisocyanate, then the remaining

isocyanate reacts with the amine group of 2-aminothiophenol.

FTIR Monitoring

FTIR were used to monitor the reactions, an example concerning a mercapto functionalized PLA segmented polyurethane synthesis monitoring by TFIR is shown in Figure 2.

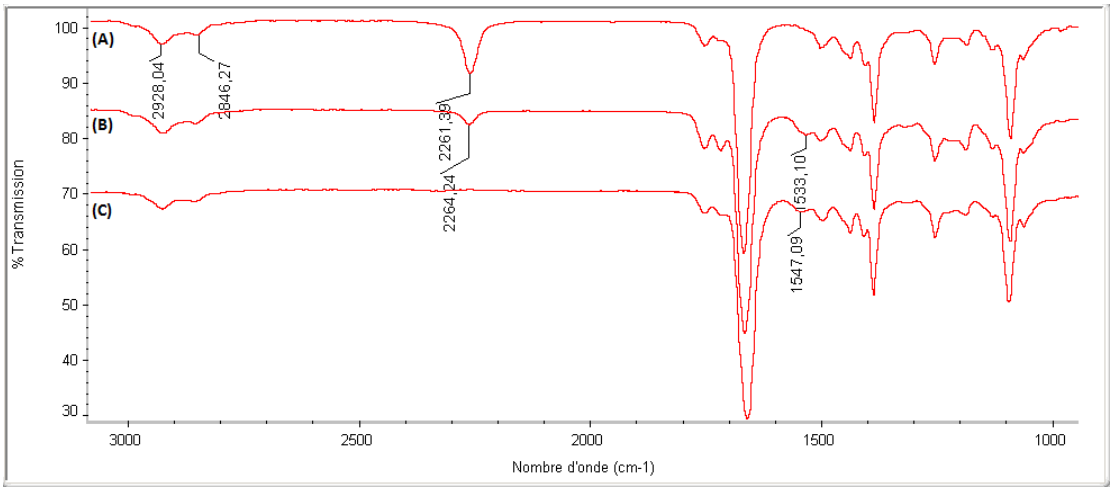

Figure 2. IR spectra of a2-step PLA segmented functionalized polyurethane synthesis (Run3): (A) reagent mixture at initial time, (B) PLA segmented PEU r after the first step, (C) mercapto functionalized PLA segmented PEU after the second step

The first steps of segmented prepolymers synthesis ended when the strength of absorption peaks at around 2260cm^{-1} (assigned to the isocyanate group) stopped decreasing, indicating the total consumption of the hydroxyl groups typically after 60mins reaction. Then, the 2-aminothiophenol was added to react with the remaining isocyante. The disappearance of N=C=O absorption indicate the end of the second step. Equivalent evolutions were performed for all the other synthesis.

5.3.3 ^{1}H NMR of mercapto functionalized PEUs

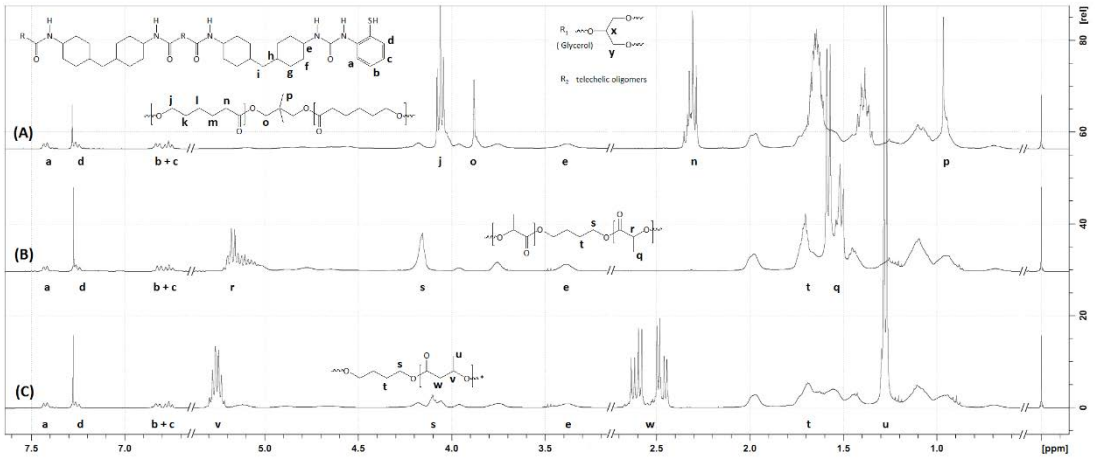

Figure 3. The ^{1}H NMR spectra of functionalized PCL / PLA / PHB segmented PEUs (A:Run2, B:Run9 and C:Run20 respectively) in $CDCl_3$ at 300K

^{1}H NMR spectra of the mercapto functionalized PEUs are presented in Figure 3, Polyester segment repeat unit versus mercapto function mole ratios can be evaluated by calculation, which is an effective way in verifying the structure of synthesized products. Comparing integrations of PCL methylene protons ”o”, PLA methine proton “r” or PHB proton “v” to the aromatic ring protons “a” at 7.4ppm that adjacent to the urethane linkage, the mole ratio of degradable segments to mercapto groups can be evaluated and compared to expected values. As seen in table 2, correct concordances are obtained confirming the structure of the PEU’s.

Table 2. The average mole ratio of repeat unit CL (or PLA and PHB) to mercapto functions in PEU moles, listed by expected value and by ^{1}H NMR calculation from products respectively. All polymerization were performed with 0.5 mol% of DBTDL at 80°C for 60mins for the first step, and at 0°C for 30mins for the second step.

Sample	Run1	Run2	Run9	Run13	Run19
Functionality with expected structure	3	3	3	5	7
Expected [mercapto]/[oligomer repeat unit], mol : mol	1 : 5.3	1 : 10.7	1 : 7.2	1 : 15.1	1 : 16.2
Calculated [mrecapto]/[oligomer repeat unit] by ^{1}H NMR analysis of the obtained products, mol : mol	1 : 5.4	1 : 11.4	1 : 7.6	1 : 13.8	1 : 14.8

5.3.4 SEC and DSC analysis of mercapto functionalized polyurethanes

DSC DSC and SEC analysis of mercapto functionalized polyurethanes results are depicted in Table 3:

Table 3. Molar mass obtained from SEC analyses and glass transition temperature by DSC analyses of mercapto functionalized polyurethanes.

Entry	[NCO] / [OH], mol / mol	M_n / M_w	degradable segment content, wt%	mercapto content, mmol/g	T_g of PEUs, °C
PCL segmented polyurethanes					
Run 1*	1.6	9200 / 29230	40.48	1.19	-24.9
Run 2*	1.43	9740 / 24991	53.71	0.79	-27.4
Run 3*	1.33	10560 / 27180	58.06	0.57	-26.9
Run 4*	1.33	17400 / 34900	73.13	0.37	-30.2
Run 5*	1.33	33800 / 60100	84.48	0.21	-31.6
Run 6*	1.22	13100 / 33710	56.28	0.40	-49.2
Run 7*	1.19	17610 / 44370	55.80	0.35	-56.1
PLA segmented polyurethanes					
Run 8*	1.6	6450 / 18770	34.78	1.20	14.0
Run 9*	1.43	10310 / 36040	47.50	0.82	17.6
Run 10*	1.33	12500 / 39170	54.17	0.62	17.3
Run 11*	1.33	11079/ 35660 2	42.22	0.79	9.5
Run 12*	1.33	18930 / 51780	69.62	0.41	35.9
Run 13*	1.22	12780 / 44230	52.35	0.43	23.9
Run 14*	1.19	19295 / 39760	51.81	0.38	34.5
PHB segmented polyurethanes					
Run 15**	1.6	5141 / 13110	37.59	1.15	8.3
Run 16**	1.43	5300 / 12970	50.55	0.77	6
Run 17**	1.33	5674 / 12530	57.11	0.58	3
Run 18**	1.22	13470 / 37870	55.32	0.40	0.8
Run 19**	1.19	5693 / 13920	54.83	0.36	1.8
Run 20**	1.33	6291 / 14880	66.61	0.45	1.4

Notes: "*"SEC with THF eluent, PS standards calibration curve

"**"SEC with chloroform eluent, universal calibration

From the SEC data in Table 3, it can be seen that for PCL, PLA and PHB segmented polyurethanes, the molar mass increased as expected with the increase of (1) the number of oligomer chains segmented in to the polyurethane, (2) the molar mass of degradable segments included in polyurethane synthesis, and (3) the functionality of the polyurethane.

Glass transition behaviors of these polyurethanes are affected by their structure. For the 3 systems, it is obvious that, the T_g of the polyurethane shift towards the T_g of the higher molar used polyester that is PHB: 0°C, PCL: -59°C and PLA 40°C. As shown in this part, different structure were designed and used for mercapto functionalized poly ester urethane syntheses.

By adapting these different formulas, poly ester urethanes with functionalities F=3-7, containing polyester segments having PCL M_n= 9000-34000 DA, PLA M_n=6500-19000 DA and , PHB M_n= 5000-13500 DA, and polyester wt% that is PCL, 40-85 wt%, PLA 35-70 wt% and PHB 35-65 wt%.

These PEU's can be used in severeal application, among them grafting of polyadducts by chain transfer reactions to mercapto groups during radical polymerization. This aspect will be developed in the following part.

5.3.5 Polymethacrylates grafting from polyester-urethanes

To evaluate the grafting reactions of methacrylates from mercapto functionalized polyurethanes, HEMA, acrylamide and MMA were reacted in THF with the chosen purified polyurethanes, then analyzed by SEC, the result are shown from Table 4 and Figure 4:

Table 4. The number averaged molar mass (M_n) of polyurethane before and after the telomerization, the molar mass were determined using universal calibration

Samples	[>C=C<]/[-SH]	M_n	ΔM_n
PCL segmented PU			
Run6	/	6307	/
Run6+MMA	6:1	7696	1389
Run6+MMA	12:1	7880	1573
Run6+HEMA	4:1	8439	2132
Run6+HEMA	8:1	8474	2167
PLA segmented PU			
Run13 (PLA-F5-A7-M870)	/	7887	/
Run13 + MMA	6:1	11720	3833
Run13 + MMA	12:1	11261	3374
Run13 + HEMA	4:1	11572	3685
Run13 + HEMA	8:1	12502	4615
PHB segmented PU			
Run19 (PHB-F7-A11-M870)	/	6314	/

Run19 + MMA	6:1	8646	1104
Run19 + HEMA	4:1	8095	1781
Run19 + HEMA	8:1	8046	1732

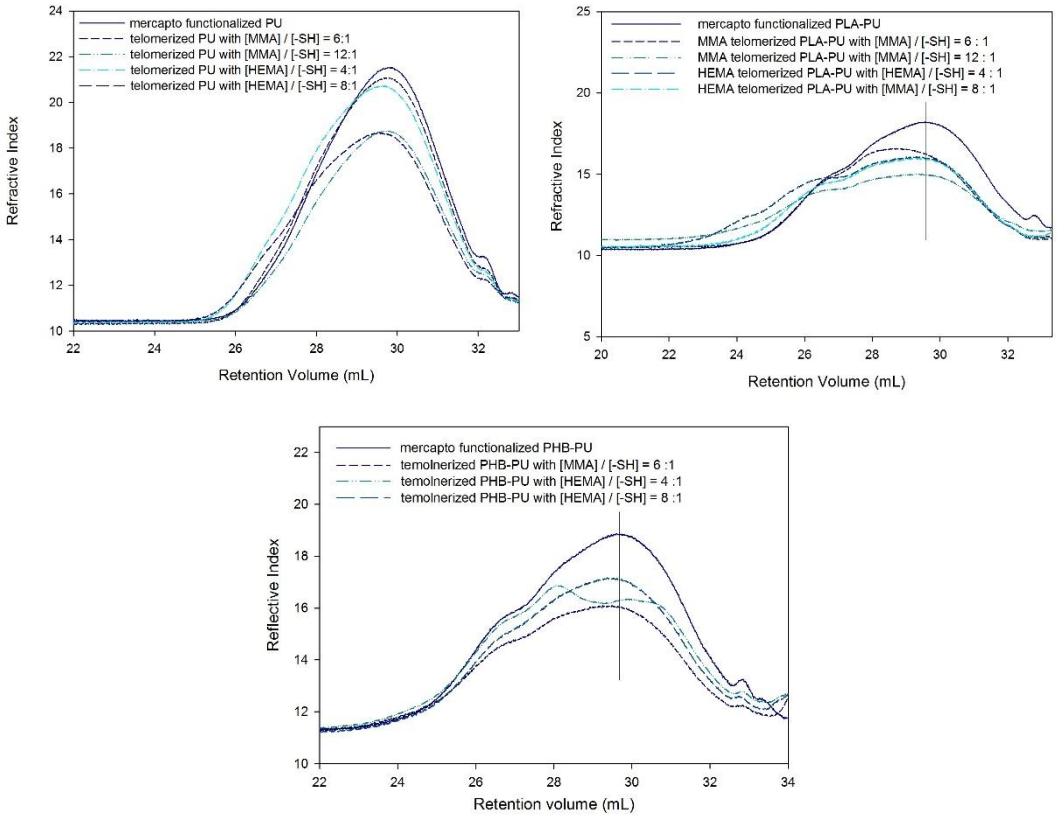

Figure 4. The SEC graph of PCL (top left), PLA (top right) and PHB (bottom) based polyurethane before and after telomerization.

Shown as Table 4 and Figure 4 from SEC analyses, obvious increase of the polyurethane number-average molecular weight can be observed after the reaction, and no other new retention peaks generated during the telomerization, indicating that the telomerization of MMA and HEMA to these mercapto functionalized polyurethanes. The polymerization degree of the ploymethacrylate grafted from the polyurethane can be calculated as:

Grafted polymethacrylate chain:

$Dp_n = (Mn-Mn_0) / F \times M_{monomer}$

Where M_n and Mn_0 is the number averaged molar mass of the polyurethane after and before

grafting, F is the expected functionality of the polyurethanes.

In order to further evaluate the structure of these polymethacrylate grafted polyurethanes, the purified products were analyzed with ^{1}H NMR and spectra are given in Figures 5-7. Figure 5 and 6 illustrate the radical grafting of MMA from PCL and PLA segmented polyurethanes. Figure 5 shows the PCL segmented polyurethanes before (upper spectrum) and after (lower spectrum) the MMA grafting. The methyl ester protons “A” from PMMA chains are present at 3.7ppm. The PMMA main chain methylene “B” and methyl protons “C” are overlapped by the cyclohexyl protons from H_{12}MDI segments and caprolactone repeat units methylene protons. Figure 6 shows the PLA segmented polyurethanes before (upper spectrum) and after (lower spectrum) the MMA grafted copolymer. Here the peaks A and B are visible and the C overlapped by protons from the prepolymer.

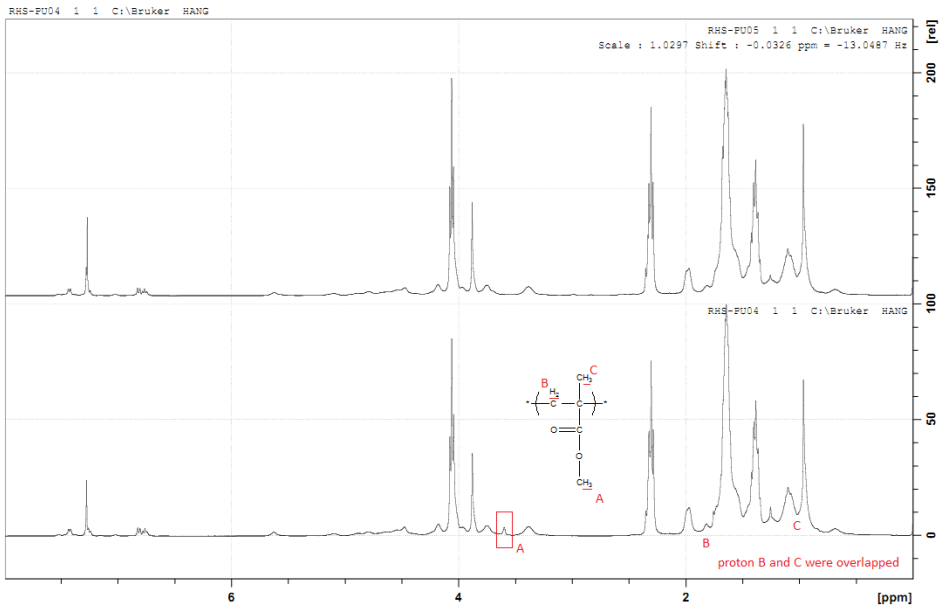

Figure 5. ^{1}H NMR spectra of PCL segmented polyurethane Run13 before and after the telomerization of MMA, the sample was purified before the analyses.

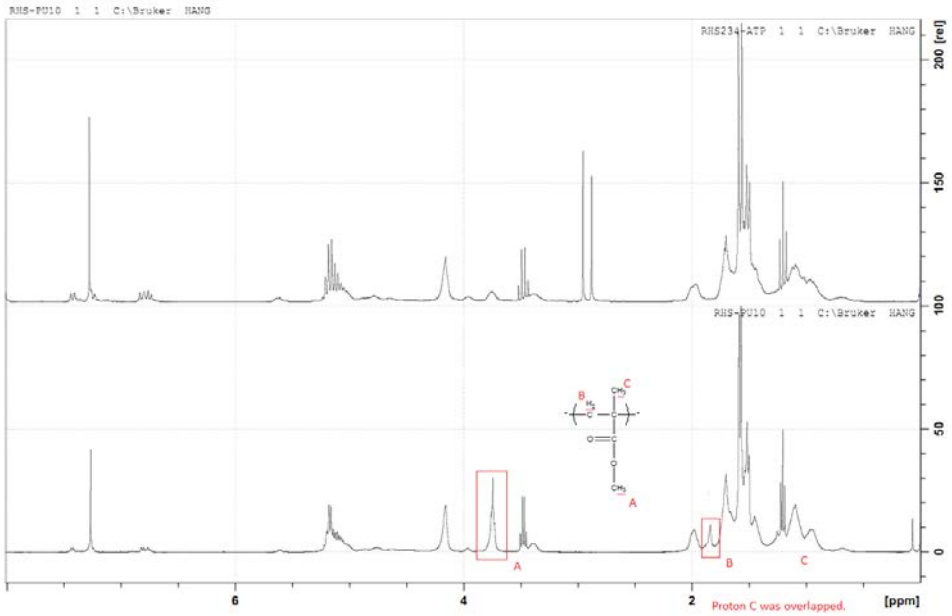

Figure 6. ^{1}H NMR spectra of PLA segmented polyurethane Run13 before and after the telomerization of MMA, the sample was purified before the analyses.

Graft of PHEMA chains to polyurethanes can also be proved. Take PHB segmented polyurethane as an example, the Figure 7 shows the PHB segmented polyurethane Run19 before (upper spectrum) and after (lower spectra) the telomeriation.

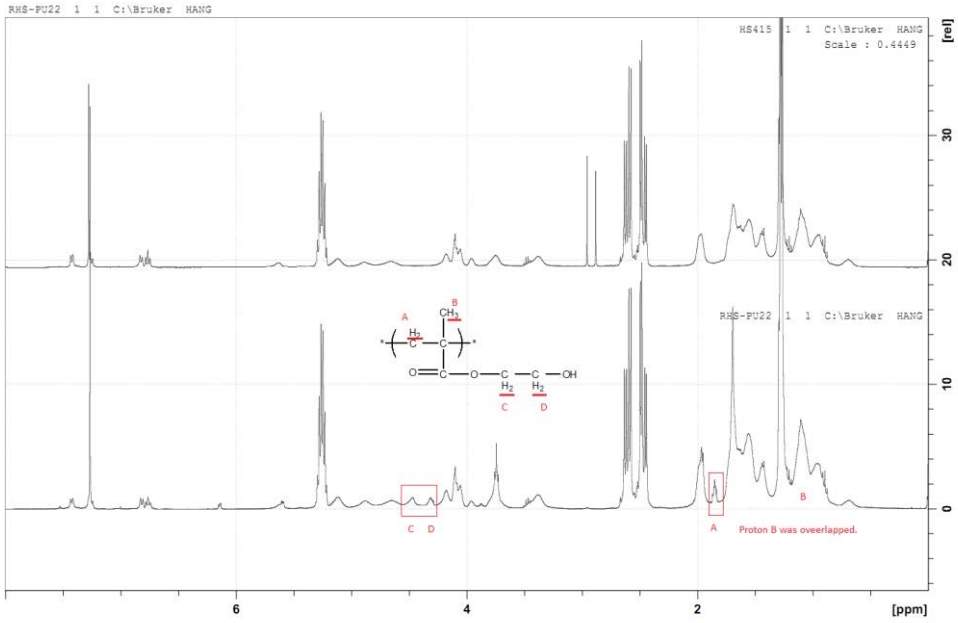

Figure 7. ^{1}H NMR spectra of PHB segmented polyurethane Run13 before and after the telomerization of HEMA, the sample was purified before the analyses.

Shown in Figure 7, compared with the mercapto functionalized polyurethane Run 19, the lower spectrum shows new peak at 4.2 and 4.5ppm, which is believed to be the ethylene ester protons C and D from PHEMA chains. The appearing peak at 1.8ppm attributed to the main chain methylene proton A of PHEMA, these peaks are evident to prove the graft of PHEMA chains onto the polyurethanes.

For PCL segmented polyurethane, methyl ester proton “A” was used to calculated the amount of MMA on the polymer chains, and MMA methylene proton “B” for PLA system, while for PHB systems, the proton C and D labeled in Figure 7 are used to calculate the amount of HEMA that grafted from the PU, by comparing the integrate of aromatic ring proton a listed in Figure 3, results are listed in table 5.

Table 5. Polymerization degree of polymethacrylate chains grafted on PU, by SEC and ^{1}H NMR calculation

Samples	Run6	Run13	Run19
Grafted polymethacrylate Dpn calculated by SEC	2.8	5.6	2.4
Grafted polymethacrylate Dpn calculated by ^{1}H NMR calculation	0.6	4.3	1.1

5.4 Conclusions:

Bio-based polyurethanes bearing reactive multi mercapto groups were synthesized. These degradable polyester segmented polymers were structured by molecular design and verified by ^{1}HNMR, SEC and DSC. The characterizations indicate that these polyurethanes can be altered by their molar mass, glass transition temperature and average mercapto functionality by adjusting the soft segment sorts, hard / soft segment compositions and [NCO] / [OH] mole ratios of the reagents. Methacrylates were used for telomerization on mercapto functions of obtained polyurethanes. The following ^{1}HNMR and SEC were performed to confirm the possibly of grafting polymethacrylate branches on these polyurethanes by telomerization, which brings the promising future for the application for these polyurethanes.

Acknowledgement

The authors thank the financial support from China Scholarship Council (state scholarship fund). This work benefited from the international cooperation between Université Jean-Monnet Saint-Etienne (France) and East China University of Science and Technology (China).

Reference:

1. Santerre JP, Woodhouse K, Laroche G, and Labow RS. Biomaterials 2005;26(35):7457-7470.
2. Laschke MW, Strohe A, Scheuer C, Eglin D, Verrier S, Alini M, Pohlemann T, and Menger MD. Acta Biomaterialia 2009;5(6):1991-2001.
3. Wang WS, Ping P, Chen XS, and Jing XB. Journal of Applied Polymer Science 2007;104(6):4182-4187.
4. Loh XJ, Sng KBC, and Li J. Biomaterials 2008;29(22):3185-3194.
5. Hiltunen K, Seppala JV, Itavaara M, and Harkonen M. Journal of Environmental Polymer Degradation 1997;5(3):167-173.
6. Lai YC and Baccei LJ. Journal of Applied Polymer Science 1991;42(12):3173-3179.
7. Zulfiqar M, Quddos A, and Zulfiqar S. Journal of Applied Polymer Science 1993;49(12):2055-2063.
8. Zdrahala RJ and Zdrahala IJ. Journal of biomaterials applications 1999;14(1):67-90.
9. Hoffman DK, Harris RF, Tefertiller NB, and Rains RC. Stable dispersions of polymers in polyfunctional compounds having a plurality of active hydrogens and polyurethanes produced therefrom. Google Patents, 1984.
10. Yu X, Grady BP, Reiner RS, and Cooper S. Journal of Applied Polymer Science 1993;49(11):1943-1955.
11. Mya KY, Gose HB, Pretsch T, Bothe M, and He C. Journal of Materials Chemistry 2011;21(13):4827-4836.
12. Huskić M and Žigon M. Polymer 2003;44(20):6187-6193.
13. Duan X, Griffith C, Dubé M, and Sheardown H. Journal of Biomaterials Science, Polymer Edition 2002;13(6):667-689.

14. Xiaoying S, Xiaohui Y, Yunhang L, and Xinling W. Journal of Polymer Science Part A: Polymer Chemistry 2004;42(10):2356-2364.
15. Coudray S, Pascault J, and Taha M. Polymer Bulletin 1994;32(5-6):605-610.
16. Henry I, Pascault JP, Taha M, Vigier G, and Flat JJ. Journal of applied polymer science 2002;83(2):225-233.
17. Mallek H, Jegat C, Mignard N, Taha M, Abid M, and Abid S. Journal of Macromolecular Science, Part A 2013;50(7):728-737.
18. Taha M, Gerard JF, and Maazouz A. Journal of Materials Science 1999;34(17):4341-4346.
19. Boutevin B, Mouanda J, Pietrasanta Y, and Taha M. Journal of Polymer Science Part A: Polymer Chemistry 1986;24(11):2891-2902.
20. Boutevin B, Pietrasanta Y, and Taha M. European Polymer Journal 1982;18(8):675-678.
21. Boutevin B, Pietrasanta Y, Taha M, and El Sarraf T. Polymer Bulletin 1983;10(3-4):157-161.
22. Boutevin B, Pietrasanta Y, and Taha M. Makromolekulare Chemie-Macromolecular Chemistry and Physics 1982;183(12):2995-3002.
23. Moad G, Chong Y, Postma A, Rizzardo E, and Thang SH. Polymer 2005;46(19):8458-8468.
24. Mayadunne RT, Rizzardo E, Chiefari J, Krstina J, Moad G, Postma A, and Thang SH. Macromolecules 2000;33(2):243-245.
25. Postma A, Davis TP, Moad G, and O'Shea MS. Macromolecules 2005;38(13):5371-5374.
26. Yamamoto K and Takasu A. Macromolecules 2010;43(20):8519-8523.
27. Liras M, García-García JM, Quijada-Garrido I, Gallardo A, and París R. Macromolecules 2011;44(10):3739-3745.
28. Roth PJ, Boyer C, Lowe AB, and Davis TP. Macromolecular rapid communications 2011;32(15):1123-1143.
29. Overberger CG and Aschkenasy H. Journal of Organic Chemistry 1960;25(9):1648-1651.
30. Overberger CG and Aschkenasy H. Journal of the American Chemical Society 1960;82(16):4357-4360.

31. Ferris C, Violante de Paz M, Zamora F, and Galbis JA. Polymer Degradation and Stability 2010;95(9):1480-1487.

32. Korhonen H, Helminen A, and Seppala JV. Polymer 2001;42(18):7541-7549.

33. Petrović ZS, Zavargo Z, Flyn JH, and Macknight WJ. Journal of Applied Polymer Science 1994;51(6):1087-1095.

Annexe

1. DMA graphs of networks did not illustrated in Chapter 4:

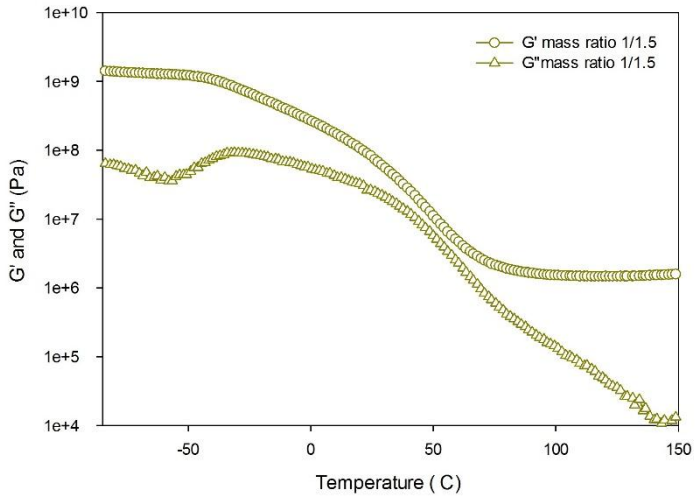

Figure 1. Storage modulus and loss modulus versus temperature curve of sample Run 20 in Chaper4, [P(GMA-co-CL)]:[HEMA]=1 : 1.5 and 10 mol% of the thiol was adapted in network synthesis.

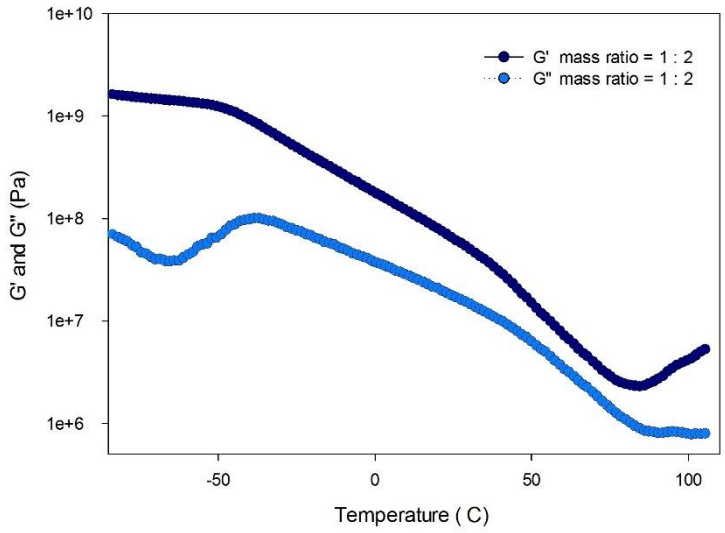

Figure 2. Storage modulus and loss modulus versus temperature curve of sample Run 21 in Chaper4, [P(GMA-co-CL)]:[HEMA]=1 : 2 and 10 mol% of the thiol was adapted in network synthesis

2. MALDI-TOF raw data for Sample Run3 mentioned in Chapter 4.

m/z	S/N	Res.	Intens.	Area		m/z	S/N	Res.	Intens.	Area		m/z	S/N	Res.	Intens.	Area
635.1669	57.4	15552	961.01	65		1205.5073	68.3	23492	1463.64	176		1802.0004	13.2	24289	212.76	50
649.3163	54.9	15244	921.82	66		1219.6600	109.3	21556	2168.69	293		1816.3684	16.9	26790	271.68	59
655.3438	100.2	15278	1872.87	135		1225.6849	82.4	23656	1864.56	232		1836.0342	9.7	20131	149.52	43
675.1595	62.8	15928	1168.55	84		1231.6561	19.1	20834	388.55	54		1848.0400	12.4	27445	193.70	43
697.1487	55.6	14989	951.41	76		1265.6975	27.5	24939	582.30	73		1876.0429	10.2	24250	149.98	38
707.3900	94.8	13196	1630.92	150		1277.7123	36.5	19732	717.91	116		1904.0636	32.2	26272	464.81	110
719.1256	69.4	16193	1310.11	103		1319.5765	54.2	24343	1090.38	149		1910.0866	13.8	25671	190.82	46
736.4323	15.0	14297	284.43	25		1323.7421	7.6	25097	151.58	20		1916.0614	11.6	26243	158.75	37
741.1052	27.2	16650	519.64	40		1333.7278	99.0	23894	1928.27	278		1990.1109	9.9	23828	124.91	34
749.2307	75.8	18712	1449.04	104		1339.7544	67.5	25450	1419.23	192		2018.1304	28.3	24929	354.54	95
763.3812	74.1	18786	1457.02	107		1345.7263	19.4	25030	430.85	60		2024.1562	11.6	23614	139.67	38
769.4077	127.2	17818	2426.56	189		1351.7394	8.2	25971	185.72	25		2030.1335	11.2	27127	133.89	33
809.4251	26.1	17000	486.17	42		1379.7698	21.6	21953	420.13	69		2040.4144	23.2	28675	270.73	63
821.4529	77.8	14291	1474.58	156		1391.7772	32.3	22094	657.83	110		2064.1664	7.4	22260	87.85	26
863.2998	105.8	21662	1957.83	150		1419.7738	16.8	21450	347.79	61		2076.1804	10.3	25615	117.43	31
877.4504	103.5	20052	2049.75	172		1433.6446	37.6	25511	734.12	111		2104.1719	9.7	25615	108.24	29
883.4766	137.0	20834	2802.54	230		1447.7975	69.5	24425	1462.51	239		2132.1999	27.6	26196	294.43	80
921.1876	26.8	19129	524.79	49		1453.8229	48.9	26019	932.76	145		2138.2205	9.7	26645	106.38	28
923.4909	31.5	19168	600.01	57		1459.7971	16.8	24730	338.56	54		2178.2288	6.5	21256	71.86	23
935.5195	59.0	14603	1153.48	146		1493.8356	15.1	20742	310.10	62		2246.2635	18.8	26246	197.67	58
943.1727	34.5	22031	673.12	57		1505.8441	20.3	21178	412.09	84		2264.4611	18.6	30406	191.58	48
965.1534	21.4	23428	436.49	37		1547.7134	24.1	21713	471.61	94		2360.3322	17.1	27829	156.24	45
977.3700	95.7	21803	2023.06	184		1561.8653	65.1	25120	1188.47	218		2474.3968	13.1	24804	106.04	37
991.5189	107.0	22537	2416.54	221		1567.8900	33.9	24841	636.75	118		2702.5281	11.4	25771	76.36	29
997.5454	136.5	21528	2660.68	255		1573.8620	16.4	26673	303.10	54						
1003.5182	18.6	18023	368.78	42		1607.9048	13.4	20291	254.65	59						
1037.5593	30.4	21411	627.24	64		1619.9116	17.2	24229	311.47	63						
1049.5838	49.5	15077	1019.21	152		1647.9081	12.2	21477	222.36	52						
1056.5525	7.8	27320	182.84	15		1661.7768	19.3	21749	338.23	76						
1077.5817	17.0	15413	361.70	55		1675.9316	48.3	24290	860.64	188						
1091.4396	81.5	22827	1842.68	193		1681.9577	22.9	24399	417.49	90						
1105.5904	132.1	22180	2619.95	291		1687.9363	13.8	23363	243.95	55						
1111.6157	111.0	22219	2245.03	251		1721.9696	10.5	20936	181.81	47						
1117.5901	18.0	19670	396.92	49		1733.9761	15.9	28541	279.75	56						
1151.6329	28.1	19574	583.83	77		1761.9816	10.5	23010	172.20	42						
1163.6500	42.5	16185	865.69	142		1775.8479	13.6	20926	219.17	57						
1167.2211	18.0	23955	357.16	40		1789.9982	40.0	26475	646.25	143						
1170.6273	6.9	21884	156.35	19		1796.0233	16.2	21272	257.71	69						

Table 1. Raw data of MALDI-TOF test for sample Run3 in Chapter 4. The sample was synthesized with [CL]:[GMA]=5, [CL]:[TBD]:[Benzyl alcohol]:[Hydroquinone]=100:1:1:1, performed at 110°C for 60mins.

Conclusion Générale

Des polyacides lactiques hydroxy téléchélique de masses molaires variées ont été synthétisés par polymérisation par ouverture de cycle du LLA en présence de 1,4 –butane diol. Des polyhydroxybutyrate hydroxy téléchéliques ont été préparés par transesterification du PHB et du 1,4-butanediol catalysée par l'acide p-toluène sulfonique .Ces oligomères ont été utilisés pour préparer des polyesters amides fonctionnalisés acrylates ou mercaptans.

Dans une approche parallèle, du PCL multi acrylate a été préparé avec succès par copolymérisation par ouverture de cycle de méthacrylate de glycidyle avec du caprolactone. Des copolymères (GMA -co- CL) ayant des masses molaires et une fonctionnalité variables ont été préparés en modifiant les paramètres de la réaction tels que le catalyseur, la nature du co-amorçeur et le rapport des stœchiométrique des différents réactifs.

Les polymères multi acrylates ont été copolymèrisés principalement avec l'HEMA sous irradiation UV pour obtenir des réseaux PLA, PHB et PCL segmentés. Les mécanismes de dégradation de ces réseaux ont été étudiés en examinant particulièrement les décompositions des liaisons uréthannes et esters. La dépolymérisation du PHEMA a été détecté avec TGA -FTIR à plus haute température (450°C).

Pour les réseaux à base de PCL, les propriétés thermo –mécaniques ont été étudiées. Le résultat montre que les phases riches en PCL ont une bonne compatibilité avec le poly HEMA. Les modules caoutchoutiques et l'étendue des températures des zones d'amortissement peuvent être contrôlées en fonction des paramètres réactionnels.

Les polymères multifonctionnels thiols du PCL, PHA et PLA ont été utilises pour faire croitre des chaines méthacrylates et construire des polymères de type étoile.

General Conclusion

Hydroxyl telechelic polylactic acids of various molecular weights were synthesized by ring opening polymerization in the presence of LLA and 1,4-butanediol. Telechelic hydroxy polyhydroxybutyrate were prepared transesterification of PHB and 1,4- butanediol catalyzed by p- toluene sulfonic acid. These oligomers were used to prepare polyesteramides functionalised acrylates or mercaptans.

In a parallel approach, the PCL multi acrylate was successfully prepared by ring-opening copolymerization of glycidyl methacrylate with caprolactone. Copolymers (GMA-co-CL) with variable molar masses and functionality were prepared by changing the reaction parameters such as catalyst, the nature of the co-initiator and the ratio of different stoichiometric reagents.

Multi-acrylated polymers were copolymerized with HEMA under UV irradiation to obtain PLA, PHB and PCL segmented networks. Degradation mechanisms of these networks have been studied by examining particular decomposition of urethane bonds and esters. Depolymerization of the PHEMA was detected with TGA -FTIR at higher temperature (450°C).

For PCL based networks , the thermo-mechanical properties were studied. The result shows that the PCL-rich phases have good compatibility with poly HEMA. The rubber and the working temperature range of the damping zones modules can be controlled as a function of reaction parameters.

Multi mercapto functionalized polymers with PCL , PLA and PHA segments were used to grow methacrylate polymer chains and build star type .